ABASTRACT

WANG, XIAOYANG. Development of a Computationally Efficient Finite Element Model of the Human Spine for the Purpose of Conducting Parametric Studies of the Stresses Induced in the Spine and in Spinal Fusion Instrumentation Hardware during Flexion, Torsion and Extension. (Under the direction of Andre Mazzoleni.)

This dissertation presents several comprehensive parametric studies of the stresses induced in the spine and in spinal fusion instrumentation during flexion, torsion and extension, by making use of a validated, computationally efficient, finite element model of the human spine. Intervertebral disc degeneration is a serious medical condition which sometimes necessitates spinal fusion in order to relieve the patient's back pain and restore spinal function. Curvature of the spine, or scoliosis, is another medical condition which may require spinal fusion. A variety of spinal fusion instrumentation constructs are studied, as invtervertebral disc conditions are varied parametrically with respect to disc stiffness. Of particular interest is the maximum stress experienced by the rods used in spinal fusion, as breakage of the rods can occur in the first few months after surgery. Also of interest is the stress induced in discs adjacent to the fused portion of the spine, as adjacent disc failure is a phenomenon which has been observed in patients who have undergone spinal fusion surgery. The human spine has a very complicated geometry, and finite element models that are based on detailed CT-scans of the spine take several hours of computer time to calculate the stresses and displacements for a single case. This dissertation presents a methodology that is based on a computationally efficient model of the spine which makes use of standard geometrical shapes. This simplified model enables the generation of results in just a few minutes of computer time, and yet produces results that are just as accurate as more complicated models when compared with experimental data. This reduced computation time makes it possible to conduct parametric studies which involve dozens or even hundreds of cases in a reasonable amount of time. This dissertation presents parametric studies which show the maximum stresses induced in the rods, and the stresses induced in adjacent discs, as the stiffness values of several of the discs are varied parametrically. The influence of the use of transforaminal lumbar interbody fusion (TLIF) and anterior lumbar interbody fusion (ALIF) spacers on rod and adjacent disc stresses are also studied. Decreased rod stress is noticed on models when TLIF and ALIF spacers are implanted, with the percentage decrease depending on

various parameters. These results have the potential to provide surgeons with guidance as to when to implant an interbody spacer to reduce the risk of rod breakage.

Some disadvantages of an anterior surgical approach (necessary to implant an ALIF spacer) have been noticed, such as vascular injury. Therefore, the possibility of implanting an interbody device posteriorly with similar function to the ALIF (e.g. a TLIF) may be an option to prevent those disadvantages. The results show that a TLIF can yield similar results to an ALIF, in terms of reducing rod stress, when it is placed as anteriorly as possible in between the vertebrae. Parametric studies of novel posterior connector structures are performed to examine their impact on reducing rod stress, and the results show that adding a truss-type structure to the instrumentation can help to reduce the stresses induced in the fusion rods, particularly under torsional loading.

Finally, three different fusion levels are studied to compare the stress level on adjacent discs after fusion surgery. Surprisingly, the results show that the stress increase on adjacent discs due to fusion surgery is less than anticipated, suggesting that factors other than stress increase may be the cause of adjacent disc failure after fusion surgery.

Development of a Computationally Efficient Finite Element Model of the Human Spine for the Purpose of Conducting Parametric Studies of the Stresses Induced in the Spine and in Spinal Fusion Instrumentation Hardware during Flexion, Torsion and Extension

by
Xiaoyang Wang

A dissertation submitted to the Graduate Faculty of
North Carolina State University
in partial fulfillment of the
requirements for the degree of
Doctor of Philosophy

Mechanical Engineering

Raleigh, North Carolina

2012

APPROVED BY:

Dr. Gregory Buckner	Dr. Carl Zorowski
Dr. Mansoor Haider	Dr. Andre Mazzoleni Chair of Advisory Committee

DEDICATION

Dedicated to

my parents

for their unconditional support.

BIOGRAPHY

Xiaoyang Wang was born in Hangzhou, Zhejiang province of China in 1985. He graduated from Hangzhou No.14 high school in 2004. Then he graduated with a Bachelor's degree in Mechanical Engineering from Zhejiang University in June, 2008, and graduated with a Master of Science degree in Mechanical Engineering from North Carolina State University in December, 2009. In December 2012, he will finish the requirements for his Ph.D. degree in Mechanical Engineering at North Carolina State University.

ACKNOWLEDGMENTS

First and foremost, I would like to thank my advisor, Dr. Andre Mazzoleni for his patient guidance, enthusiastic encouragement and generous support throughout my study and research at NC State University. Especially, he encouraged me to pursue new ideas throughout and took time to share his insight into the research.

I would like to thank my committee members, Dr. Gregory Buckner, Dr. Carl Zorowski, and Dr. Mansoor Haider for their generosity with their time and valuable suggestions in completing this thesis.

Finally, my gratitude goes to my parents for their endless love and continuous encouragement.

TABLE OF CONTENTS

LIST OF FIGURES

LIST OF TABLES

Chapter 1

Introduction

This dissertation presents several comprehensive parametric studies of the stresses induced in the spine and in spinal fusion instrumentation during flexion, torsion and extension, by making use of a validated, computationally efficient, finite element model of the human spine. Intervertebral disc degeneration is a serious medical condition which sometimes necessitates spinal fusion in order to relieve the patient's back pain and restore spinal function. Curvature of the spine, or scoliosis, is another medical condition which may require spinal fusion. A variety of spinal fusion instrumentation constructs are studied, as invtervertebral disc conditions are varied parametrically with respect to disc stiffness. The motivation for conducting these studies is to develop computational tools which can be used to help surgeons predict potential surgical outcomes prior to surgery, and hence provide some guidance as to what type of surgery may be most beneficial for a given patient, given the pre-operative condition of their spine. Although previous researchers have developed finite element models of the spine, most only cover a subsection of the spine, e.g. the lumbar spine, and the model presented here covers the entire thoracic-lumbar spine. Also, most finite element models of the spine which have been developed run very slowly, due to the fact that they are based on detailed CT scans of a particular patient, while the model presented here is based on simpler geometrical shapes which make it an order of magnitude faster to run. This computationally efficient model has proven to be just as accurate as more anatomically complicated models, as will be shown in Chapter 2, and its efficiency enables detailed parametric studies to be performed in a reasonable amount of time; these studies will be presented in later chapters.

The computationally efficient spine model developed and presented in this dissertation is used primarily to study the stresses induced in the rods used in spinal fusion surgeries, and the stresses induced in intervertebral discs adjacent to the fused section of the spine, under various loading conditions, while parametrically varying the stiffness values of selected intervetertebral discs. Calculating the stresses induced in the rods is important, because one of the primary causes of failed outcomes after surgery is breakage of the rods prior to completion of the spinal fusion process (which can take several months after surgery to be complete). Calculating the stresses in adjacent discs is important because some patients experience failure of adjacent discs after spinal fusion surgery, and it is an open question as to whether these failures were inevitable

due to a patient's propensity for disc failure, or whether the structural changes in the spine due to the fusion surgery cause the adjacent discs to fail. Surgeons currently have many different options available to them when performing spinal fusion surgeries, such as using interbody spacers, and different types of reinforcing structures placed between the fusion rods (e.g. cross-links or truss structures). In this dissertation, we show how the computationally efficient finite element model which has been developed can be used to evaluate the performance of a particular configuration of fusion hardware (instrumentation) in terms of the stresses induced in the hardware and in adjacent discs. Parametric studies are also conducted to give insight into which types of surgeries might be most effective for a particular patient, given the condition of the patient's intervertebral discs, namely the modulus of elasticity of the disc, i.e. its stiffness.

Further details of the computationally efficient model discussed above, and how it was validated, will be discussed in chapter 2. Chapter 2 also presents studies of how the use of interbody spacers can reduce the stresses experienced by the rods used in spinal fusion surgery, and gives guidance as to when it might be prudent to use these spacers. The studies also examine how the placement of the spacers (anterior vs. posterior) affects the stresses experienced by the rods.

The fact that using this model enables results to be generated quickly makes it possible to conduct detailed parametric studies, as will be presented in later chapters. The basic outline of the rest of this dissertation is outlined below.

Chapter 2 of this dissertation presents a computationally efficient model of the human spine, which is validated by correlating results generated using the model with experimental data and results obtained from other validated finite element models. Parametric studies are performed by varying the elastic properties of selected discs . Models with interbody devices (spacers placed as supporting structures between vertebrae) are created and used to investigate their ability to reduce rod stress and reduce the risk of rod breakage. Different interbody spacer locations are investigated, as well as the use of different types of interbody devices, in order to gain insight as to which types of spacers (and locations) are most able to reduce rod stress under flexion, extension, and torsion. To our knowledge, this work is first to study the effect of the disc

degeneration process on rod stress, and also presents the longest rod-screw spinal fusion construct that has been investigated via finite element studies of the spine.

Chapter 3 presents two novel posterior connector structures, and conducts parametric studies to investigate the effect of these structures on rod stress over a wide range of parametrically varied disc stiffness values.

Chapter 4 studies three different fusion levels to investigate the stress level on adjacent discs after fusion surgery, where the adjacent disc stresses in the fused spine are compared with a non-fused control case.

Finally, Chapter 5 summarizes the conclusions of this dissertation and its most important contributions.

Chapter 2

Development of Computationally Efficient Finite Element Model of the Human Spine for Instrumentation Studies

2.1 Introduction

In order to relieve patients' back pain caused by degenerative (e.g. collapsed) discs or scoliosis (excessive curvature of the spine), and to maintain proper spinal intervertebral spacing, surgeons often perform fusion surgeries on the lumbar and thoracic portions of the spine. Pedicle screws and rods are implanted as fusion instrumentation constructs to hold the spine in proper position and avoid degenerative or traumatic disorders [1, 2]. However, infectious and neurological complications and instrumentation failure have been reported. Studies show the occurrence of these breakage complications is at least 5% to 6 % [3, 4]. Non-union and vertebral structures collapse may occur due to the breakage of rods and screws implanted in the spine to assist the fusion process [5]. One method that has been used to try and increase spinal stability and reduce rod stress during the post-surgical fusion process is to implant interbody fusion devices between some of the vertebrae to be fused. Among various lumbar fusion technologies, the transforaminal lumbar interbody fusion (TLIF) (Figure 2.1) developed by Harms et al.[6] is reported as a modification of the posterior lumbar interbody fusion (PLIF) [7], and has been popular due to the fact that it is easier to implant. Clinical data indicates that the TLIF can provide equivalent performance to the PLIF as far as fusion rates and complication rates are concerned [6]; for this reason, this dissertation develops finite element models of the spine which incorporate TLIF spacers, but not PLIF spacers. In some cases, more stability is needed, leading surgeons to implant an anterior lumbar interbody fusion (ALIF) device [8]. Although the ALIF provides a more solid connection between the vertebrae, it is also much more difficult to implant, since it requires that an incision be made in the abdomen, in addition to making an incision along the spine. Due to its clinical relevance, this dissertation presents finite element models of the spine which incorporate the ALIF spacers [9-11]. Given the wide range of options available to a surgeon preparing to perform spinal surgeon on a patient, it would be highly valuable to have a finite element model of the human spine which could be used to evaluate the stresses experienced by the spine, and the fusion hardware implanted in the spine, for various fusion constructs. Such a finite element model has been developed, and is presented in this dissertation, as will be described in the next section. Rather than base the model on CT-

scans which incorporate very fine details particular to a specific patient, our model has been simplified to capture the essential geometric properties (taken from the biomechanics literature [12-14]), while still generating valid results; the validation of the model is presented in a following section.

In this simplified finite element model, parameters can be changed easily, and new results generated in just a few minutes, as opposed to the several hours of computer time required to generate results from a more complicated model. This reduced computation time makes it possible to conduct parametric studies in a reasonable amount of time. To our knowledge, this work is the first to conduct parametric studies of the stresses induced in spinal fusion hardware for different instrumentation configurations over a wide range of disc stiffness parameters.

In this chapter, a spine model from L1 (Lumbar) to S1 (Sacrum) is compared with both experimental and finite element analysis data (from other sources) to validate the accuracy of the model. Some parametric studies which involve spinal fusion hardware are then presented to illustrate the utility of the model.

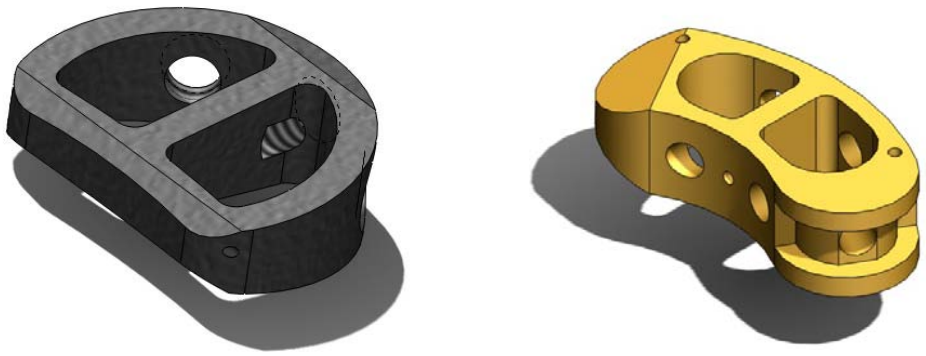

Figure 2.1. Interbody devices 3-dimensional models (ALIF (left) and TLIF (right))

2.2 Development of a computationally efficient finite element model of the spine

In the current literature, spine finite element analysis is mostly based on computed tomography (CT) scan images of individual human spines. The models generated from those CT scan images are full of very small and intricate geometries. In finite element software packages, smaller and finer meshing elements are required to represent these geometries, resulting in very long computational times to finish analyses.

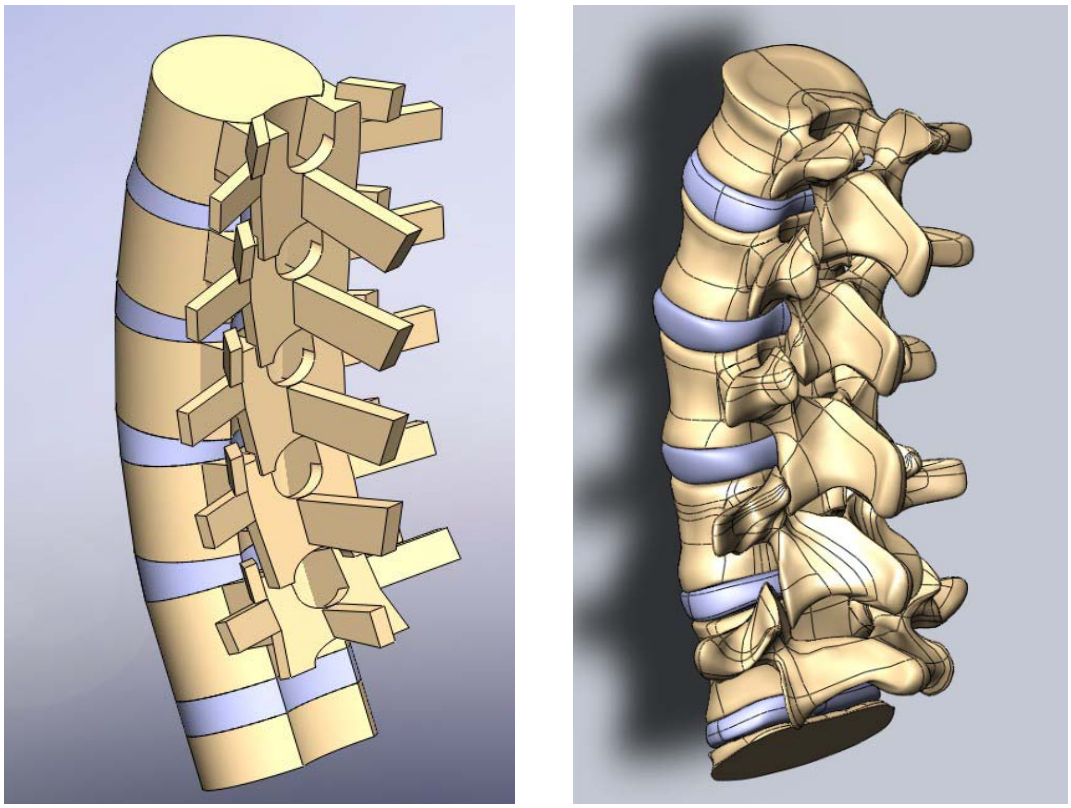

Figure 2.2. Computational efficent model (left) and detailed 3D model (right)

A 3D model based on one patient's CT scan is presented in Figure 2.2. With tiny and intricate geometries (mainly on facet joints), the computer run time for this model is over 24 hours. The main objective of our research is analyzing the stresses induced in the spine (mainly disc) and spinal instrumentation hardware. Therefore, the detailed geometries on facet joints are irrelevant to our study purposes and make the model computationally inefficient. In order to make the analysis computationally efficient, a 3D spine model based on geometrical details based on statistical anatomical dimensions [12-14] has been created (Figure 2.2). The most important spinal geometries (such as vertebra heights, vertebra widths, angles between vertebrae, disc heights, and etc) are strictly based on data from the literature. The main geometries of the spine are created as simple blocks and cylinders, which make the simplified model very easy to mesh and generate results in very short time (in some cases, an analysis can be run in as little as 10 minutes). Solidworks 2010 (Dassault Systèmes, Vélizy, France) is used to develop the 3D geometry. The solid model is then imported into a finite element analytical program (ABAQUS 6.10, Hibbitt, Karlsson and Sorenson, Inc., Providence, RI) to perform the analysis.

In our model, cortical bone is modeled by using thin shell elements [15]. 3D solid elements are applied to model the trabecular bone, posterior elements of the vertebrae, annulus fibrosus, and the nucleus pulposus of intervertebral discs. All seven ligaments are incorporated into the model as spring elements: anterior longitudinal, posterior longitudinal, intertransverse, ligamentum flavum, capsular, interspinous, and supraspinous ligaments [16-18]. 3D surface-to-surface contact is established to simulate the interaction between the facet joints surfaces.

2.2.1 Model validation

In order for a finite element model to generate useful results, the model must be validated by comparing predicted results with available experimental data, and with results generated by other validated finite element models. No published data is available for models of the spine which extend from T1 to the pelvis, but experimental data does exist for L1-S1 cadaver specimens. The available experimental data is taken from Yamamoto et al [19] on a model from L1 to the sacrum. Therefore, in order to validate our model with experimental data, an L1-S1 model is

created with the same lumbar geometry as the T1-pelvis model (shown in Figure 2.3). The annulus fibrosus in the intervertebral discs is modeled using two different approaches. In the first approach, the annulus fibrosus is assumed to follow an isotropic hyperelastic law, i.e. neo hookean method is used, where the coefficients are set as C_{10}=0.3448, D_1=0.3 [24]. The stress and strain curve of this hyperelastic definition is shown in Figure 2.4. In the second approach, the annulus fibrosus is modeled as a linear elastic material (Young;s modulus of 4 MPa) [23]. For both approaches, the nucleus pulposus is set as nearly incompressible as the Poisson's ratio is defined very close to 0.5 [16, 25, 26]. As discussed earlier, spinal ligaments are modeled as spring elements. The vertebrae are modeled using two different materials corresponding to whether or not the bone is cortical or trabecular. All the material and mechanical properties including Young's modulus, Poisson's ratio, and cross-sectional area are gathered from values reported in the biomechanics literature [16-18,25-28] (Table 2.1).

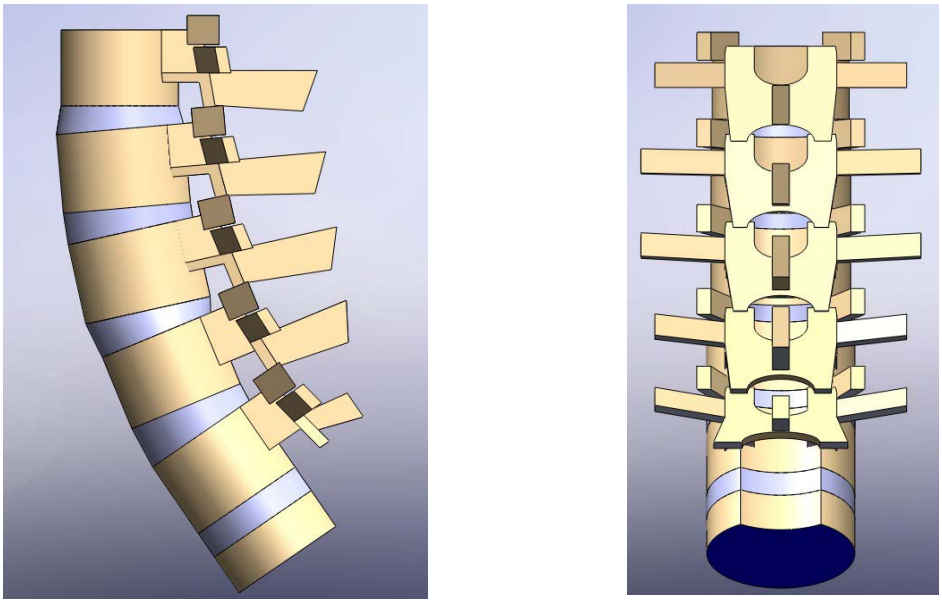

Figure 2.3. The side view (left) and posterior view (right) of intact L1-S1 spine model

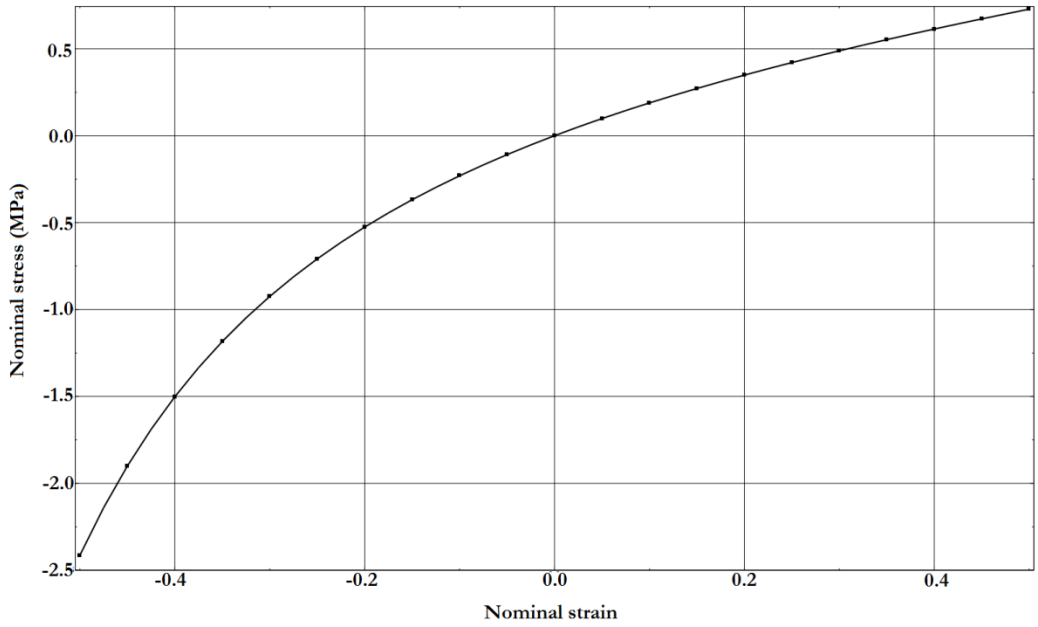

Figure 2.4. Stress and strain curve (hyperelastic definition)

Table 2.1. Material and mechanical properties used in L1-S1 model

Component	Element type	Young's Modulus (MPa)	Cross-section (mm^2)	Poisson's ratio
Cortical bone	Shell	12000	-	0.3
Trabecular bone	Solid	100	-	0.2
Annulus fibrosus	Solid	Parametric Study	-	0.3
Nucleus pulposus	Solid	1	-	0.499
Posterior elements	Solid	3500	-	0.25
Ligaments	Spring			
Anterior longitudinal		7.8(<12%) 20(>12%)	63.7	-
Posterior longitudinal		10(<11%) 20(>11%)	20.0	-
Intertransverse		10(<18%) 58.7(>18%)	1.8	-
Interspinous		10(<14%) 11.6(>14%)	40.0	-
Ligamentum flavum		15(<6.2%) 19.5(>6.2%)	40.0	-
Capsular		7.5(<25%) 32.9(>25%)	30.0	-
Supraspinous		8(<20%) 15(>20%)	30.0	-
Sacrum	Solid	12000	-	0.3

For this L1-S1 model, the nodes on the bottom surface of sacrum were constrained for all degrees-of-freedom. Coupled forces are imposed on the top surface of L1 to simulate the moments. In order to validate the model, the same loading conditions are used on this model as the ones in Yamamoto's experiment [19]. A 150 N preload is applied on the L1 vertebra, and 10 Nm flexion, 10 Nm extension, 10 Nm torsion, and 10 Nm lateral bending (Figure 2.5) moments are imposed (separately) at L1. The range of motion of all segments is recorded, and the results are compared with Yamamoto's data.

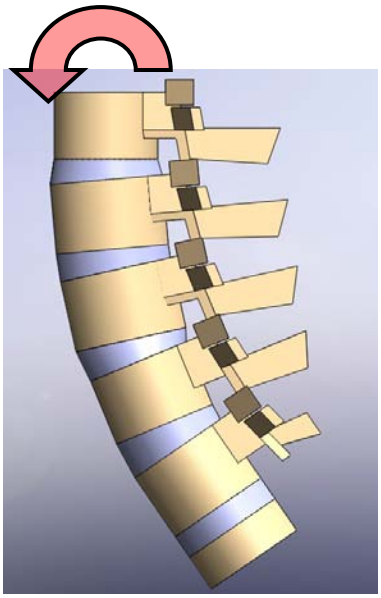

a). flexion

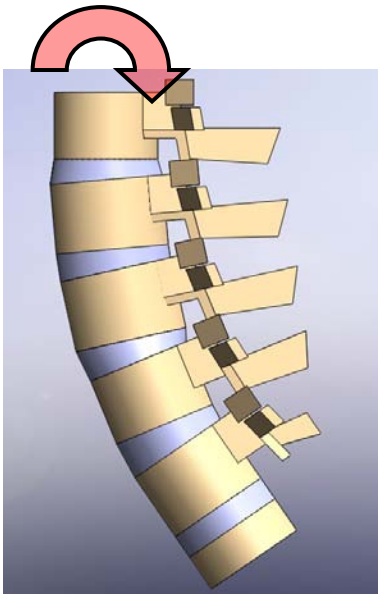

b). extension

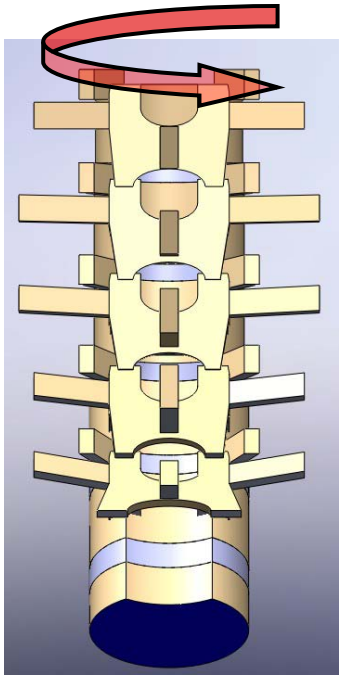

c). torsion

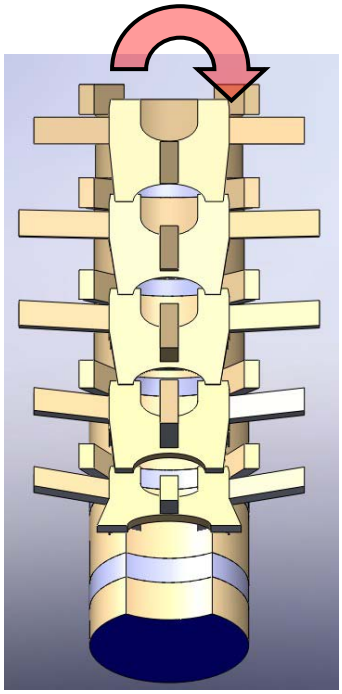

d). lateral bending

Figure 2.5. Spine motions

The range of motion comparison is listed in Table 2.2 and depicted in Figure 2.8. Both hyperelastic and elastic annulus fibrosus models are analyzed in this validation study. Yamamoto et al's [19] (Figure 2.6 shows the experiment setup) experimental data and C.S Chen et al's [16] finite element results (Figure 2.7 shows the three-dimensional model) are compared with our finite element analysis results. As can be found in Table 2.2, four datasets are compared for the four loadings, which include extension, flexion, torsion, and lateral bending. Both models (elastic and hyperelastic) in our study correlate with Yamamoto's experimental data. In extension and lateral bending loadings, our validation study has better correlation with Yamamoto's data than C.S. Chen's. To explain some of the differences between our validation study and Yamamoto's data, the different geometrical models in the two methods must be taken into account. In our validation study, spinal dimensions were gathered from the literature to represent a typical spinal geometry. Since the values found in the literature are obtained by averaging the values obtained from examining multiple patients, there is a natural spinal geometrical difference between our validation study and Yamamoto's study (which experimentally tests a single cadaver spine). Also, the material properties in our validation study were chosen by examining the spinal finite element analysis literature. The material properties in the cadaver spine used in Yamamoto's spine study may be different than the average values found in the literature. These possible differences in parameter values can explain the slight difference between the ranges of motion found for our validation study and those found in Yamaoto's experimental study.

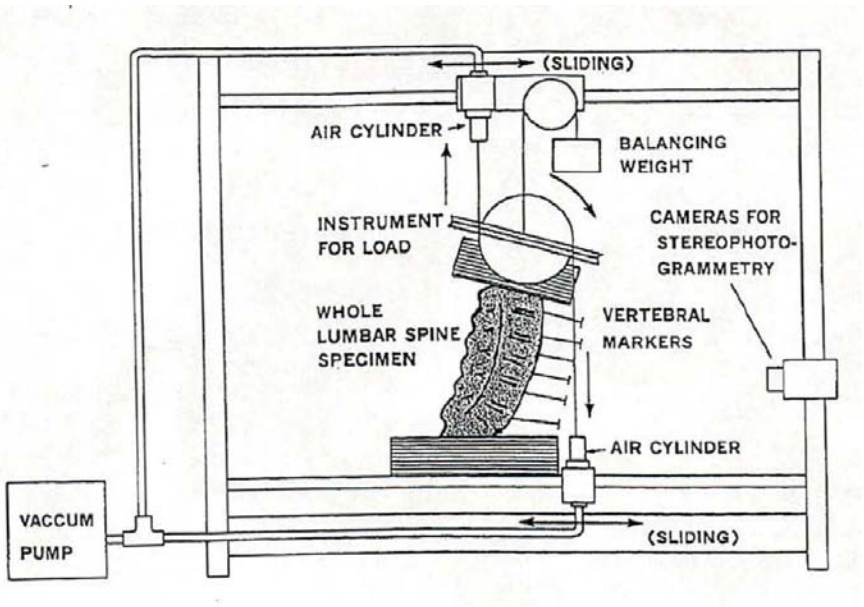

Figure 2.6. Yamamoto's experiment setup [19]

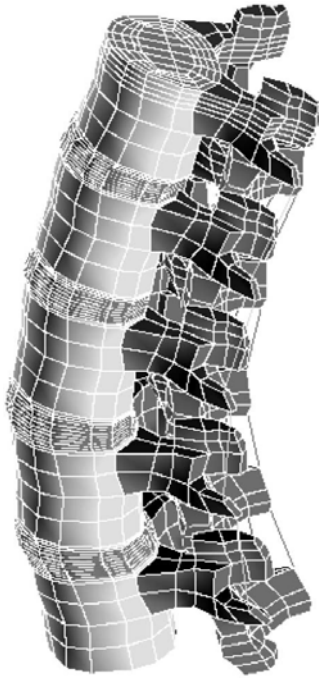

Figure 2.7. C.S Chen's lumbar spine finite element model [16]

Table 2.2. Comparison between the present study and the in vitro experimental study in the 3D angular motion (hyperelastic and elastic (in parenthesis))

	Extension			Flexion		
	Present Study	Yamamoto et al. (1989)	C.S. Chen et al. (2001)	Present Study	Yamamoto et al. (1989)	C.S. Chen et al. (2001)
L1-L2(degree)	3.81(3.65)	2.8	2.64	4.10(3.98)	4.2	3.05
L2-L3(degree)	3.72(4.12)	3.3	2.32	3.98(4.12)	5.4	3.28
L3-L4(degree)	3.61(4.07)	2.3	1.18	4.01(3.78)	6.1	3.58
L4-L5(degree)	3.70(3.23)	4.0	2.89	4.04(3.91)	7.1	4.49
	Torsion			Lateral Bending		
	Present study	Yamamoto et al. (1989)	C.S. Chen et al. (2001)	Present study	Yamamoto et al. (1989)	C.S. Chen et al. (2001)
L1-L2(degree)	1.81(1.72)	1.4	2.28	3.26(3.45)	3.5	2.85
L2-L3(degree)	1.85(1.73)	1.9	2.56	4.08(4.17)	5.0	3.31
L3-L4(degree)	1.90(1.85)	1.9	2.21	3.80(4.23)	4.3	3.33
L4-L5(degree)	1.80(1.74)	1.9	2.08	3.75(3.90)	4.0	2.08

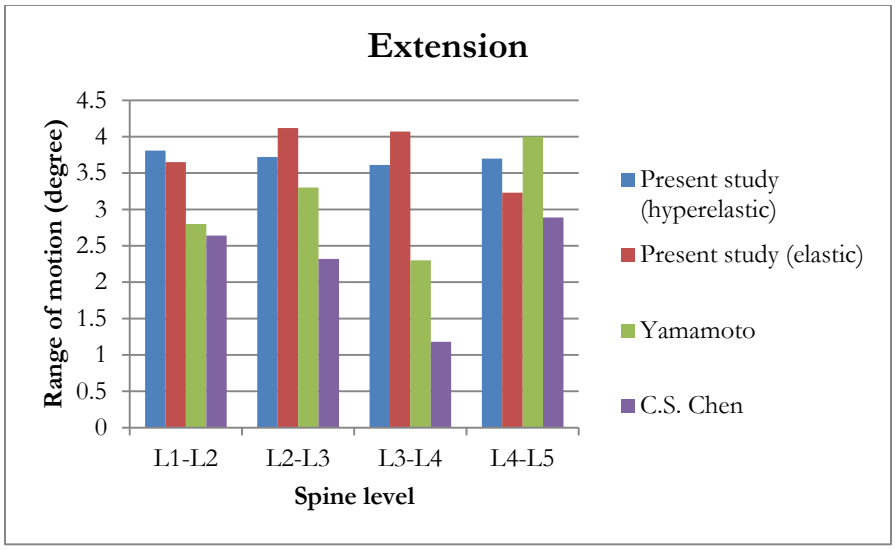

Figure 2.8. Comparison between the present study and the in vitro experimental study in the 3D angular motion under extension motion

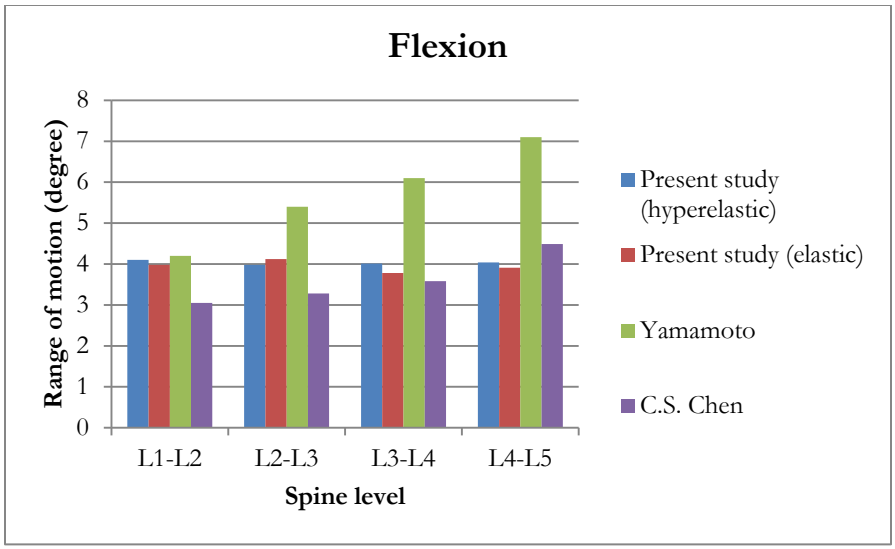

Figure 2.9. Comparison between the present study and the in vitro experimental study in the 3D angular motion under flexion motion

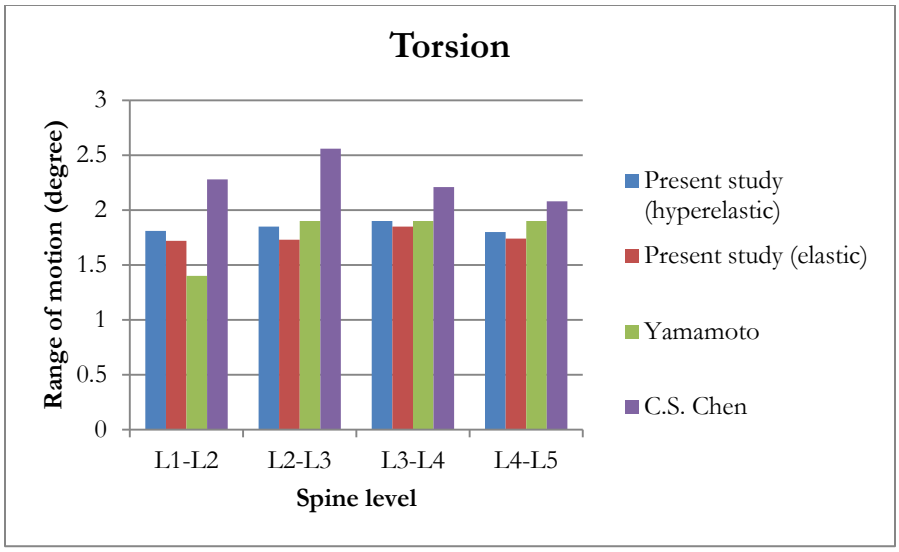

Figure 2.10. Comparison between the present study and the in vitro experimental study in the 3D angular motion under torsion motion

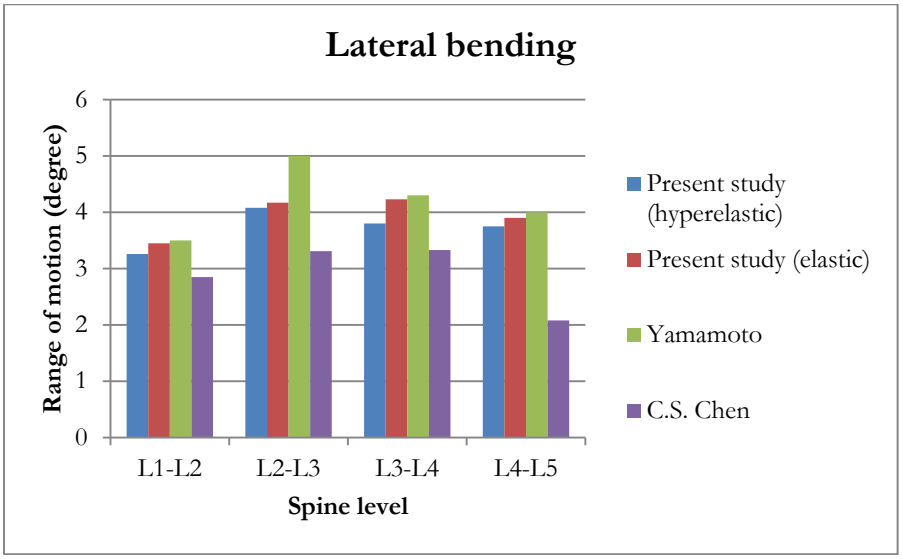

Figure 2.11. Comparison between the present study and the in vitro experimental study in the 3D angular motion under lateral bending motion

The range of motion comparison is also presented in Figure 2.8-2.11 under all four loading motions (extension, flexion, torsion and lateral bending). The good correlation between our finite element analysis and Yamamoto's experimental data gives us confidence that our finite element model will be able to represent and analyze spinal responses effectively under various loading scenarios. Note that although the model presented extends from T1 to the sacrum, only the L1-S1 portion was validated with experimental data, since no experimental data is available for T1-L1.

2.3 Some parametric studies using the model

2.3.1 Parametric study of stresses induced in the spine and in associated spinal fusion hardware, as intervertebral disc conditions are varied parametrically with respect to stiffness

A 3D spine model from T1 to the pelvis is used in this study to examine the effects of spinal fusion regarding stresses induced in the spine and in associated spinal fusion hardware, as intervertebral disc conditions are varied parametrically with respect to stiffness. The rod-screw construct fusion in this model starts from T2 and proceeds all the way down to iliac wing. For this parametric study, the thoracic spine from T1 down to T10 is modeled as one rigid solid part to simulate its natural attachment to the human rib cage. In TLIF implant models, in accordance with surgical procedures, one side of the facet joint is removed to allow for TLIF penetration [6]. Therefore, one side of the facet joint's contact definition is removed in these models. Based on standard surgical practices, the TLIF is placed as anterior as possible between the vertebrae. The

finite element model presented in Figure 2.9 is developed with 80,634 nodes and 291,034 elements. A variety of spinal fusion instrumentation constructs are studied. The ALIFs are placed at the center between vertebrae, and the TLIFs are located as anteriorly as possible.

Interbody devices are commonly used to strengthen the spine and relieve patients' back pain. In order to further support the spine, surgeons sometime implant a second interbody device into the lumbar spine to provide it with more spinal rigidity. In this study, finite element analysis is used to show its potential to provide surgeons with guidance as to when to implant one or two interbody devices to reduce the risk of rod breakage.

All nodes on the bottom of the pelvis are fixed in all directions. The annulus fibrosus in the intervertebral discs is modeled as linear elastic material in this work. Interbody devices (TLIF and ALIF) are made out of poly ether ether ketone (PEEK) [29]. The other material properties are the same as the ones used in L1-S1 validation model. All material properties information for this T1-Pelvis model is listed in Table 2.3.

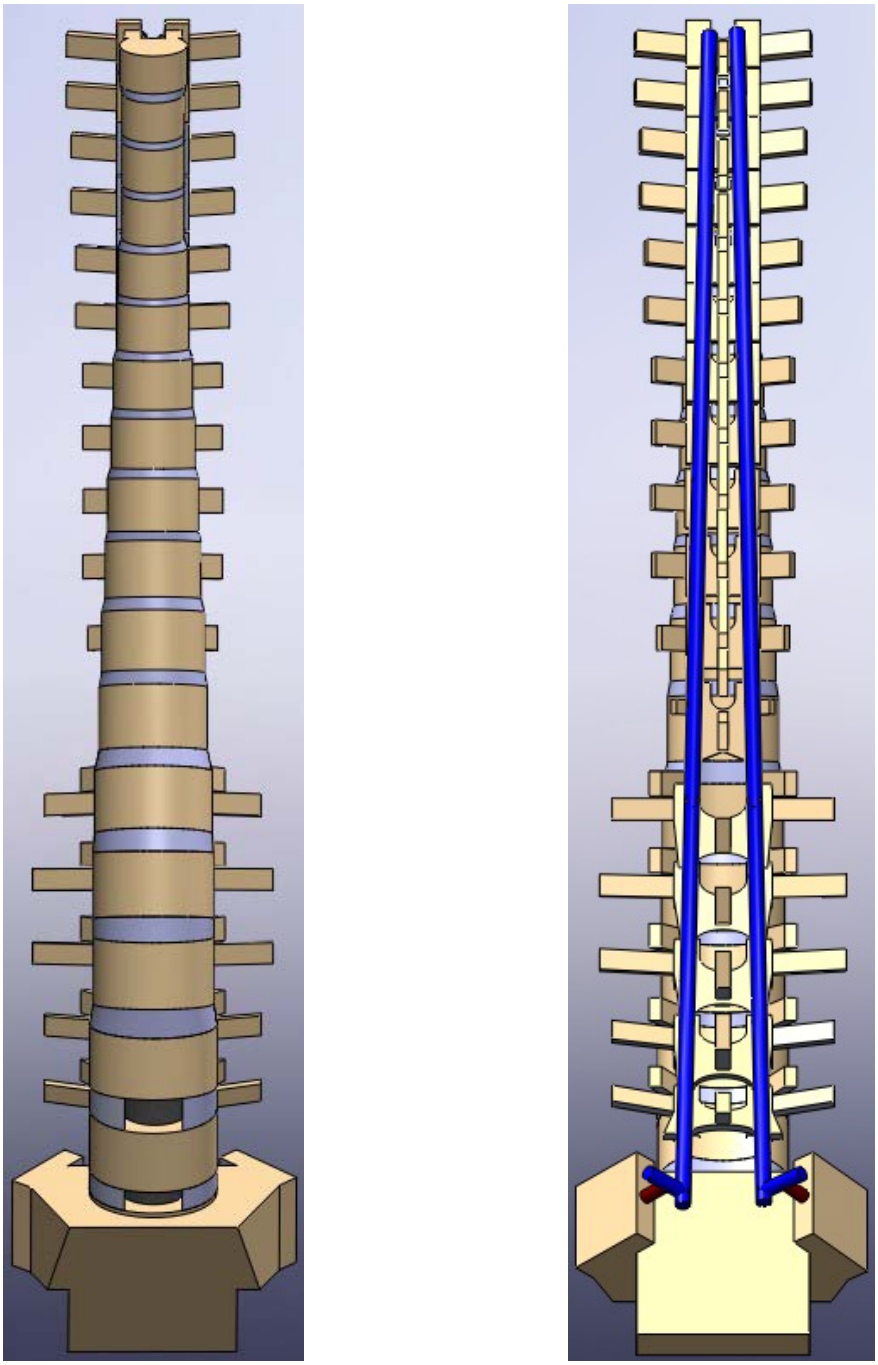

Figure 2.12. The anterior view (left) and posterior view (right) of T1-Pelvis spine model with 2 ALIFs implanted

Table 2.3. Material and mechanical properties in T1-Pelvis model

Component	Element type	Young's Modulus (MPa)	Cross-section (mm^2)	Poisson's ratio
Cortical bone	Shell	12000	-	0.3
Trabecular bone	Solid	100	-	0.2
Annulus fibrosus	Solid	Parametric Study	-	0.3
Posterior elements	Solid	3500	-	0.25
Ligaments	Spring			
Anterior longitudinal		7.8(<12%) 20(>12%)	63.7	-
Posterior longitudinal		10(<11%) 20(>11%)	20.0	-
Intertransverse		10(<18%) 58.7(>18%)	1.8	-
Interspinous		10(<14%) 11.6(>14%)	40.0	-
Ligamentum flavum		15(<6.2%) 19.5(>6.2%)	40.0	-
Capsular		7.5(<25%) 32.9(>25%)	30.0	-
Supraspinous		8(<20%) 15(>20%)	30.0	-
Sacrum	Solid	12000	-	0.3
Fusion rods (Cobalt)	Solid	209000	-	0.31
Fusion screws (Titanium)	Solid	116000	-	0.32
Interbody device (PEEK)	Solid	3800	-	0.3

According to standard surgical practice, a TLIF cannot be implanted on the spinal level below the level where there is already an ALIF implanted. Therefore, there are a total of 8 models that need to be created to include all the possible interbody device combinations at the L4-L5 and

L5-S1 levels (Table 2.4).

A 40 N concentrated force is applied at the center of the spine model in the posterior and anterior directions to simulate extension and flexion motions, respectively. A 10 Nm moment is imposed on the spine to create the torsional motion.

Table 2.4. Models with different spinal interbody devices

Level \ Model No	1	2	3	4	5	6	7	8
L4-L5 implant	Disc	Disc	ALIF	ALIF	TLIF	TLIF	TLIF	Disc
L5-S1 implant	ALIF	TLIF	Disc	ALIF	Disc	TLIF	ALIF	Disc

Figure 2.13-2.15 show the maximum rod stress on models with no spacers implanted and with spacers implanted in the L4-L5 spacer model models during extension, flexion and torsion motions, as the L4-L5 and L5-A1 disc stiffness parameters are varied parametrically from 1 MPa to 3000 MPa; these values are chosen to reflect the range of stiffness values which have been observed in the human spine during cadaver studies, with the normal stiffness value of the human spine being 4 MPa [23]. For this study all of the discs above L4-L5 are assumed to be healthy, i.e. their disc stiffness values are set to 4 MPa. As the results show, during extension and flexion motions, larger maximum rod stresses occur when the disc properties are set as degeneratively soft (Young's modulus of 1 MPa). As mentioned above, in accordance with the biomechanics literature, a healthy disc is modeled as having a Young's modulus of 4 MPa [23]. Once disc properties are stiffer than 4 MPa, the maximum rod stress decreases and becomes lower than the stresses that occur when the discs are healthy; this is most likely due to the fact that more rigid discs take up more of the load than do healthier, softer discs. Disc properties can become stiffer during a process called self-fusion, in which the discs become more rigid; this

of course reduces flexibility in the spine, but does have the positive effect of reducing the maximum rod stress which occurs in the rods used in spinal fusion surgery. Of course, during the months after the implantation of spinal fusion rods, the discs which are now immobilized tend to self-fuse and become rigid, leading to less stress on the rods, but the initial disc stiffness is very important in that it affects the stresses induced in the rods in the months occurring immediately after surgery. Based on the results, we see that replacing a degeneratively soft L4-L5 disc with an interbody device can significantly reduce the maximum rod stress. However, if the discs are already stiffer prior to surgery due to a degenerative process, the implantation of an interbody device may not be necessary.

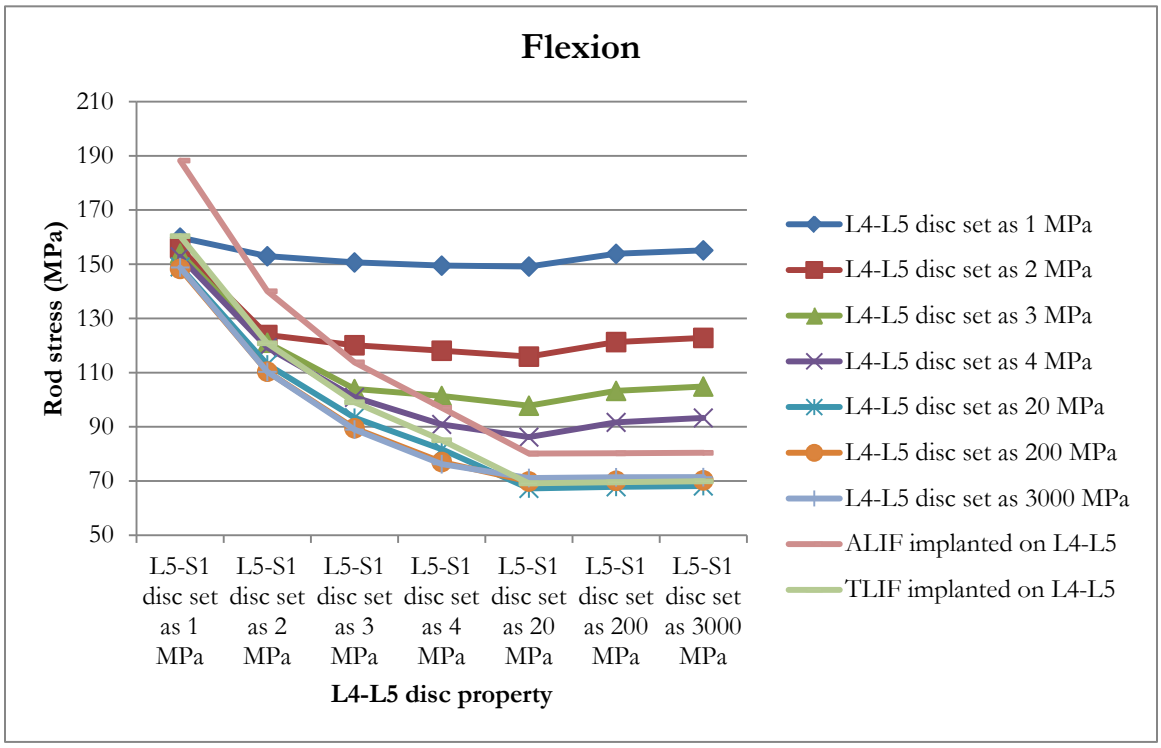

Figure 2.13. Maximum rod stress (MPa) on non-spacer model and L4-L5 spacer models during disc degeneration in flexion motion

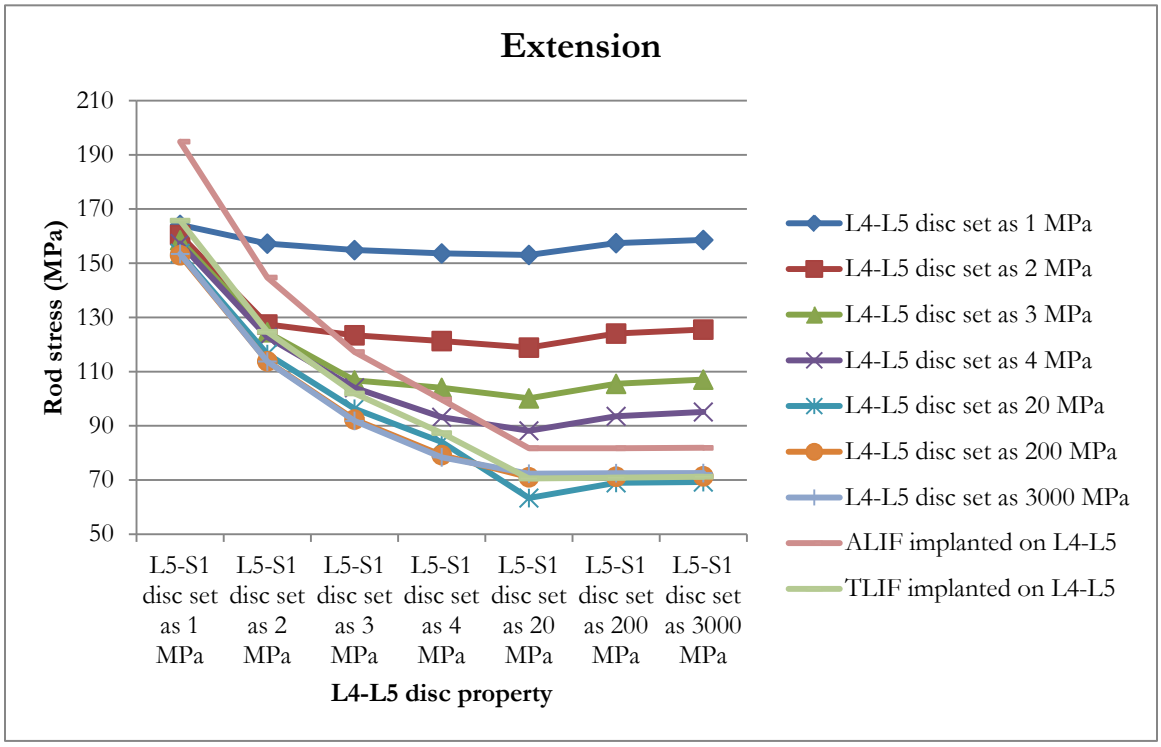

Figure 2.14. Maximum rod stress (MPa) on non-spacer model and L4-L5 spacer models during disc degeneration in extension motion

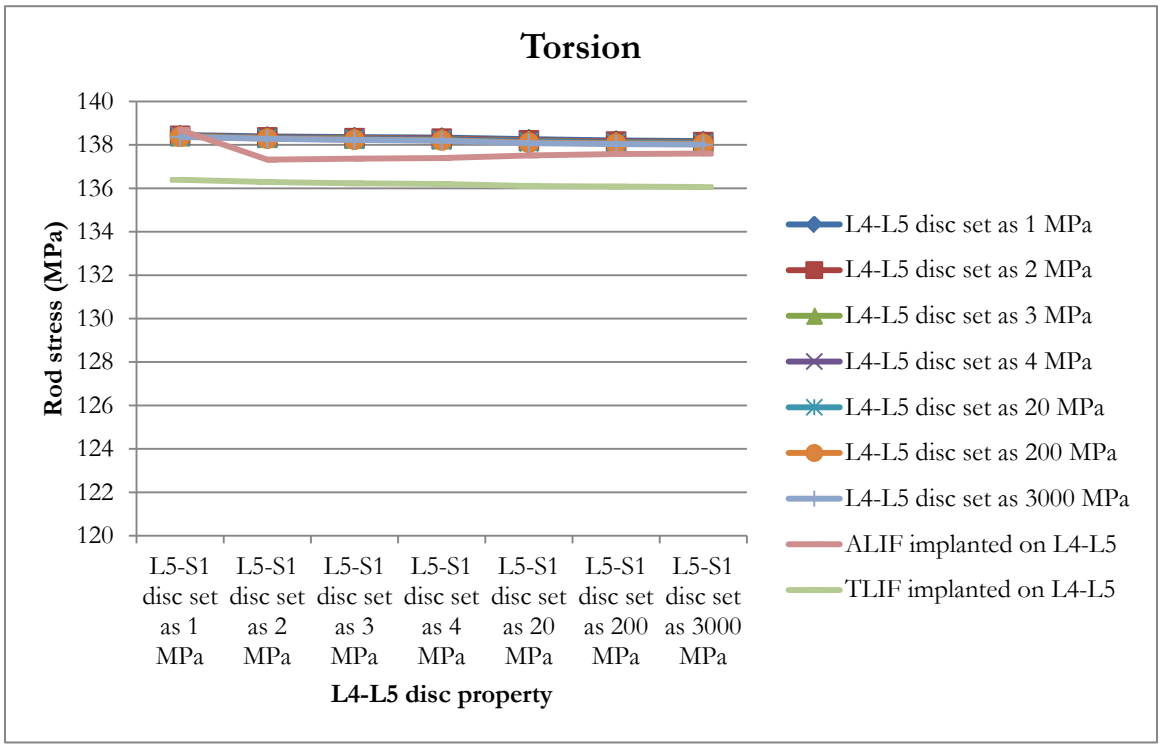

Figure 2.15. Maximum rod stress (MPa) on non-spacer model and L4-L5 spacer models during disc degeneration in torsion motion

Figure 2.13-2.15 also illustrate if both L4-L5 and L5-S1 discs are degeneratively soft (i.e. with a Young's modulus of 1 MPa), just replacing L4-L5 disc with an interbody device doesn't reduce the maximum rod stress during extension and flexion motions. In fact, in some cases adding an interbody device induces an even larger maximum rod stress. For example, in the model with an ALIF implanted on L4-L5 (yellow dot curve), when L5-S1 is degeneratively soft we have that in extension the maximum rod stress is 18.7% higher than the model where both discs are degeneratively soft. A similar situation also occurs during flexion motion.

Figure 2.16-2.18 depict the maximum rod stress on models with an ALIF implanted at the L4-L5 level, and the L5-S1 stiffness varied parametrically (including a case where an ALIF is also implanted at L5-S1, as discussed below), during extension, flexion, and torsion. The motivation for this study is to investigate when a second interbody device should be implanted to reduce the risk of rod breakage. As discussed previously, if the L5-S1 disc is degeneratively soft, an interbody device implanted on L4-L5 doesn't reduce the maximum rod stress. In surgical practice, a second interbody device is often implanted to further provide the spine with more rigidity. In this case, an ALIF is already placed between L4 and L5. According to surgical protocols, a TLIF normally wouldn't be implanted between spinal levels below ALIF implant. Therefore, one model with an additional ALIF implanted at the L5-S1level is created.

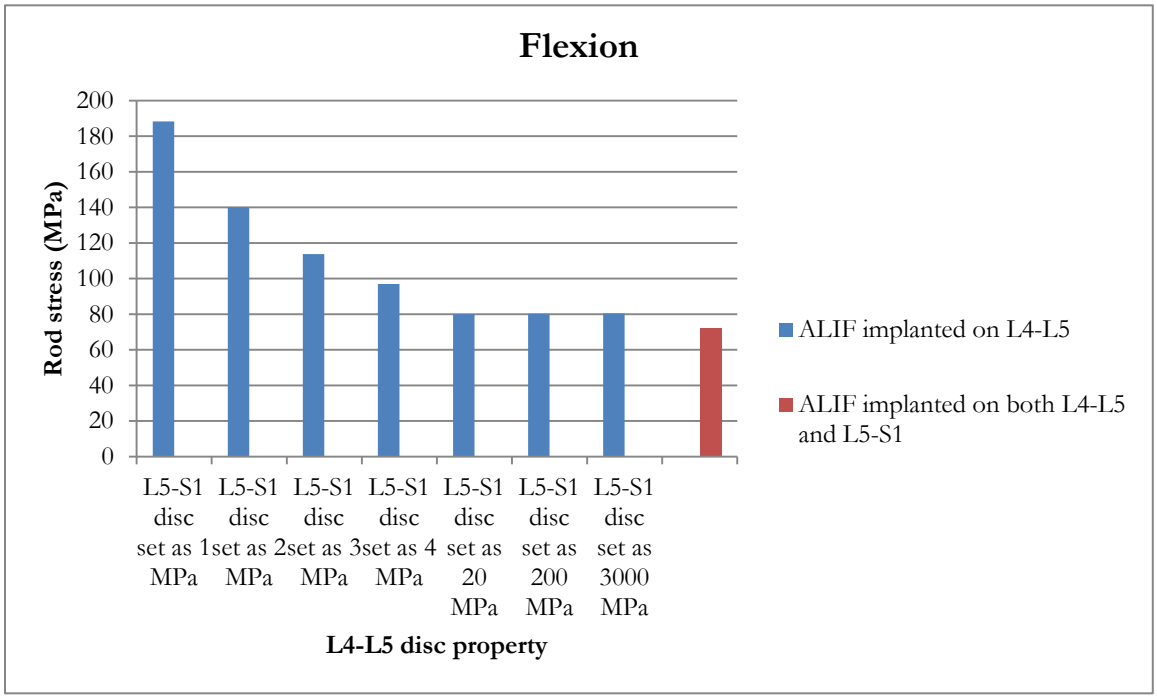

Figure 2.16. Maximum rod stress (MPa) on models with ALIF implanted on the L4-L5 level during disc degeneration in flexion motion

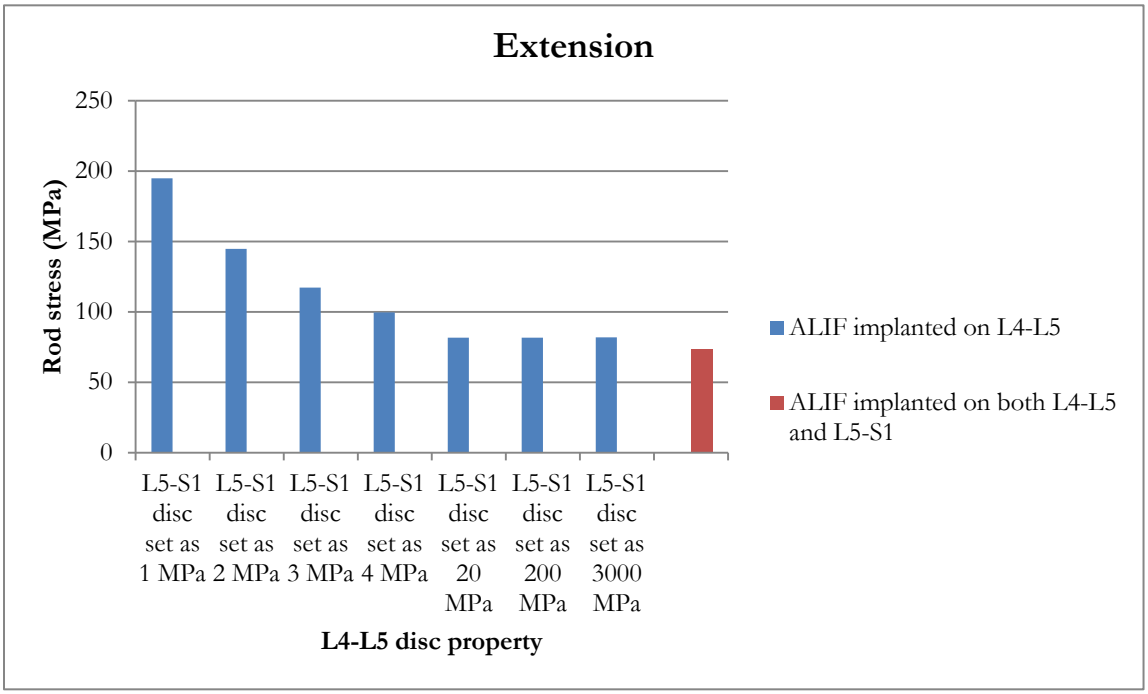

Figure 2.17. Maximum rod stress (MPa) on models with ALIF implanted on the L4-L5 level during disc degeneration in extension motion

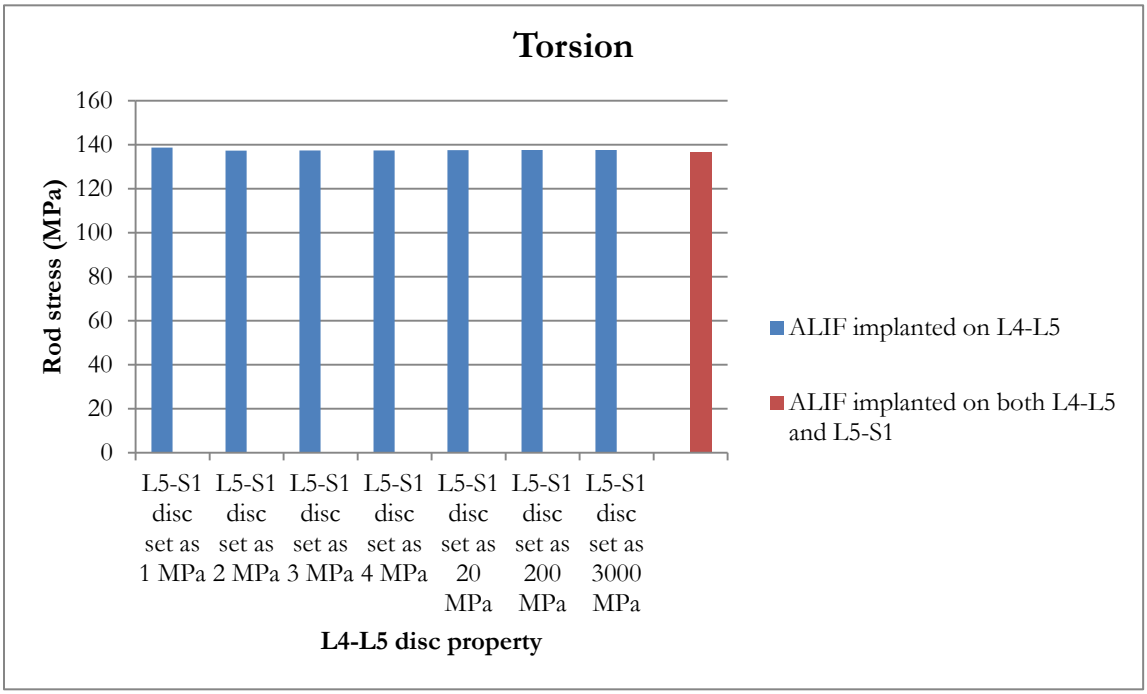

Figure 2.18. Maximum rod stress (MPa) on models with ALIF implanted on the L4-L5 level during disc degeneration in torsion motion

Von Mises stress of each model is tabulated to compare the maximum rod stress. For the model with an ALIF implanted on L4-L5 (blue bars), we see that the highest maximum rod stress occurs when the L5-S1 disc's Young's modulus is set as 1 MPa. For extension and flexion motions, the maximum rod stress decreases when the L5-S1 disc becomes stiffer, as expected. The maximum rod stress decreases 58.0% as the L5-S1 disc property is varied from 1 MPa to 3000 MPa under extension. The percentage difference is 57.3% under flexion.

During extension and flexion motions, a second ALIF spacer (red bars) can significantly reduce the maximum rod stress if the L5-S1 disc is degeneratively soft. If the L5-S1 disc is stiffer than normal (i.e. its Young's modulus is higher than 4 MPa), the second ALIF on L5-S1 has no significant impact on reducing the maximum rod stress. Similarily, there is no significant difference between the two models under torsional loading for all of the parameter values investigated.

Figure 2.19-2.21 demonstrate the maximum rod stress on models with a TLIF implanted on L4-L5 during disc degeneration in extension, flexion and torsion motions. The study assumes the surgical scenario of a patient who has a TLIF implanted between L4 and L5 disc already. In surgical practice, either an ALIF or a TLIF can be implanted at the L5-S1 disc level if necessary. To match standard surgical protocols, two models with either an ALIF or TLIF implanted at the L5-S1 level are modeled.

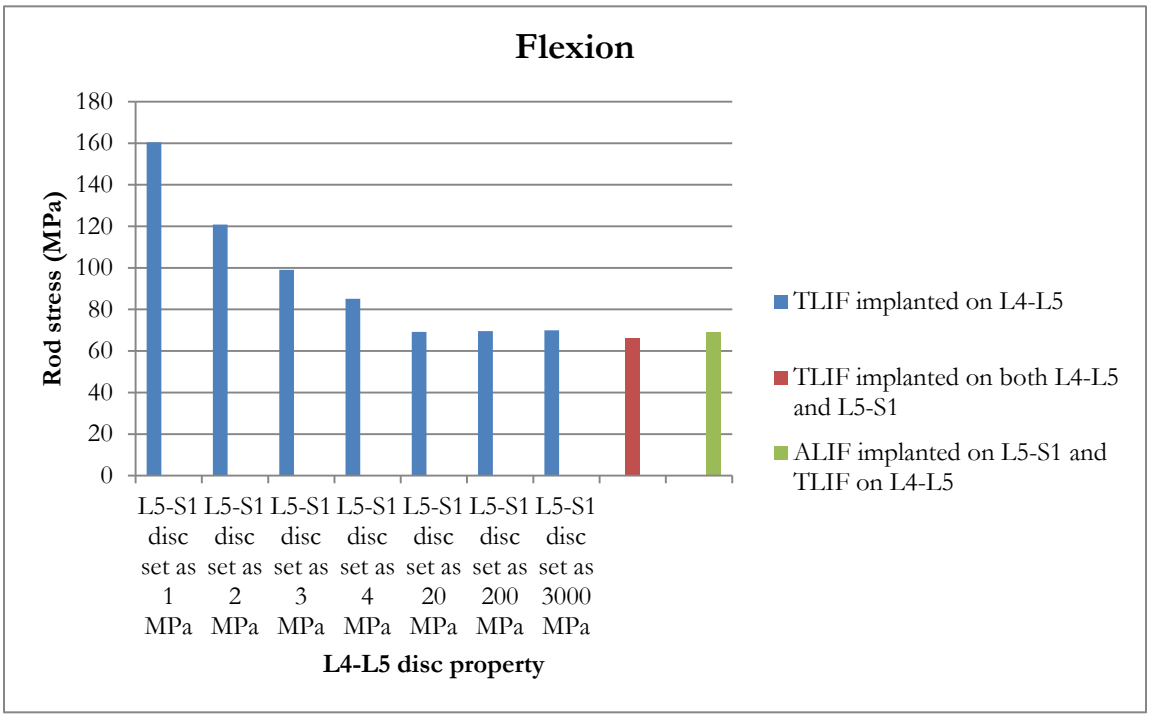

Figure 2.19. Maximum rod stress (MPa) on models with TLIF implanted on the L4-L5 level during disc degeneration in flexion motion

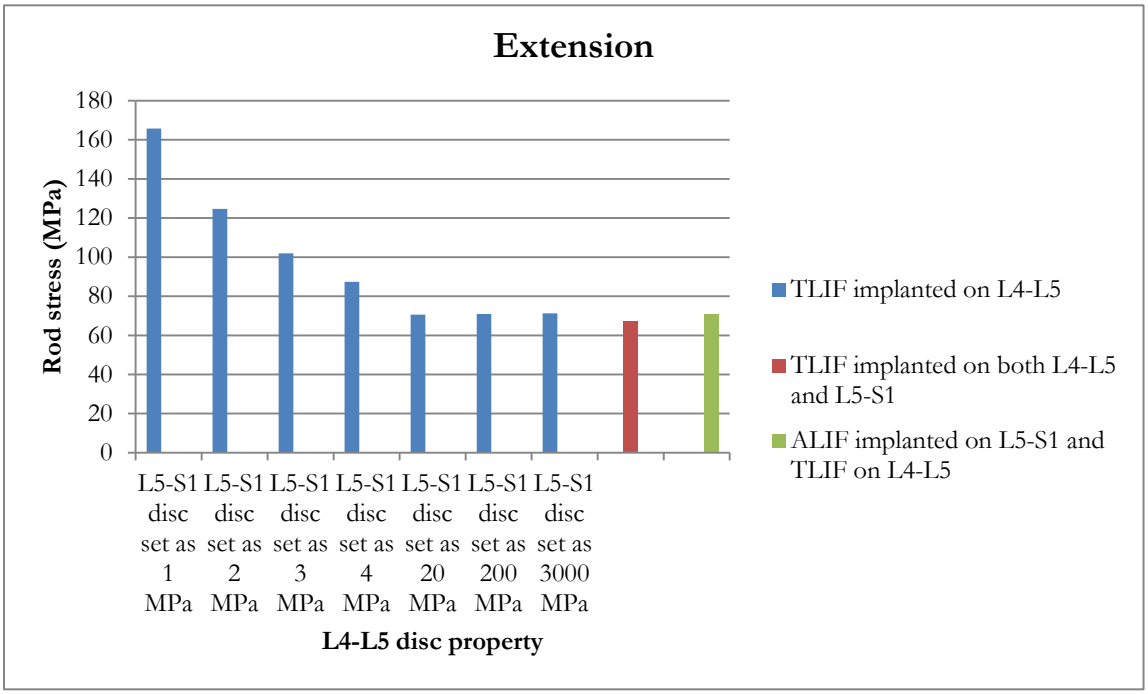

Figure 2.20. Maximum rod stress (MPa) on models with TLIF implanted on the L4-L5 level during disc degeneration in extension motion

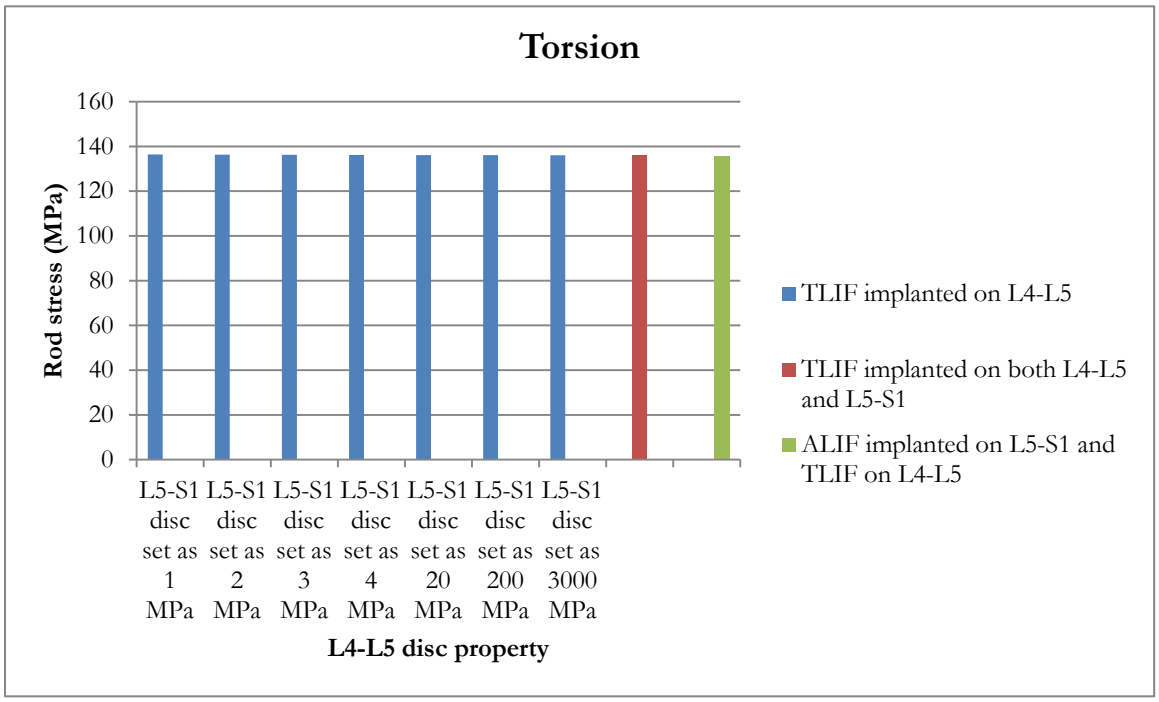

Figure 2.21. Maximum rod stress (MPa) on models with TLIF implanted on the L4-L5 level during disc degeneration in torsion motion

For the model with a TLIF implanted on L4-L5 (blue bars), the maximum rod stress decreases when the L5-S1 disc gets stiffer under extension and flexion motions. 57.0% and 56.4% percentage differences are noticed, respectively, for extension and flexion when the L5-S1 disc stiffness property is changed from 1 MPa to 3000 MPa.

As Figure 2.19-2.21 depict, either ALIF (green bars) or TLIF (red bars) can significantly reduce the maximum rod stress if L5-S1 disc is degeneratively soft. In this case, a second spacer can be critical to prevent the risk of rod breakage. Similarly as discussed earlier, no spacer would be necessary if the disc is already degeneratively stiff prior to surgery. During torsion motion, we see that all the models generate similar maximum rod stresses.

Note that there is no significant difference between an ALIF and TLIF at reducing the maximum rod stress. As the name implies, ALIF requires surgeons to operate from the anterior side of the patient. Currently, most of the spinal fusion is implanted on the posterior side, such as rod-screw constructs, so implanting an ALIF increases both the surgical difficulty and time, which are directly related to the surgical cost and also increase the possibility of post-surgical complications. Also, in some cases, vascular injuries have been seen to occur with the anterior surgical approach. A TLIF, however, can be implanted from the posterior side, where the rod-screws construct is located; since a TLIF serves a similar function in reducing the risk of rod breakage, a TLIF may be a better option than an ALIF for some cases in which the spacer is being implanted to replace a degeneratively soft disc for the purpose of reducing the stresses induced in the fusion rods.

Figure 2.22-2.24 present the maximum rod stresses for the non-spacer model and the L5-S1 spacer models during extension, flexion, and torsion motions. As discussed earlier, the interbody devices implanted on L4-L5 are already studied. In Figure 2.13, the simulation focuses on how the interbody devices influence on spinal performance when they are implanted on L5-S1.

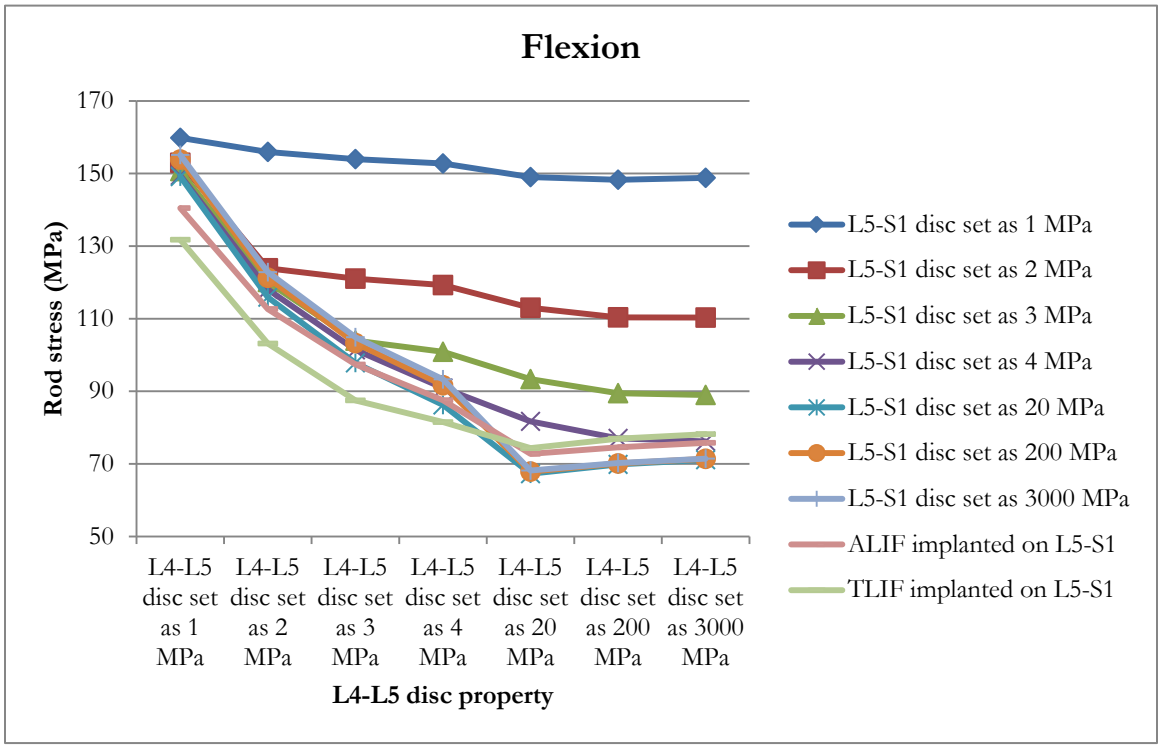

Figure 2.22. Maximum rod stress (MPa) on non-spacer model and L5-S1 spacer models during disc degeneration in flexion motion

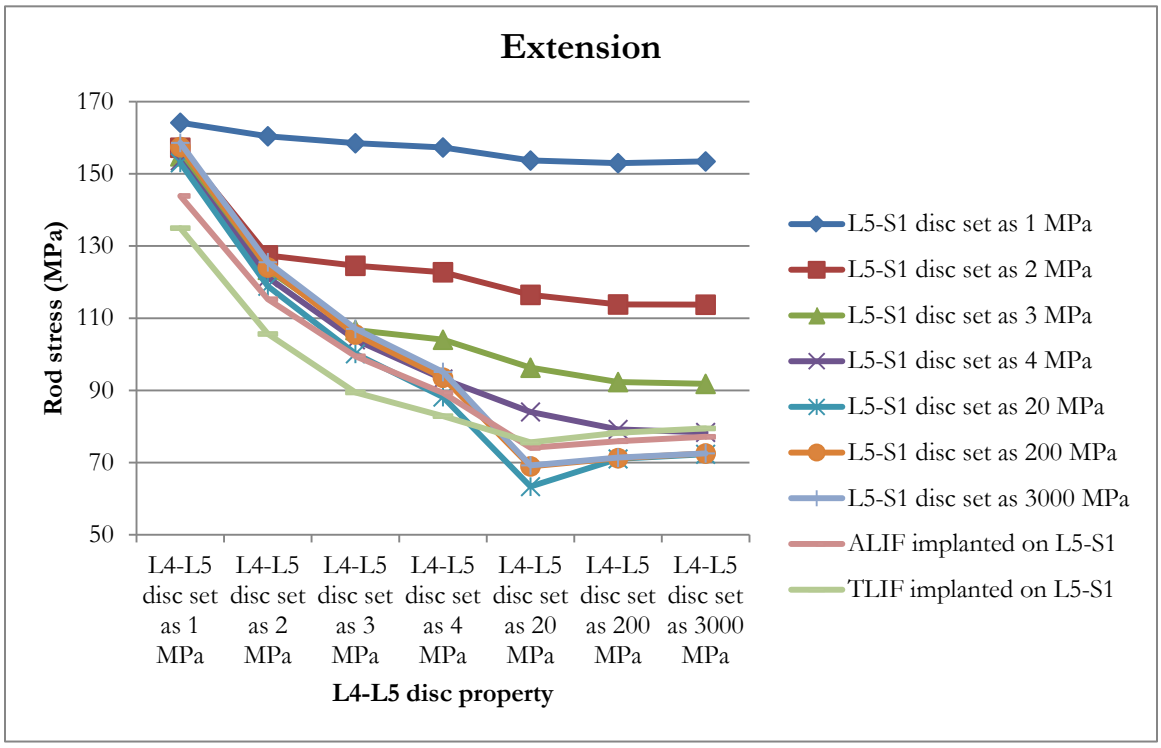

Figure 2.23. Maximum rod stress (MPa) on non-spacer model and L5-S1 spacer models during disc degeneration in extension motion

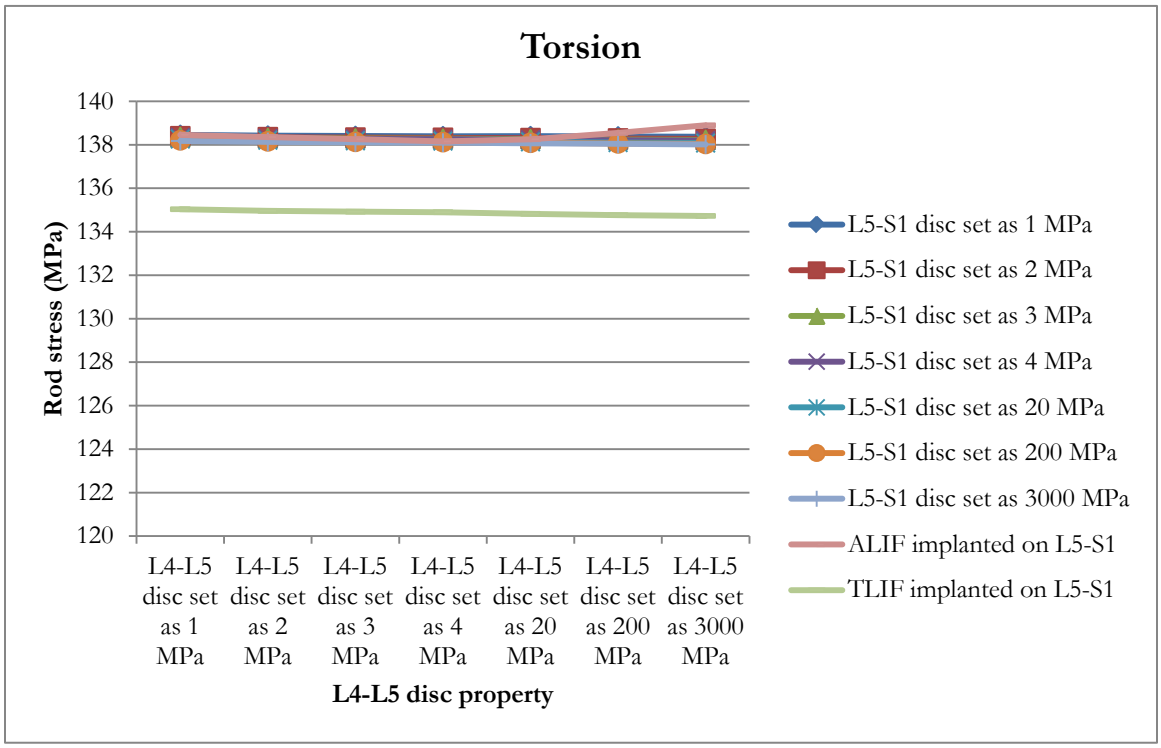

Figure 2.24. Maximum rod stress (MPa) on non-spacer model and L5-S1 spacer models during disc degeneration in torsion motion

During extension and flexion motions, the results show that an interbody device can significantly reduce the maximum rod stress if the L5-S1 disc is degeneratively soft. When the L5-S1 disc gets stiffer (i.e. its Young's modulus is higher than 4 MPa), neither an ALIF nor a TLIF affects a significant reduction of the maximum rod stress. However, it is also noticed that the maximum rod stress is still considerably high even with interbody device implanted when L4-L5 disc is degeneratively soft, which necessitates the requirement of a second interbody device. Under torsional loading, all the models generate similar maximum rod stress. Figure 2.25-2.27 show the maximum rod stress on models with an ALIF implanted on the L5-S1 level in extension, flexion, and torsion motions. In this simulation, an ALIF is already implanted to replace the L5-S1 disc. L4-L5 disc conditions are varied parametrically with respect to disc stiffness to study its influence on rod stresses. Since an ALIF is first placed at the bottom lumbar disc level (L5-S1), either ALIF or TLIF can be placed at L4-L5 based on surgical protocol. Therefore, two additional models are created.

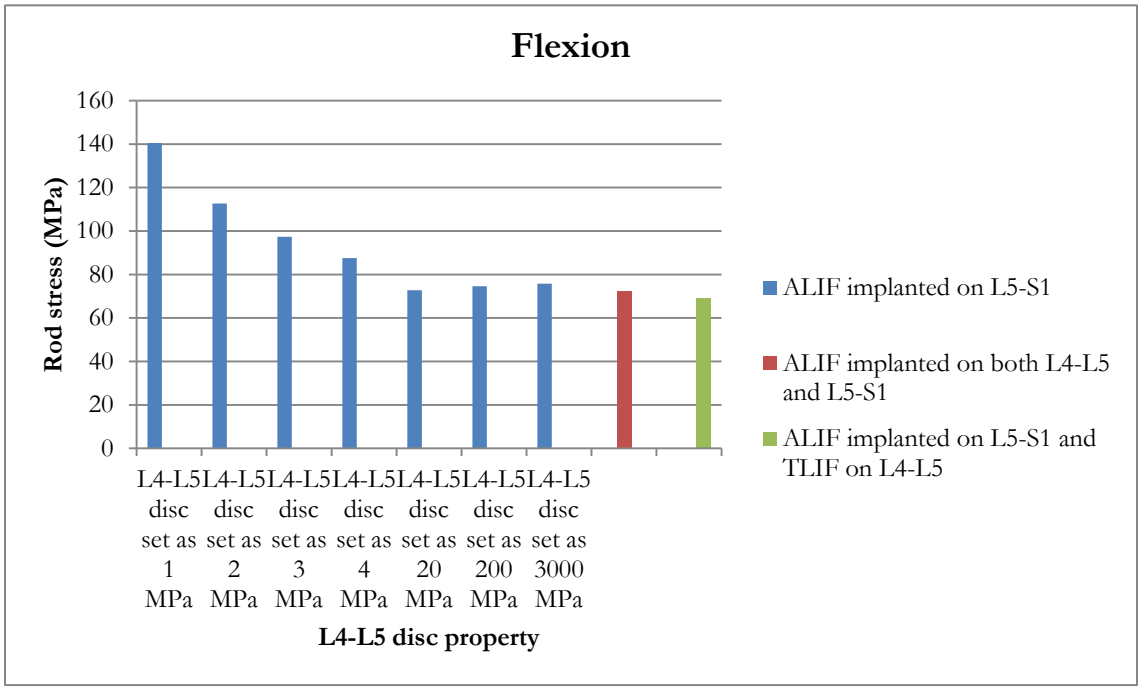

Figure 2.25. Maximum rod stress (MPa) on models with ALIF implanted on the L5-S1 level during disc degeneration in flexion motion

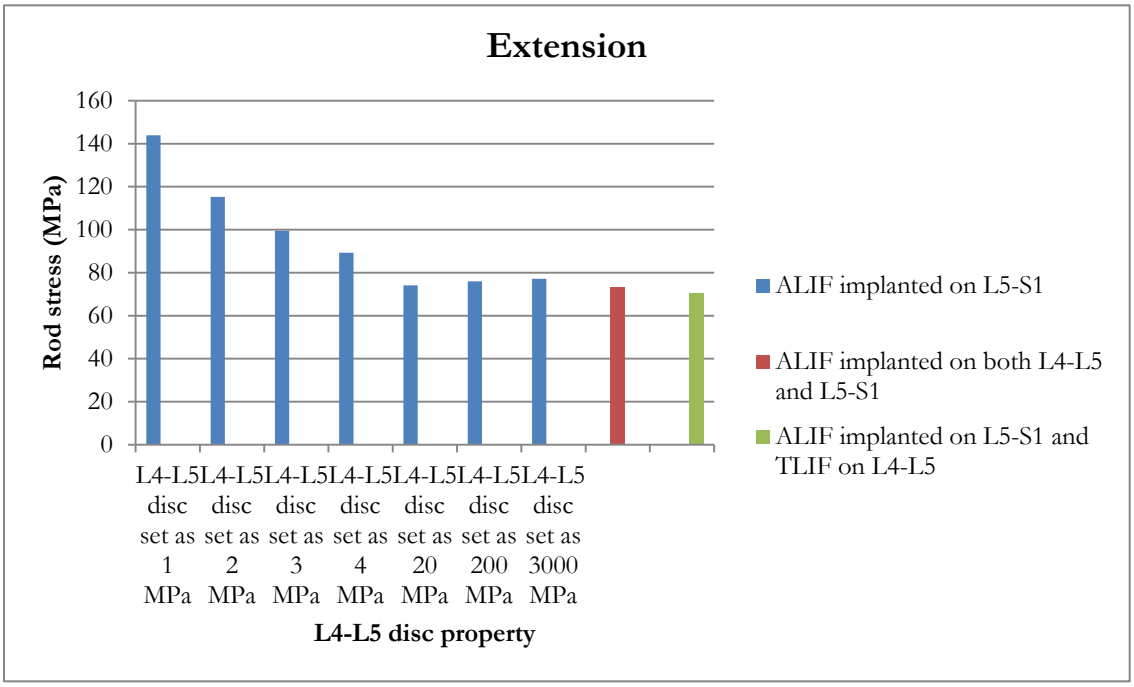

Figure 2.26. Maximum rod stress (MPa) on models with ALIF implanted on the L5-S1 level during disc degeneration in extension motion

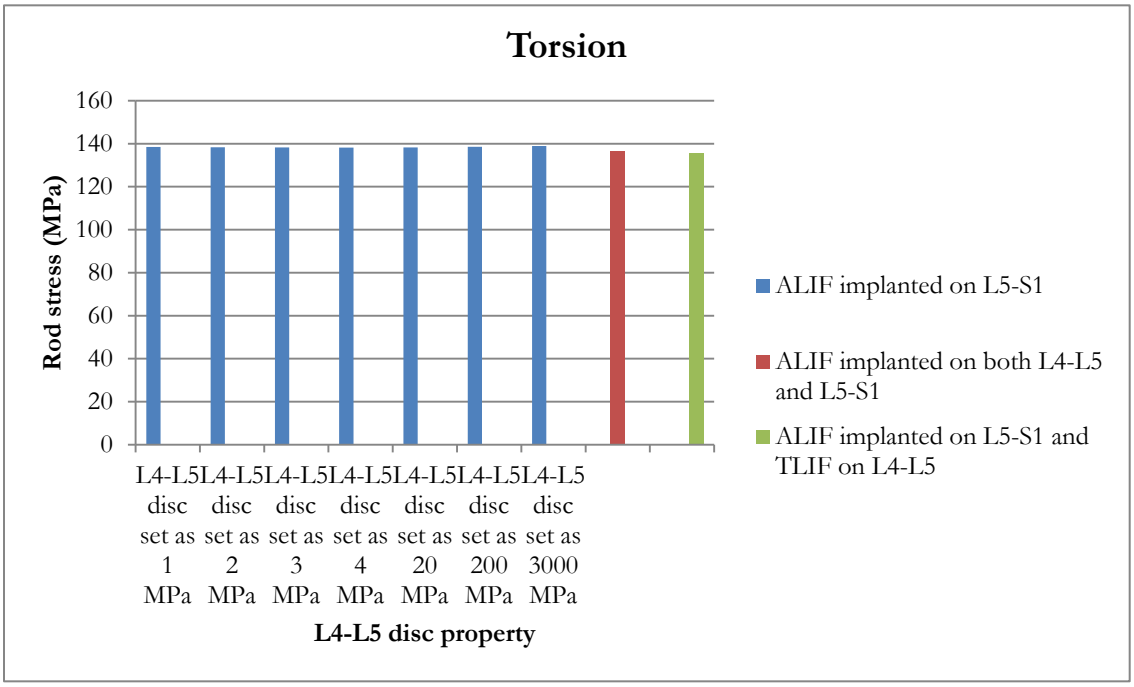

Figure 2.27. Maximum rod stress (MPa) on models with ALIF implanted on the L5-S1 level during disc degeneration in torsion motion

For the model with an ALIF implanted on L5-S1 (blue bars), the maximum rod stresses are reduced by 46.4% and 46.0% under extension and flexion respectively as the L4-L5 disc property is varied from 1 MPa to 3000 MPa. As discussed earlier, the maximum rod stress is still quite high when the L4-L5 disc is degeneratively soft. A second interbody device replacement on the L4-L5 level (red and green bars) can significantly reduce the maximum rod stress when L4-L5 disc is degeneratively soft. If the L4-L5 disc becomes stiffer (Young's modulus is higher 4 MPa), a second interbody device implant is not necessary. The maximum rod stress decreased automatically due to the higher spinal rigidity provided by stiffer discs. No significant difference is noticed between an ALIF and TLIF at reducing the maximum rod stress as they are used as the second interbody device.

Finally, in the last simulation, a TLIF is first placed at L5-S1 level. Similarly, two additional models with either ALIF or TLIF implanted on L5-S1 are modeled to investigate the necessity of a second interbody device. The maximum rod stress on models with a TLIF implanted on the L5-S1 level during disc degeneration in extension, flexion and torsion motions are presented in Figure 2.28-2.30.

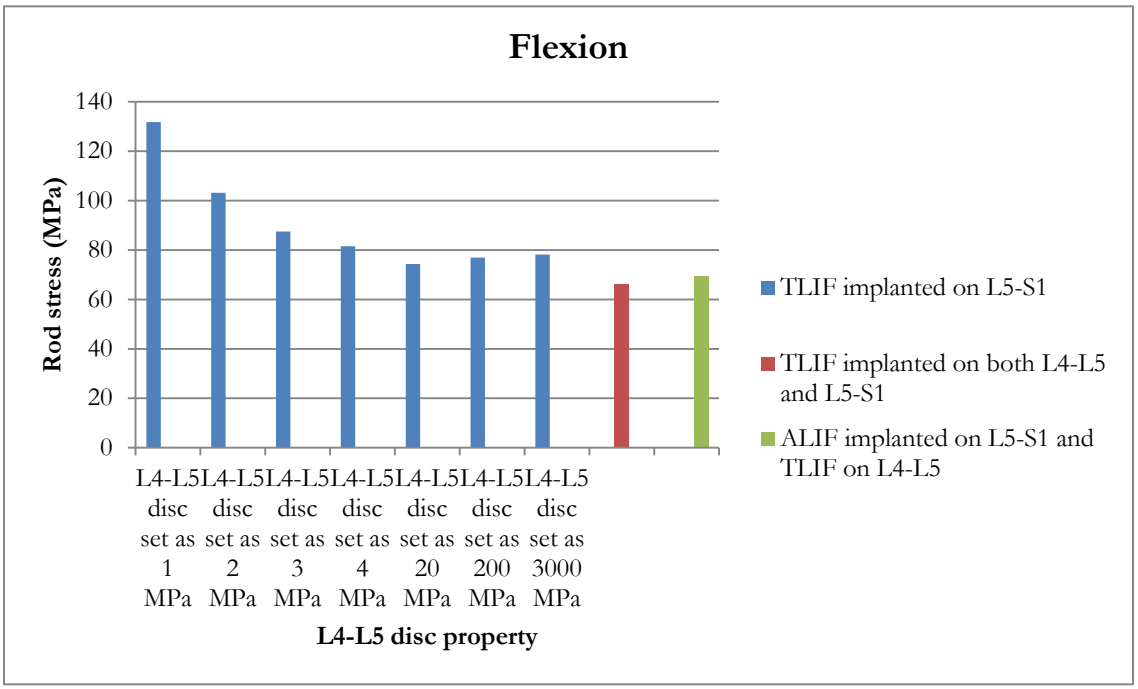

Figure 2.28. Maximum rod stress (MPa) on models with TLIF implanted on the L5-S1 level during disc degeneration in flexion motion

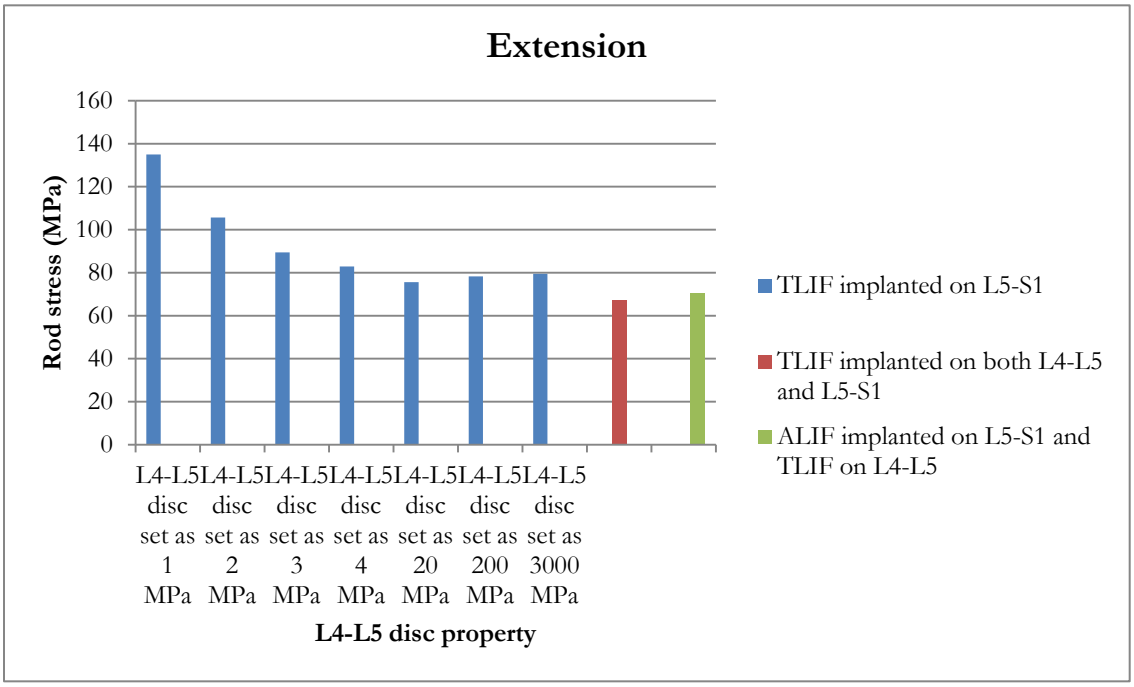

Figure 2.29. Maximum rod stress (MPa) on models with TLIF implanted on the L5-S1 level during disc degeneration in extension motion

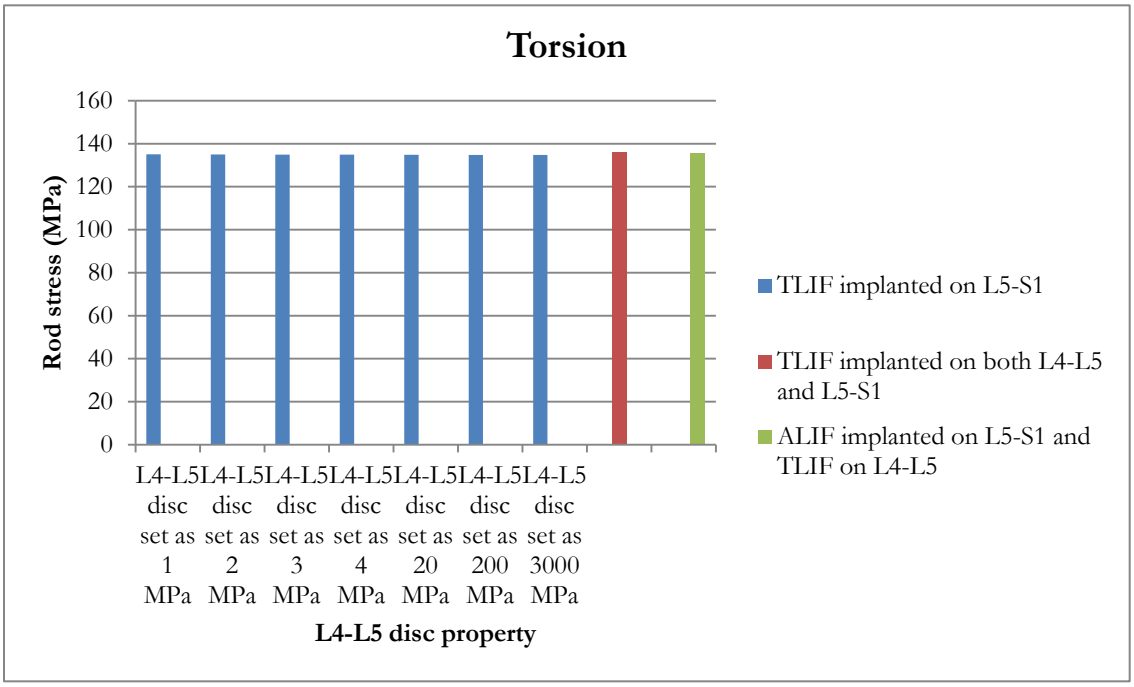

Figure 2.30. Maximum rod stress (MPa) on models with TLIF implanted on the L5-S1 level during disc degeneration in torsion motion

During extension and flexion motions, 41.1% and 40.7% percentage decreases are noticed in the maximum rod stresses respectively when the L4-L5 disc property is varied from 1 MPa to 3000 MPa. It is critical to use a second interbody device at the L4-L5 level if the disc is diagnosed as degeneratively soft, in terms of reducing the maximum rod stress.

Currently, surgeons implant either an ALIF or a TLIF as the second interbody device on the L4-L5 level in this situation. However, our results indicate the a TLIF can yield similar results to an ALIF, as far as reducing the maximum rod stress is concerned, when it is placed as anteriorly as possible between in vertebrae. As we mentioned before, considering the surgical difficulty and associated cost of implanting an ALIF, a TLIF should be considered as a simpler alternative to an ALIF when replacing a degeneratively soft disc, if the primary reason for implanting a spacer is to reduce rod stress.

2.3.2 Interbody device location and type selection study

In this section, a revision surgery case is studied. The case concerns a situation where the patient's spine is already fused with rod-screw construct from L5-S1 and T12-L4. The original fusion was intended to extend from T12 to the sacrum, but failure occurred to rod breakage, necessitating a revision surgery. For the revision surgery, in addition to replacing the rods, an interbody spacer was placed at the L4-L5 level (Figure 2.31). This study compares the maximum stresses induced in the fixation rods (during a 90 degree torso bend) for both a TLIF and an ALIF, implanted at L4-L5, and also examines how the location of the TLIF (varies from full anterior to full posterior) affects the maximum stresses on the rods. A 40 N concentrated force was applied at the center of the thoracic lumbar to simulate a 90 degree torso bend.

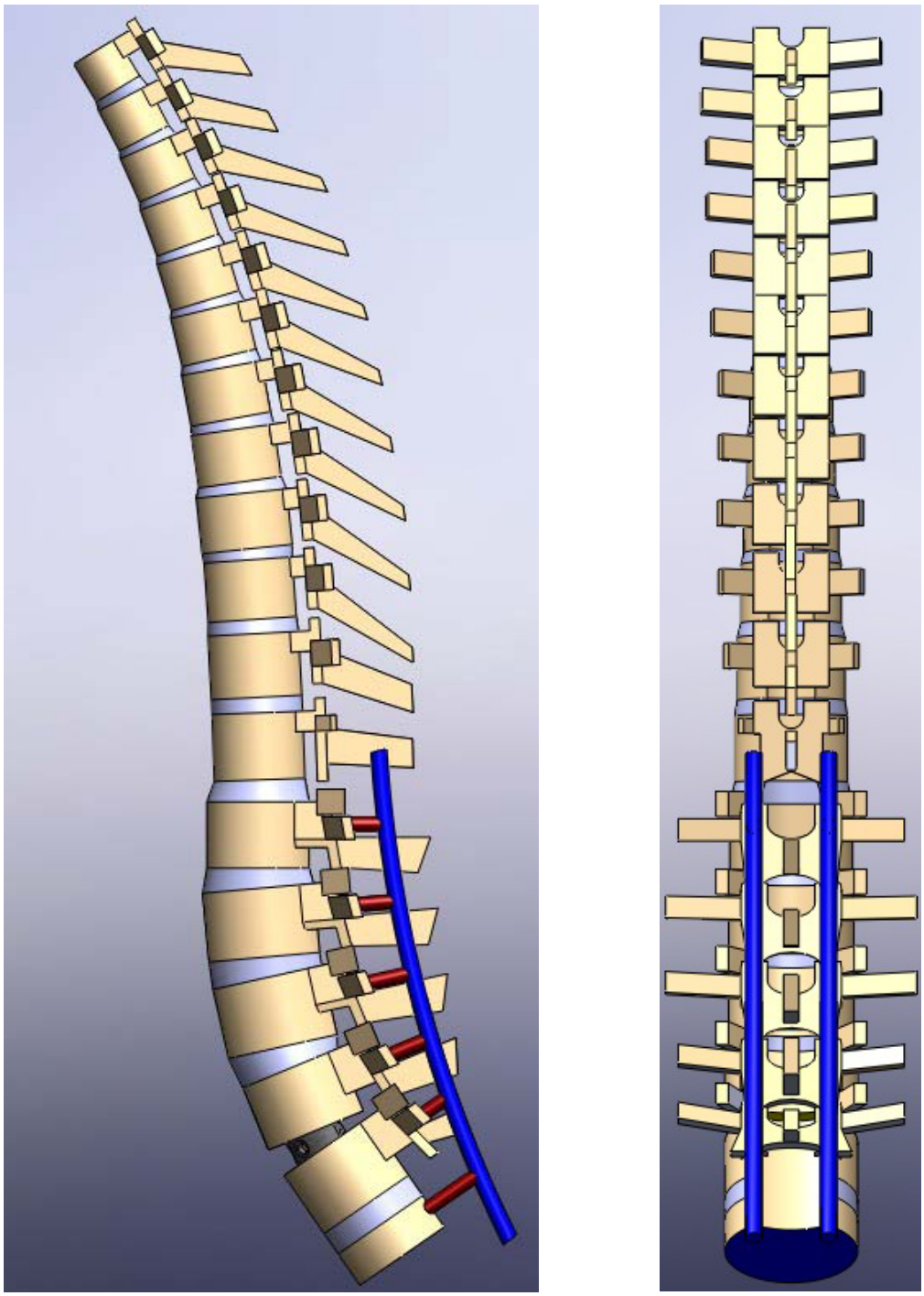

Figure 2.31. The side view (left) and posterior view (right) of instrumented T1-S1 spine model

In order to investigate how the TLIF location effects on rod stress, six different locations (Figure 2.32) are modeled with the TLIF implanted on L4-L5, from fully anterior (case 1) to fully posterior (case 6), in 5.4 mm increments. Due to surgical practice and the size of the ALIF, only one case for ALIF placement is considered, where it is assumed to be placed at the center of the space between the L4 and L5 vertebrae.

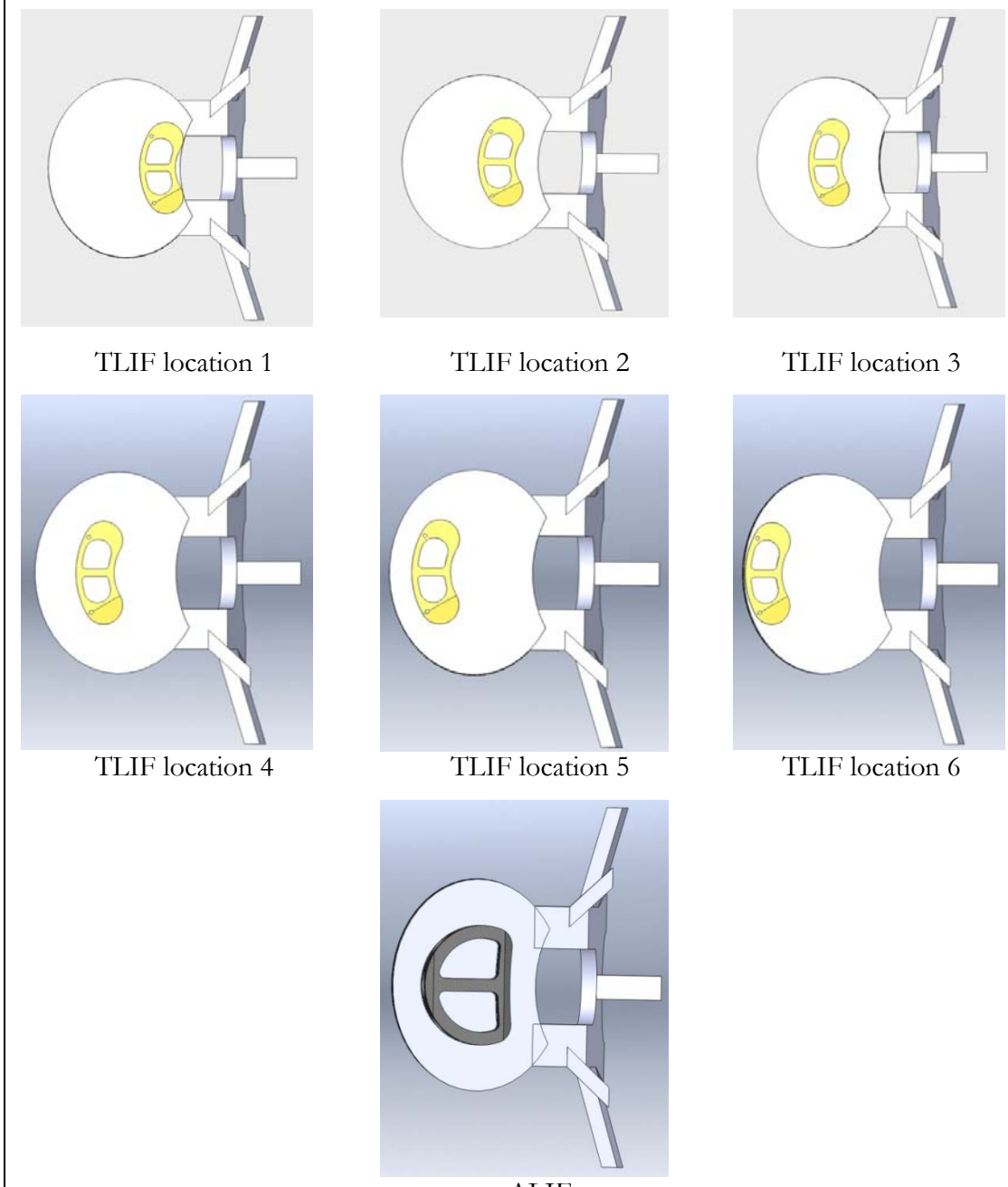

Figure 2.32. Interbody device locations

(TLIF location moves 5.4 mm from posterior to anterior; ALIF is placed at center)

The finite element analysis results are listed in Table 2.5. The maximum stress induced on rods is tabulated for each case, where case 7 is the simulation with the ALIF. As can be seen from Table 2.5, placement of the TLIF is very critical to the maximum stresses experienced in the rods during a torso bend, as placing the TLIF fully posteriorly results in a 61% increase in maximum rod stress (relative to an ALIF), while placing the TLIF fully anteriorly results in a 10% decrease in maximum rod stress (relative to an ALIF). Figure 2.33 also presents the maximum stress in the rods for each case. The percentage difference is shown in Figure 2.34. As can be seen in the chart and the figures, a TLIF can be just as effective (if not more so) at reducing rod stress during flexion, so given the relative ease of implanting a TLIF (as opposed to and ALIF), implanting a TLIF may be preferable to implanting an ALIF in certain situations.

Table 2.5. Maximum stress on rods and for all studies

Spacer	Case No.	Maximum stress on rods (MPa)	Percentage difference relative to ALIF on rods
TLIF	1	42.6	61%
	2	42.1	59%
	3	37.8	43%
	4	31.8	21%
	5	29.1	10%
	6	23.7	-10%
ALIF	7	26.4	0%

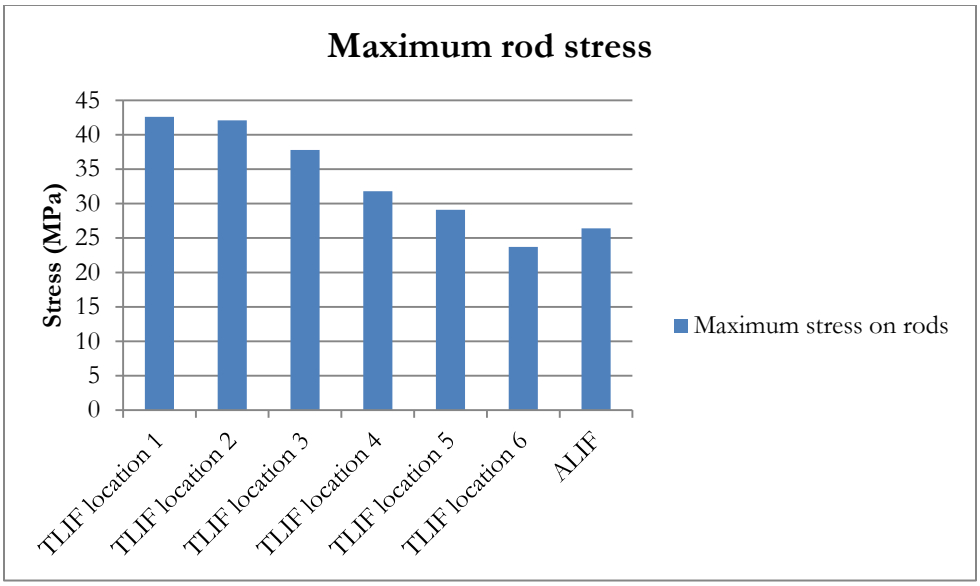

Figure 2.33. Maximum stresses on rods for all cases

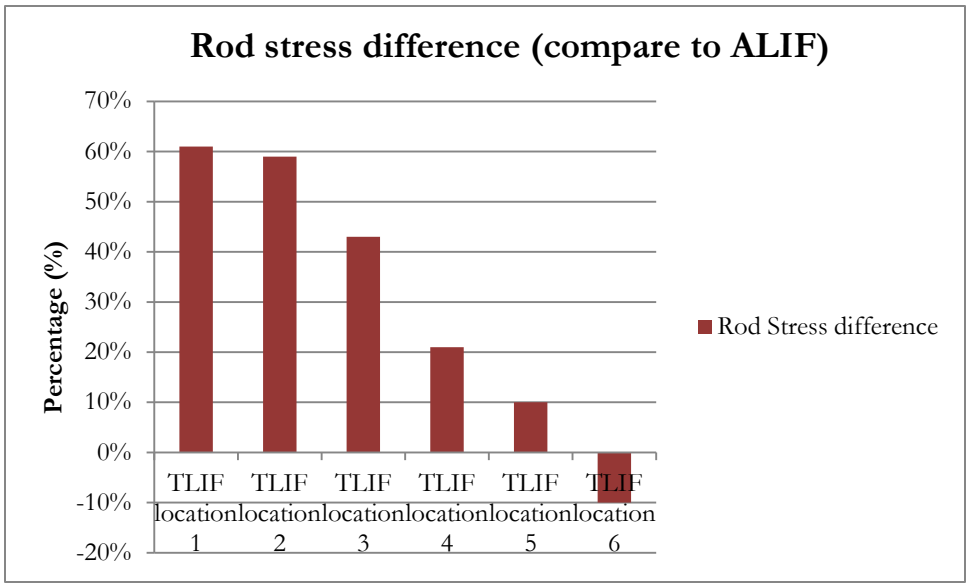

Figure 2.34. Maximum stress comparison between ALIF and TLIF studies on rods

2.4 Conclusion

In this chapter, a computationally efficient L1-S1 spine model is compared with experimental and finite element analysis data and shown to be a validated model. The model is then extended to include the T1-L1 portion of the spine. With less complicated geometries, the model presented is very computationally efficient, enabling the rapid conduction of detailed parametric studies. In the interbody device selection and disc degeneration study presented in this chapter, eight models with all possible interbody device (ALIF and TLIF) implant combinations (for L4-L5 and L5-S1) are modeled for a rod-screw fusion from T2 to the iliac wing. Extension, flexion and torsional loads are applied to investigate the spinal response and the stresses induced in the fusion rods. The results show that implanting an interbody device (ALIF of TLIF spacer) can significantly reduce the rod stress during extension and torsion motion by replacing a degeneratively soft (1 MPa) disc. If an interveterbral disc has begun the self-fusion process (i.e. is stiffer than a healthy disc), an interbody device may not be required, since our results show that replacing a degeneratively stiff disc with an interbody spacer has only minimal effect on rod stress. Little difference was noticed between an ALIF implant and a TLIF placed very close to the anterior edge of the intervertebral space. Due to the procedural difficulty of ALIF surgery, our sutdies show that a TLIF may be a preferable alternative to ALIF spacers for many patients.

In the interbody device location and type selection study presented in this chapter, seven models are created to represent the different interbody device types and locations. The results show that a TLIF can yield similar results to an ALIF, in terms of reducing rod stress, when it is placed as anteriorly as possible in between the vertebrae. Based on the fact that TLIF spacers are easier than ALIF spacers to implant, the suggestion is made to use a TLIF instead of an ALIF, and to place the TLIF as close as possible to the anterior edge. This study illustrates how finite element analysis can be used to analyze different surgical options for a particular patient case, and to provide guidance to the surgeon regarding proper implant choice and placement.

Chapter 3

Novel Spinal Connectors Provide Potential to Reduce Rod Stress on the Lumbar Rod-Screw Construct

3.1 Introduction

Currently, pedicle screw and rod fixation for fusion surgeries has become the standard method for fusing the spine to treat a variety of degenerative and traumatic conditions [1, 2, 5]. To enhance the rigidity of the rod-screw system, mechanical transverse connectors are often used as part of spinal instrumentation to provide a connection between the left and right fusion rods [30-48]. Studies have shown a 44% torsional segmental stiffness increase with use of a transverse connector in an in vitro spine model, with little effect on flexion and extension motions [49]. Pedicle screw fixation is well known to be most effective at stabilizing spinal surgical instrumentation during extension and flexion motions [50]. It is also suggested that the application of two transverse connectors is more effective in providing torsional stiffness than one connector [51]. Despite its effectiveness in providing increased spine segmental stiffness, the necessity of using a transverse connector is still controversial [52]. In addition to the extra costs and surgical time involved, the higher surgical construct profile that results from implanting a transverse connector is another limitation. Medical cases have been presented in the literature where implant removal was necessitated due to the discomfort caused by a high posterior spinal construct profile [53].

The objectives of posterior connectors are to provide immediate stability after surgery and to facilitate healing while maintaining the desired correction in the shape of the spine. This chapter focuses on comparing two novel posterior connector constructs to standard transverse connectors with respect to their ability to reduce rod stress and reduce the risk of rod breakage.

3.2 Development of posterior connector constructs

Spinal components from T1 (thoracic) down to the pelvis have been developed in Solidworks 2010 (Dassault Systèmes, Vélizy, France). "IGES" or "Parasolid" files are generated from Solidwork and then imported into an analytical finite element software package ABAQUS 6.10 (Hibbitt, Karlsson and Sorenson, Inc., Providence, RI) to analyze the stresses induced under

various load conditions.

In this chapter, rod-screw constructs are used to simulate an L1-iliac spinal fusion for several different models, where different types of posterior connectors are considered to provide support between two rods. Following standard surgical protocol, the traditional connector model is modeled with two transverse connectors on both the L1-L2 and L4-L5 levels (Figure 3.1(a)). Novel connector structures are then proposed and studied in this chapter to evaluate the potential of these novel structures to reduce the rod stress. In one of the novel structures, a truss-type connector links the left and right rods between L3 and the sacrum (Figure 3.1 (c)). In another one of the novel structures, a DLink-type connector is placed on the side of each rod and is connected between L3 and the sacrum. In surgical practice, a D-Link connector is recommended to be implemented along with truss connector (Figure 3.1 (e)). For each connector model, the situation with a transfominal interbody lumbar fusion (TLIF) located on L5-S1 as anteriorly as possible is also studied.

Therefore, there are six different configurations of models in this chapter: (1) a T1-Pelvis spine model with L1-iliac fusion and transverse connectors on both L2-L3 and L4-L5; (2) a T1-Pelvis spine model with L1-iliac fusion, TLIF on L5-S1, and transverse connectors on both L2-L3 and L4-L5; (3) a T1-Pelvis spine model with L1-iliac fusion and truss connector; (4) a T1-Pelvis spine model with L1-iliac fusion, TLIF on L5-S1, and truss connector; (5) a T1-Pelvis spine model with L1-iliac fusion and truss-DLink connectors; (6) a T1-Pelvis spine model with L1-iliac fusion, TLIF on L5-S1, and truss-DLink connectors as shown in Figure 3.1.

The procedures of model development and geometrical connections are discussed earlier in Chapter 2. The overall view of T1-Pelvis spine model with L1-iliac fusion, TLIF on L5-S1, and transverse connectors on both L2-L3 and L4-L5 is presented in Figure 4.2. In the finite element model associated with this 3D model, there are 71,330 nodes and 268,214 elements. The mechanical and material parameters are given in Table 3.1.

In all six models, vertebrae and intervertebral discs between T1 to T10 in thoracic region is modeled as one part to represent its natural attachment to the human rib cage. All degrees of

freedom on the pelvis bottom are fixed. Extension and flexion motions are simulated by a 40 N concentrated force applied at the center of the spine. A 10 Nm moment is imposed on the spine to create the torsion motion.

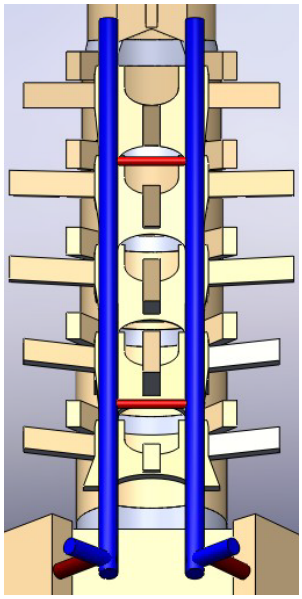

a). Transverse connectors on L1-L2 and L4-L5

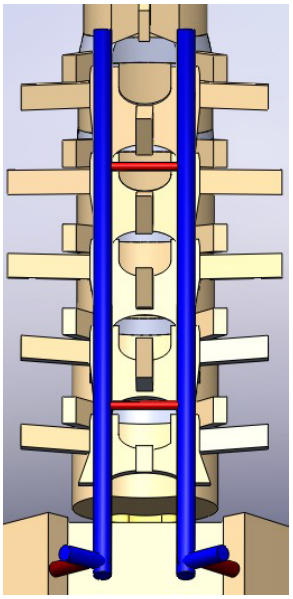

b). Transverse connectors on L1-L2 and L4-L5 with TLIF on L5-S1

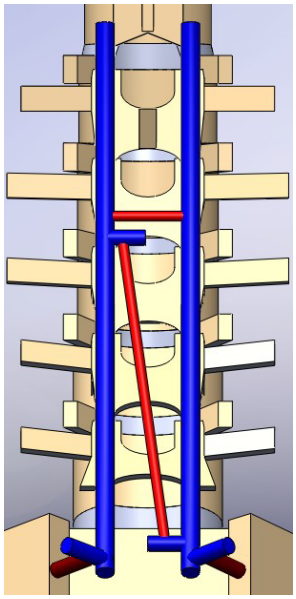

c). Truss connector

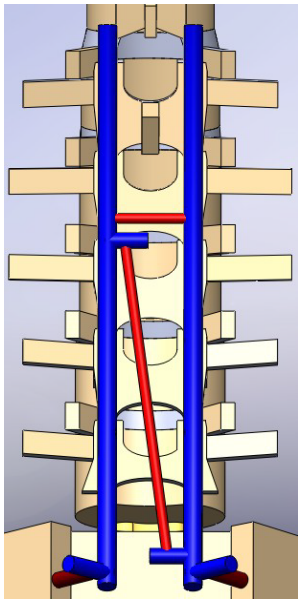

d). Truss connector with TLIF on L5-S1

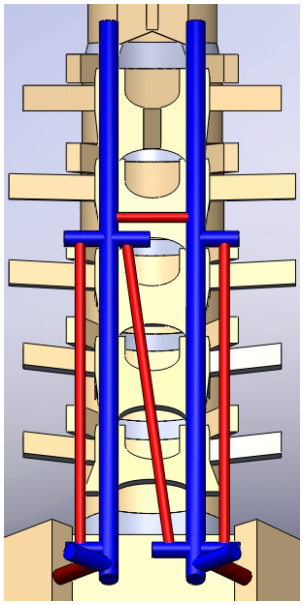

e). Truss-DLink connectors

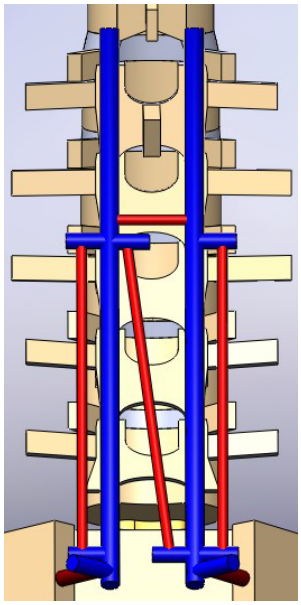

f). Truss-DLink connectors with TLIF on L5-S1

Figure 3.1. Different configurations of models used in connector study

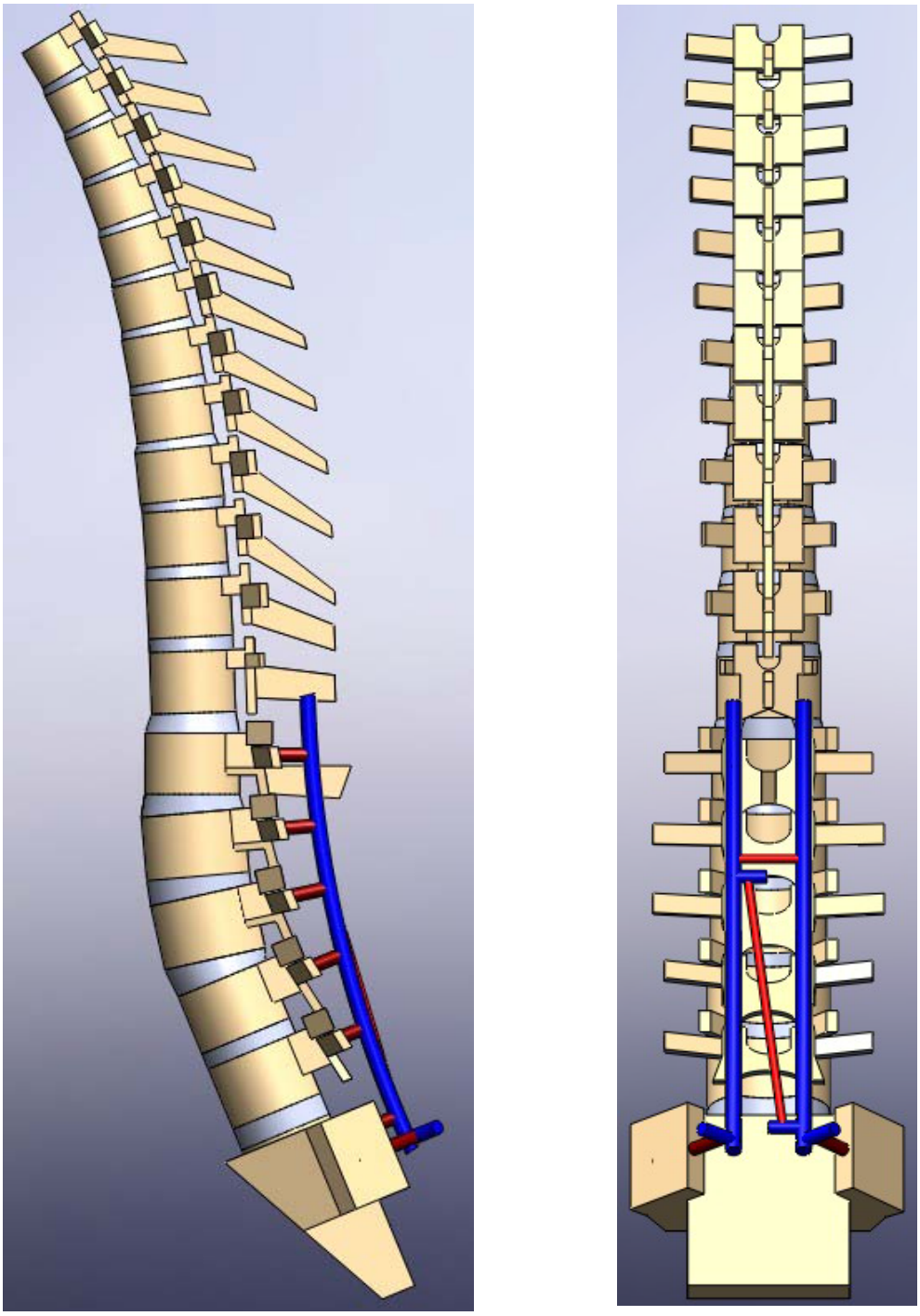

Figure 3.2. The side view (left) and posterior view (right) of a L1-iliac fusion model with TLIF, transverse connector, and truss connector implanted

Table 3.1. Material and mechanical properties used in connector study

Component	Element type	Young's Modulus (MPa)	Cross-section (mm^2)	Poisson's ratio
Cortical bone	Shell	12000	-	0.3
Trabecular bone	Solid	100	-	0.2
Annulus fibrosus	Solid	Parametric Study	-	0.3
Posterior elements	Solid	3500	-	0.25
Ligaments	Spring			
Anterior longitudinal		7.8(<12%) 20(>12%)	63.7	-
Posterior longitudinal		10(<11%) 20(>11%)	20.0	-
		10(<18%) 58.7(>18%)	1.8	-
Intertransverse		10(<14%) 11.6(>14%)	40.0	-
Interspinous		15(<6.2%) 19.5(>6.2%)	40.0	-
Ligamentum flavum		7.5(<25%) 32.9(>25%)	30.0	-
Capsular		8(<20%) 15(>20%)	30.0	-
Supraspinous				
Sacrum	Solid	12000	-	0.3
Fusion rods (Cobalt)	Solid	209000	-	0.31
Fusion screws (Titanium)	Solid	116000	-	0.32
Interbody device (PEEK)	Solid	3800	-	0.3
Connector (Titanium)	Solid	116000	-	0.32

3.3 Posterior constructs analysis

In this chapter, all six models are analyzed under extension, flexion, and torsion motions. For those models with L4-L5 and L5-S1 discs intact, sensitivity analysis is conducted by varying the Young's modulus of both intervertebral discs parametrically with respect to disc stiffness. For models with TLIF implanted on L5-S1, L4-L5 disc property is varied to simulate the disc degeneration process. The maximum rod stress resulted are collected to study the trends.

The maximum rod stress on models with L1-iliac fusion and a transverse connector is depicted in Figure 3.3-3.5. The simulation first focuses on investigating whether a TLIF can reduce the rod stress and prevent the risk of rod breakage when the posterior construct changes (i.e. additional connector structures are added). As expected, during extension and flexion motions, larger maximum stress (blue curve) is found on rods as the disc properties are set to be degeneratively soft (Young's modulus is 1 MPa). Once disc property is defined to be stiffer than 4 MPa (healthy disc), the decreased maximum rod stress is noticed. Based on the results, replacing a degeneratively soft L5-S1 disc with a TLIF can significantly reduce the maximum rod stress (yellow curve). Among all five different L4-L5 disc properties, a TLIF reduces the maximum rod stress by up to 56.0% and 55.5% by replacing a degenerative disc in extension and flexion respectively. If the discs become stiffer, the spinal rigidity increases, which reduces the maximum rod stress automatically. In this case, a TLIF isn't necessary in fusion surgery (if the pupose of implanting the spacer is to reduce rod stress). In torsion motion, maximum rod stress is less sensitive to the disc properties on L4-L5 and L5-S1 discs. A TLIF can reduce the maximum rod stress by up to 8.7%.

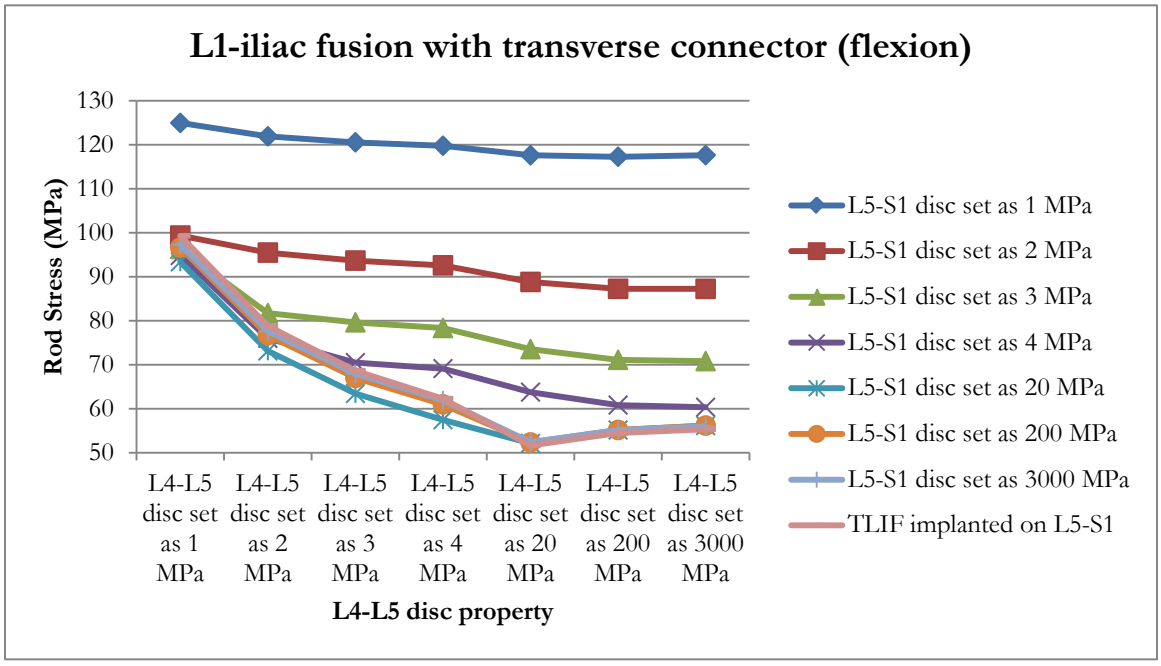

Figure 3.3. Maximum rod stress (MPa) on L1-iliac fusion models with transverse connector during disc degeneration in flexion motion

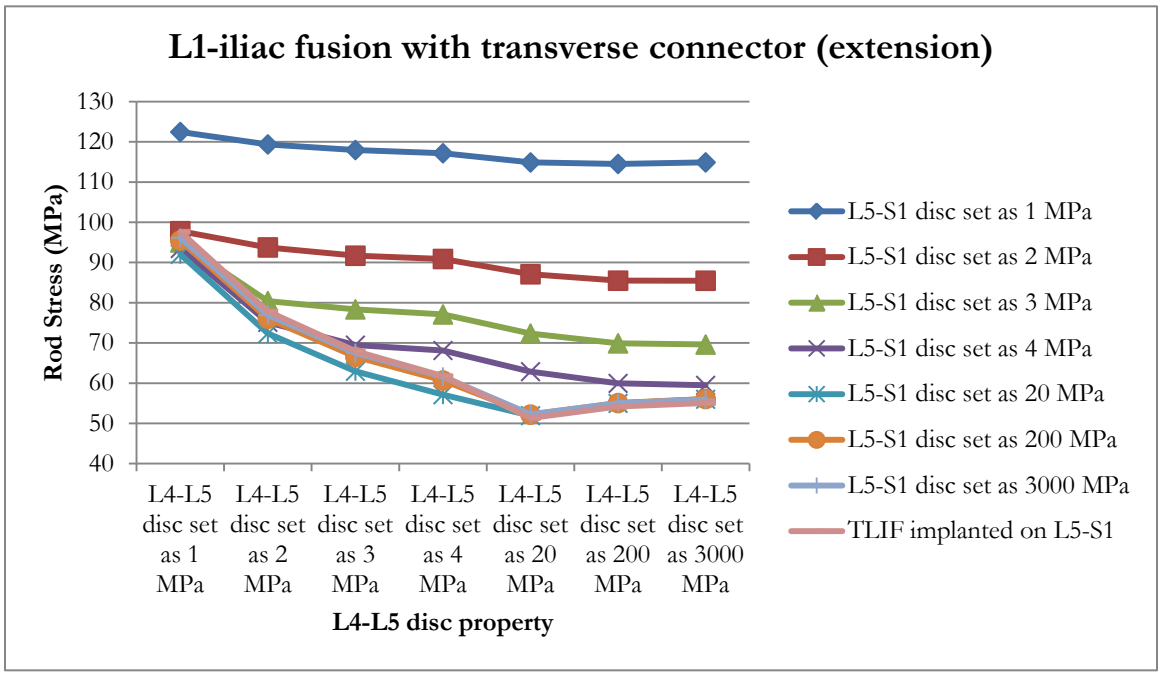

Figure 3.4. Maximum rod stress (MPa) on L1-iliac fusion models with transverse connector during disc degeneration in extension motion

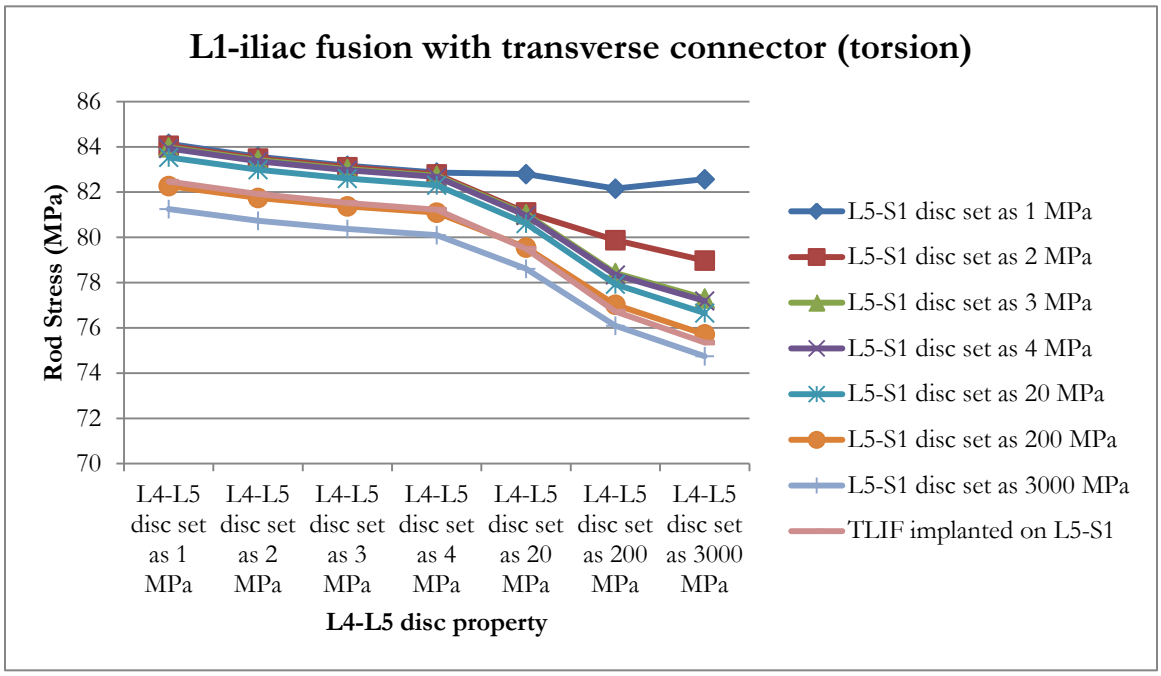

Figure 3.5. Maximum rod stress (MPa) on L1-iliac fusion models with transverse connector during disc degeneration in torsion motion

The maximum rod stress on L1-iliac fusion models with truss connector during all motions is presented in Figure 3.6-3.8. As anticipated, a TLIF becomes very valuable at reducing the maximum rod stress if L5-S1 disc is degeneratively soft during extension and flexion motions. The maximum rod stresses are reduced by up to 57.3% and 56.3% during extension and flexion respectively by implanting a TLIF to substitute degeneratively soft L5-S1 disc. In torsion, the bottom disc properties have less influence on the maximum rod stress; for torsion, the TLIF substitution reduces the maximum rod stress by a maximum of 15.3%.

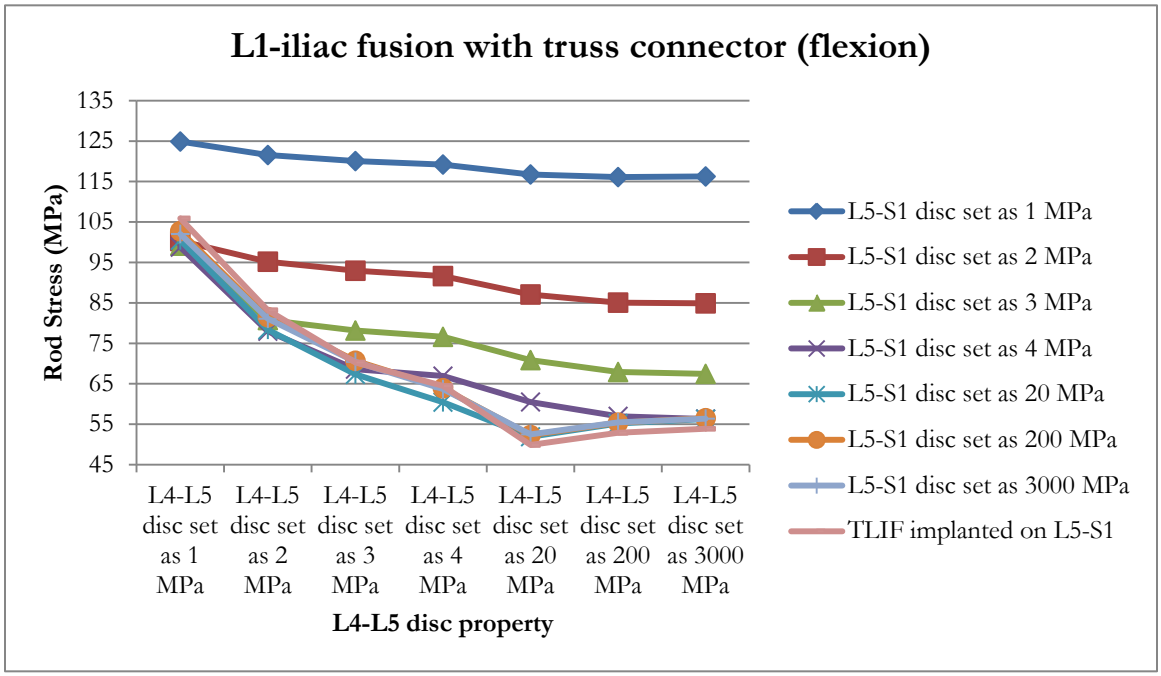

Figure 3.6. Maximum rod stress (MPa) on L1-iliac fusion models with truss connector during disc degeneration in flexion motion

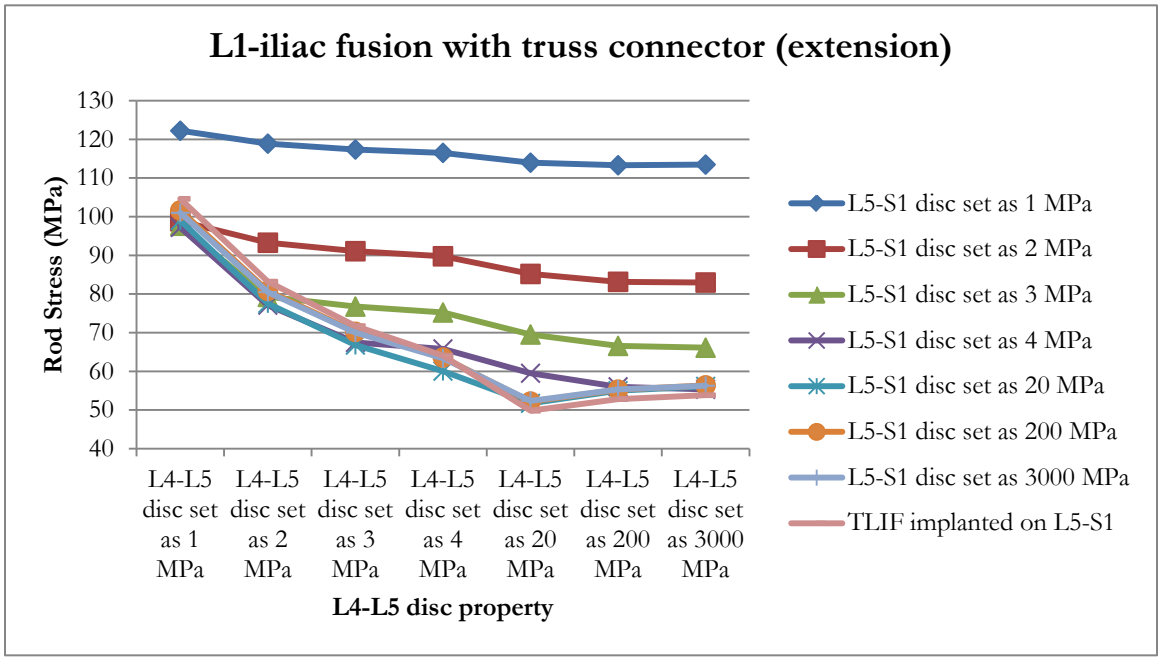

Figure 3.7. Maximum rod stress (MPa) on L1-iliac fusion models with truss connector during disc degeneration in extension motion

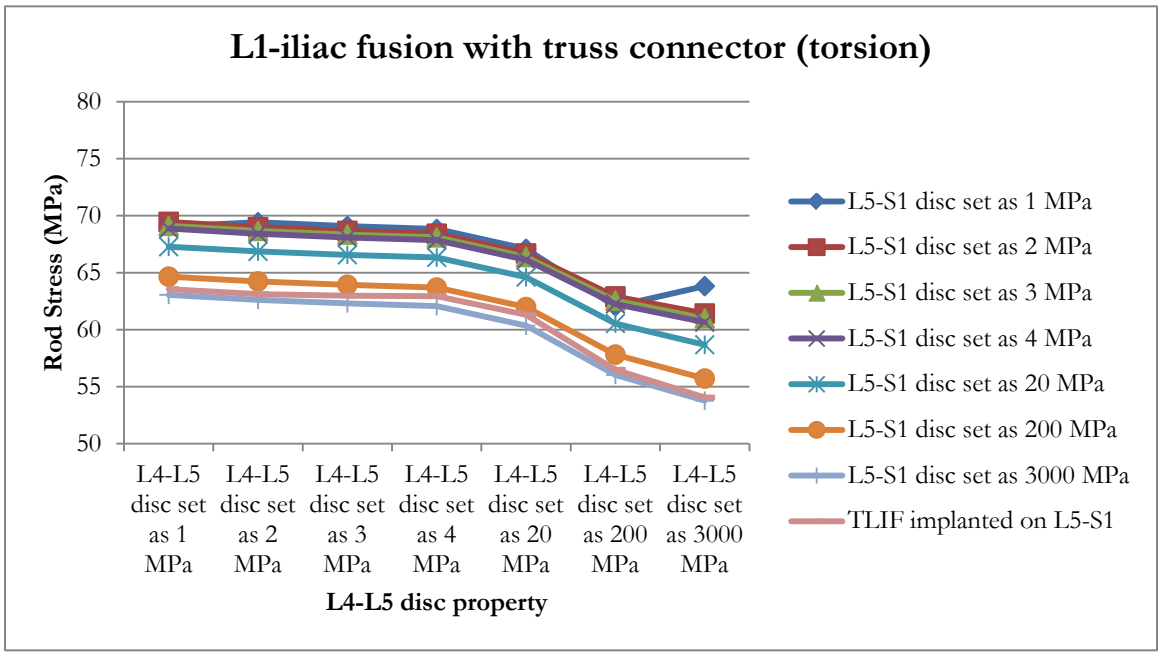

Figure 3.8. Maximum rod stress (MPa) on L1-iliac fusion models with truss connector during disc degeneration in torsion motion

The resultes on L2-ilac fusion models with truss and DLink connectors are depicted in Figure 3.9-3.11. Similarly, the maximum rod stresses decrease up to 59.1% and 58.2% during extension and flexion respectively by implanting a TLIF at L5-S1. It is also noticed that maximum rod stress is less sensitive to the material properties at the bottom two lumbar discs. A TLIF is shown to be able to reduce the maximum rod stress by up to 15.7% under torsional loading.

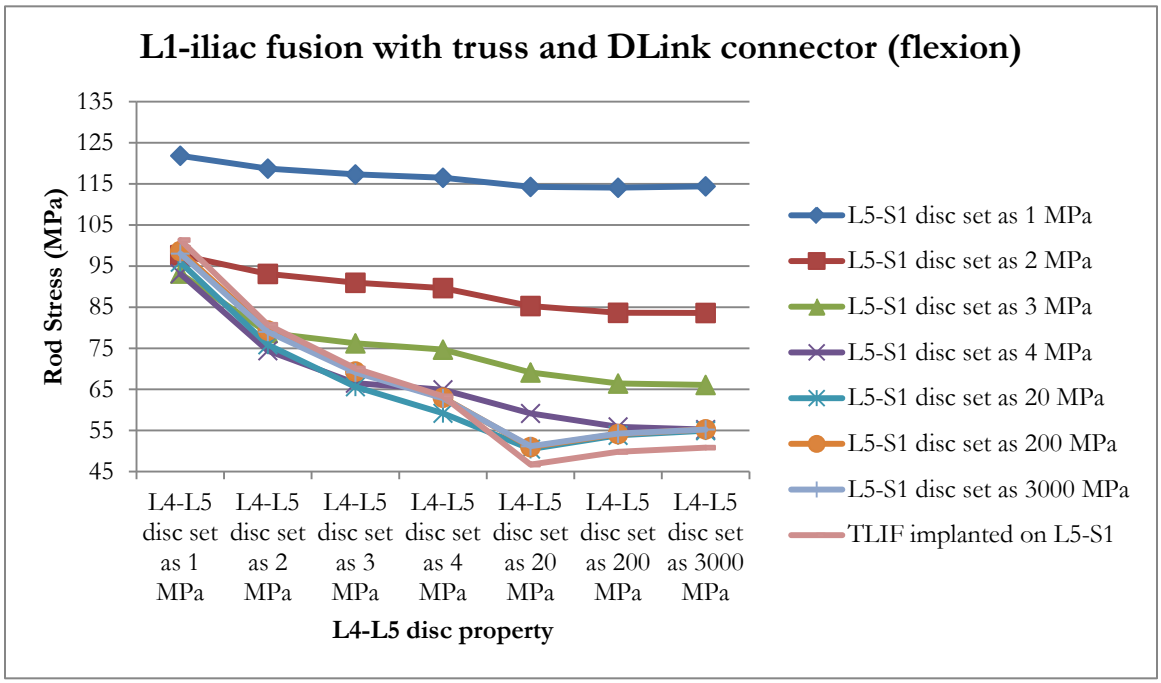

Figure 3.9. Maximum rod stress (MPa) on L1-iliac fusion models with truss and DLink connector during disc degeneration in flexion motion

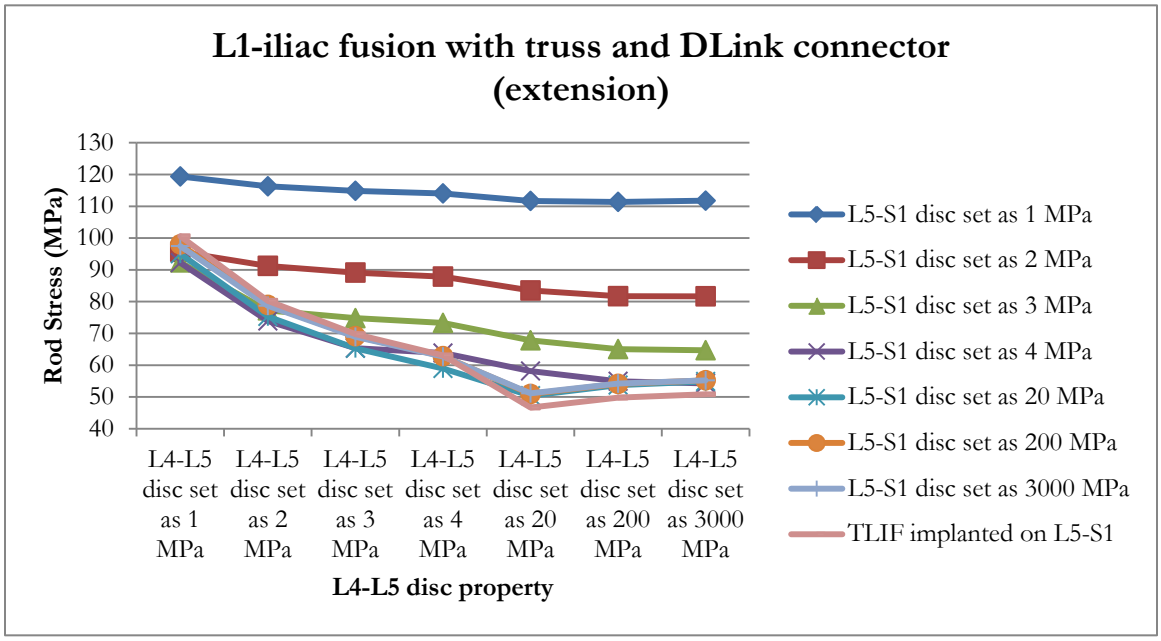

Figure 3.10. Maximum rod stress (MPa) on L1-iliac fusion models with truss and DLink connector during disc degeneration in extension motion

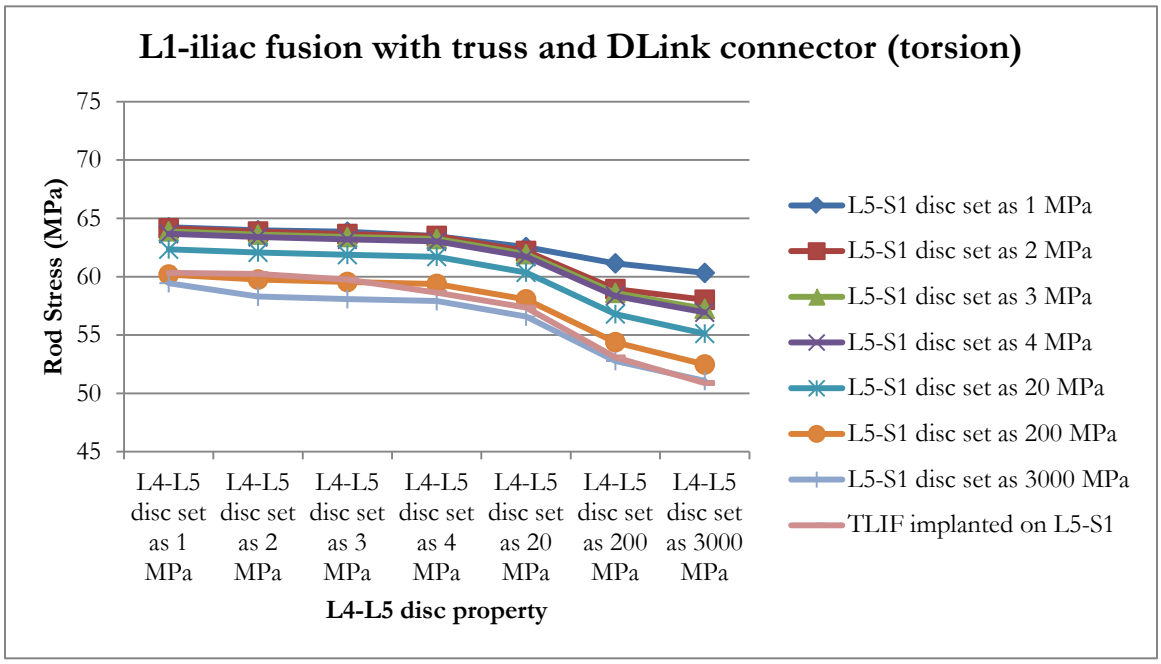

Figure 3.11. Maximum rod stress (MPa) on L1-iliac fusion models with truss and DLink connector during disc degeneration in torsion motion

The maximum rod stresses among three different posterior connector structures are compared in Figure 3.12-3.14. It is reported that the traditional connectors are quite effective at providing spinal support and increasing rigidity, especially torsional rigidity. However, hardware breakage are often caused by high stresses induced on rod-screw constructs.

For extension and flexion motions, no significant difference among all three models. Our proposed connector structures (truss connector and truss-DLink connector) share the similar maximum rod stresses with the traditional tranverse connector structure. In our analysis, the maximum stress induced on rods during extension and flexion motions is mainly related to interverbral disc properties. The posterior connector structures have trivial influence for those two motions. Under this circumstance, replacing the degeneratively soft L4-L5 disc by an interbody device would be the best option to reduce the maximum rod stress and prevent the risk of rod breakage as discussed in Chapter 2.

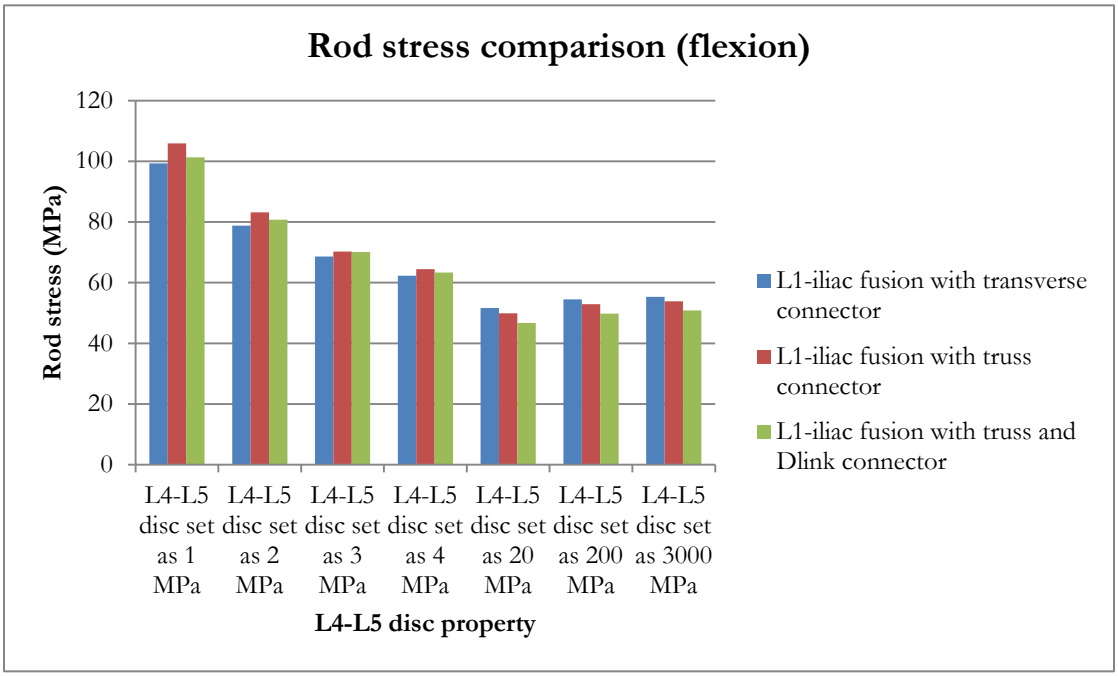

Figure 3.12. Maximum rod stress (MPa) comparison among different connectors during disc degeneration in flexion motion

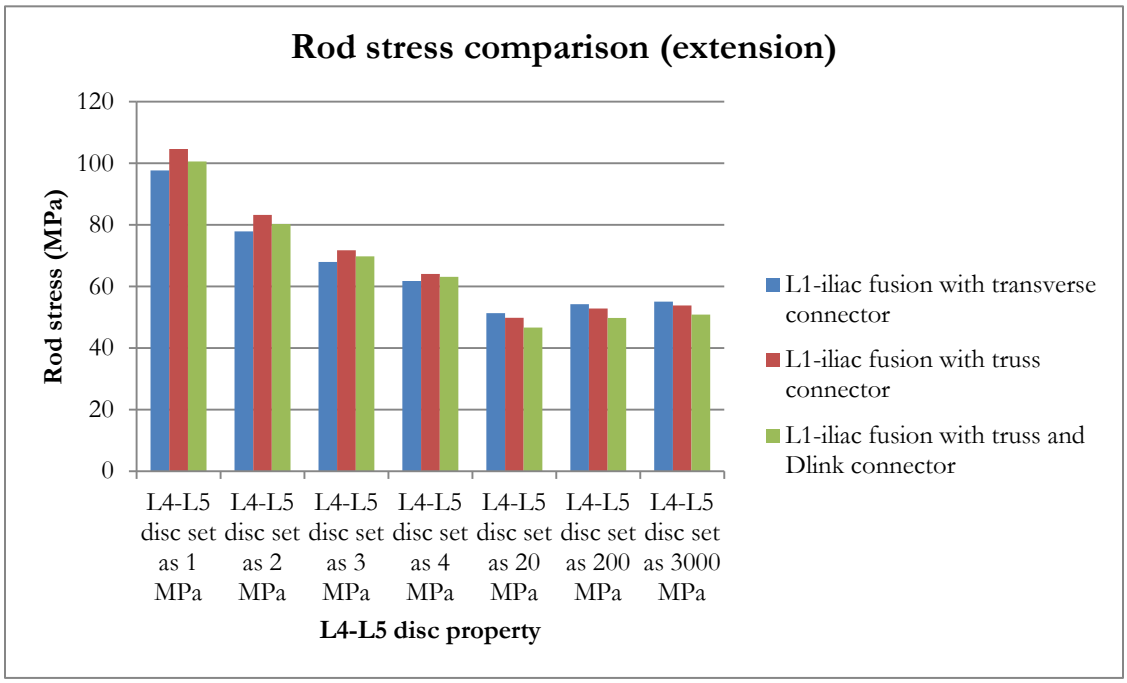

Figure 3.13. Maximum rod stress (MPa) comparison among different connectors during disc degeneration in extension motion

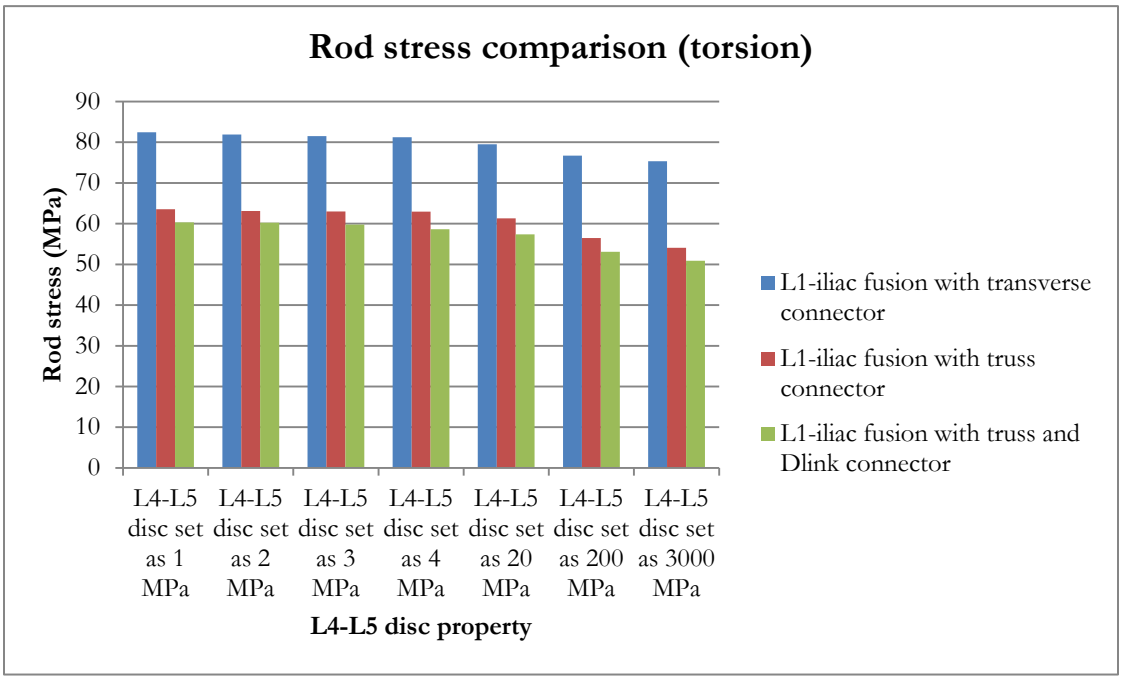

Figure 3.14. Maximum rod stress (MPa) comparison among different connectors during disc degeneration in torsion motion

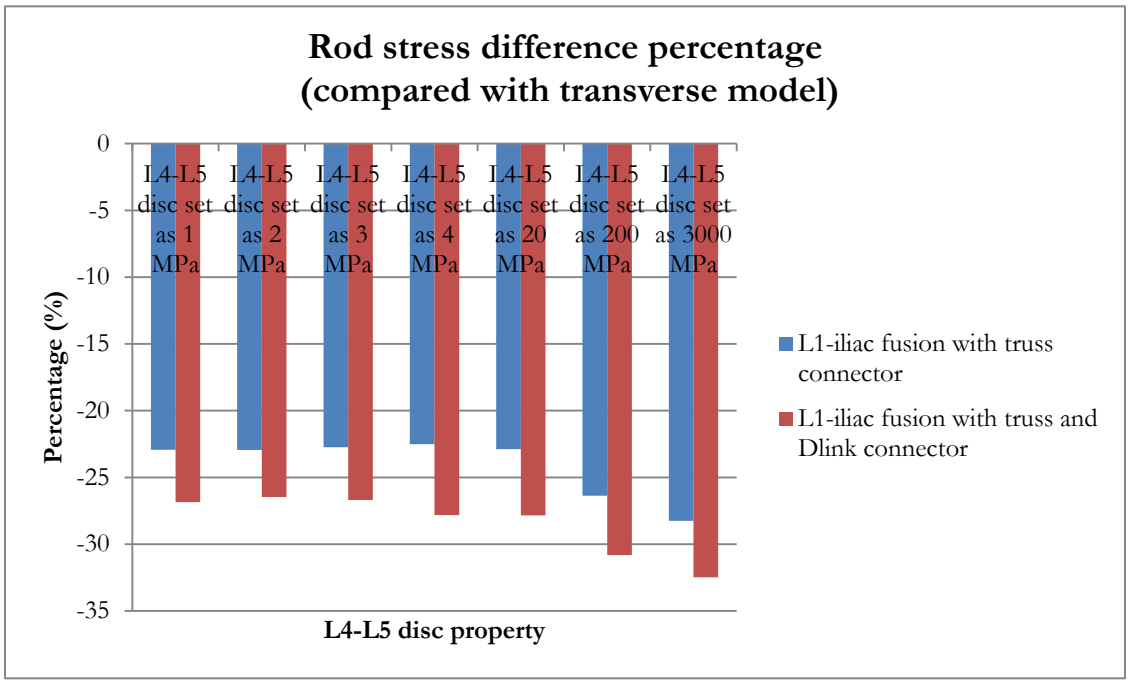

Figure 3.15. Novel connector models maximum rod stress difference percentage compared to transverse connector in torsion motion

In torsion motion, Figure 3.15 shows both proposed connector structrues reduce the maximum rod stress significantly compared to transverse connector structure. If a truss connector is implemented rather than a transverse connector, the maximum rod stress can be reduced from 22.9% to 28.3%. A truss-DLink connector can help to reduce the maximum rod stress from 26.8% to 32.5% compared with the transverse connector. Approximately, adding two DLink connectors to the truss model yields another 4% to 5% deceased rod stress under torsion motions. Based on the surgical cost the related difficulites, it is recommended to use just the truss connector. However, if an additional 4% to 5% decease is very critical to certain patients, truss-DLink connectors can also be considered.

3.4 Conclusion

In this chapter, six models are developed to study how posterior connectors can affect rod stress on rod-screw constructs under various loading conditions. The results show that implanting a TLIF can significantly reduce the maximum rod stress when used to replace a degeneratively soft disc, regardless of the type of posterior connectors used. Two novel connector structures are proposed and evaluated in this chapter. Parametric studies are performed to examine their impact on reducing rod stress, and the results show that adding a truss-type structure to the instrumentation can help to considerably reduce the stresses induced in the fusion rods, particularly under torsional loading. Under some specific surgical circumstances, the use of DLink connectors can also be considered to further reduce the rod stress.

Chapter 4

Adjacent Disc Biomechanics after Spine Fusion

4.1 Introduction

Intervertebral disc degeneration is a serious medical condition which sometimes necessitates spinal fusion in order to relieve the patient's back pain and restore spinal function. Two common surgical treatments are often used for degenerative disc disease: spinal fusion and disc replacement (e.g. the interbody devices discussed in Chapter 2). However, it is widely known that spinal fusion result in increased rigidity of the spine, some loss of motion, and may possibly lead to adjacent level degeneration [54-69].

Studies have indicated that patients with spinal fusion appear to be at greater risk for adjacent segment disease, and sometimes revision surgeries are required due to the failure of adjacent discs. Hilibrand et al. [70] studied over 300 patients after fusion surgery for 10 years and found the rate of adjacent level failure was approximately 3% per year. Goffin et al. [71] reported a 92% incidence of adjacent disc degeneration after anterior fusion surgery. In Gore and Sepic's [72] study, the incidence rate is recorded as 98% in a 21-year follow-up after the surgeries. To help shed light on the possible causes of adjacent disc failure, we have used our finite element model to study how spinal fusion affects the adjacent disc stresses compared to a non-fused spine under the same loadings.. Several intervertebral discs above the fusion level (along with the immediately adjacent disc) are analyzed for three different spinal fusion constructs (covering different levels) to conduct a comprehensive study of the stresses induced in adjacent discs after spinal fusion surgery.

4.2 Development of spine fusion models

A solid spine model from T1 (thoracic) all the way down to the pelvis is designed in Solidworks 2010 (Dassault Systèmes, Vélizy, France) and then imported into finite element modeling software ABAQUS 6.10 (Hibbitt, Karlsson and Sorenson, Inc., Providence, RI). In this chapter, seven different configurations of the model are considered: (1) a noninstrumented T1-Pelvis spine model with healthy spinal parameters used as a reference control case; (2) a T1-pelvis spine

model with L1-iliac fusion; (3) a T1-pelvis spine model with L1-iliac fusion and a TLIF implanted at L5-S1; (4) a T1-pelvis spine model with L2-iliac fusion; (5) a T1-pelvis spine model with L2-iliac fusion and a TLIF implanted at L5-S1; (6) a T1-pelvis spine model with T10-iliac fusion; (7) a T1-pelvis spine model with T10-iliac fusion and a TLIF implanted at L5-S1(as shown in Figure 4.1).

The components and details of this noninstrumented model are provided in Chapter 2 Section 2. The rod-screw constructs are implemented to create different spinal fusion levels. The 3D T1-Pelvis spine model with L1-iliac fusion is presented in Figure 4.2. Its finite element model includes 71,330 nodes and 268,214 elements. The sensitivity analysis is conducted by varying the Young's modulus of intervertebral discs parametrically with respect to disc stiffness. The mechanical and material parameters are listed in Table 4.1.

In all seven models, all nodes on the bottom of the pelvis are fixed in all directions. A 40 N concentrated force is loaded at the center of the spine model to simulate the extension/flexion loads. A 10 Nm moment is applied on the spine to create the torsional load.

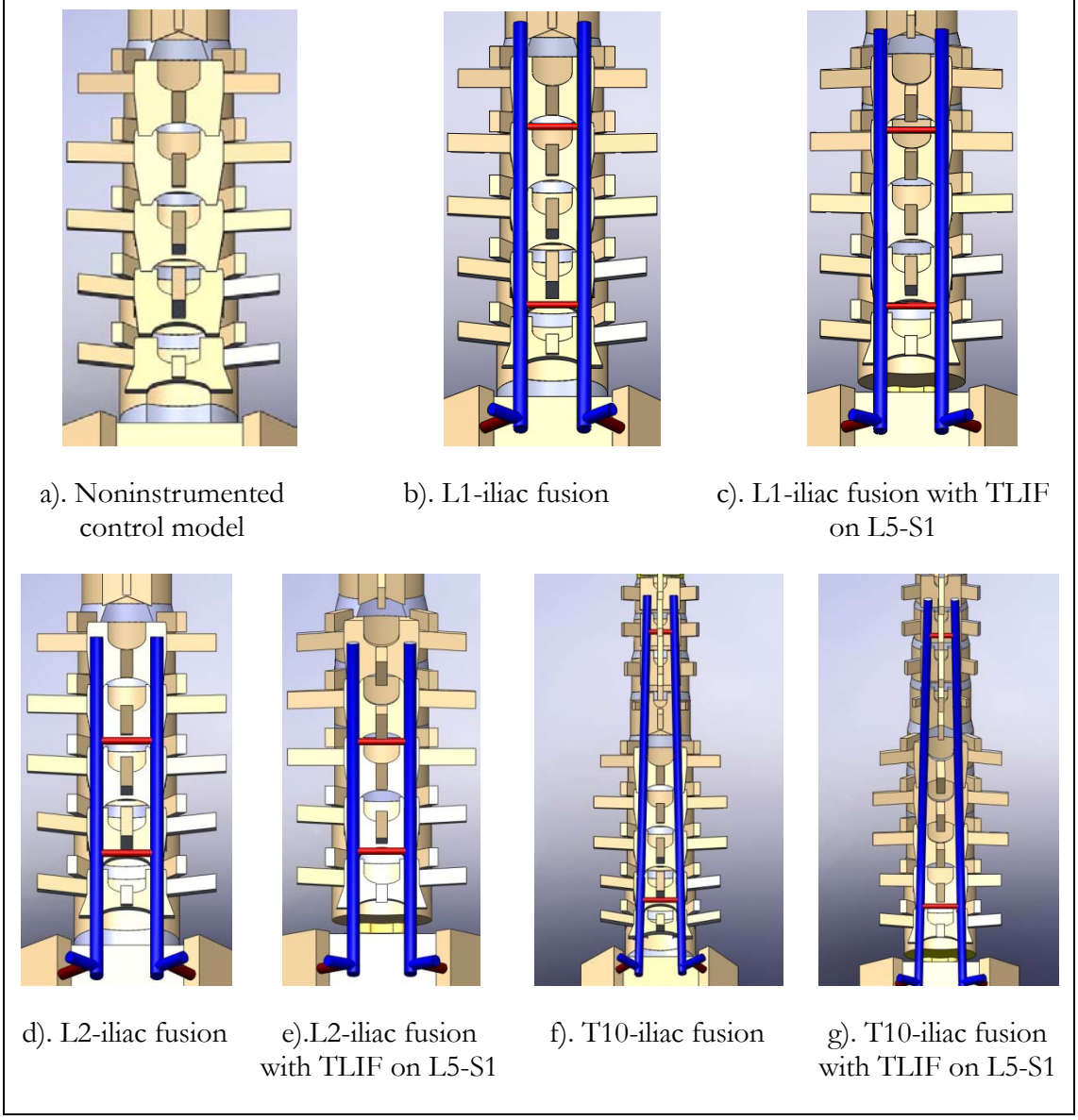

Figure 4.1. Different configurations of models used in adjacent disc study

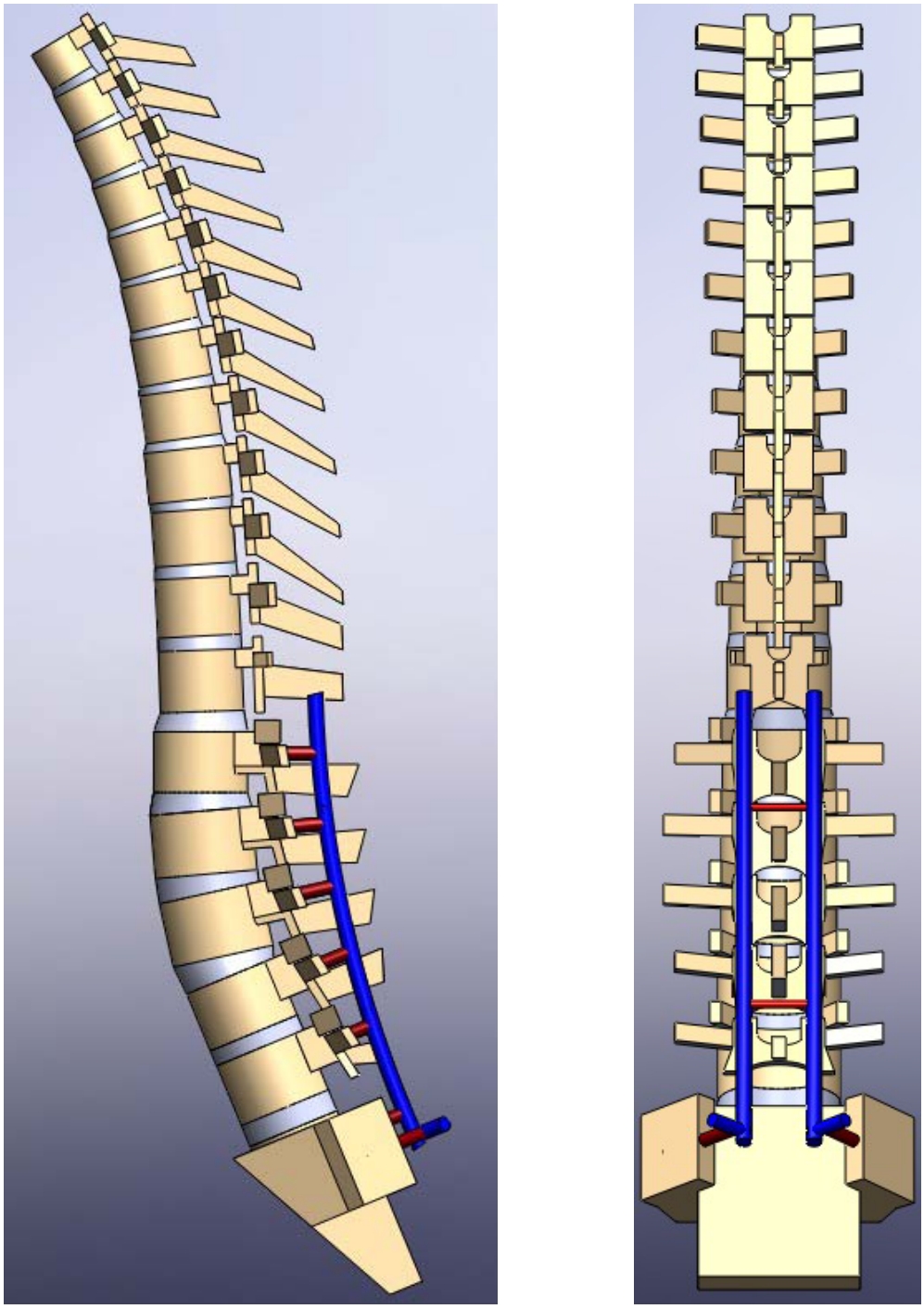

Figure 4. 2. The side view (left) and posterior view (right) of a L1-iliac fusion model

Table 4.1. Material and mechanical properties used in adjacent disc study

Component	Element type	Young's Modulus (MPa)	Cross-section (mm^2)	Poisson's ratio
Cortical bone	Shell	12000	-	0.3
Trabecular bone	Solid	100	-	0.2
Annulus fibrosus	Solid	Parametric Study	-	0.3
Posterior elements	Solid	3500	-	0.25
Ligaments	Spring			
Anterior longitudinal		7.8(<12%) 20(>12%)	63.7	-
Posterior longitudinal		10(<11%) 20(>11%)	20.0	-
Intertransverse		10(<18%) 58.7(>18%)	1.8	-
Interspinous		10(<14%) 11.6(>14%)	40.0	-
Ligamentum flavum		15(<6.2%) 19.5(>6.2%)	40.0	-
Capsular		7.5(<25%) 32.9(>25%)	30.0	-
Supraspinous		8(<20%) 15(>20%)	30.0	-
Sacrum	Solid	12000	-	0.3
Fusion rods (Cobalt)	Solid	209000	-	0.31
Fusion screws (Titanium)	Solid	116000	-	0.32
Connector (Titanium)	Solid	116000	-	0.32

4.3 Adjacent disc stress analysis

T12-L1 disc stresses under L1-iliac spinal fusion during extension, flexion and torsion are depicted in Figure 4.3-4.5. As both the L4-L5 and L5-S1 discs' stiffness values are varied parametrically, no significant difference in the stresses in the T12-L1 disc is observed during all three motions. As we know, the T12-L1 disc is a long distance away from the bottom two lumbar discs. Therefore, it is not surprising that there is not a large influence from the L4-L5 and L5-S1 discs on the T12-L1 disc. Adjacent disc stress is mainly affected by the spinal rigidity provided by the screw-rod constructs. Since the results indicate that adjacent disc stresses are not sensitive to the material properties on bottom discs, in Figure 4.3 any case can be selected to represent L1-iliac fusion model to make the comparison among different fusion levels. Therefore, for all the models, both the L4-L5 and L5-S1 discs' Young's modulus are set to 4 MPa (i.e. the healthy disc parameter value) to investigate the influence of different spinal fusion levels on adjacent disc stresses.

It is also noticed that a TLIF on the L5-S1 level provides no benefit in terms of reducing the adjacent disc stress. Therefore, an interbody device isn't recommended as being necessary to reduce the risk of the adjacent level degeneration.

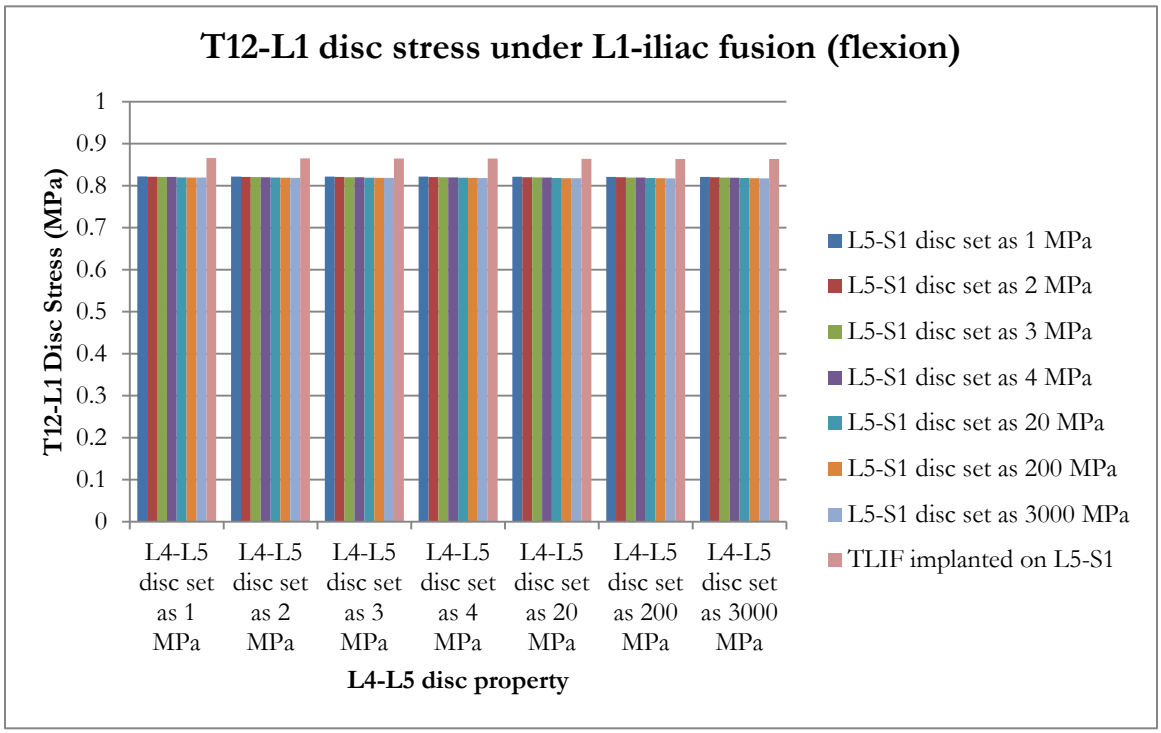

Figure 4.3. T12-L1 disc stress with L1-iliac fusion during flexion motion

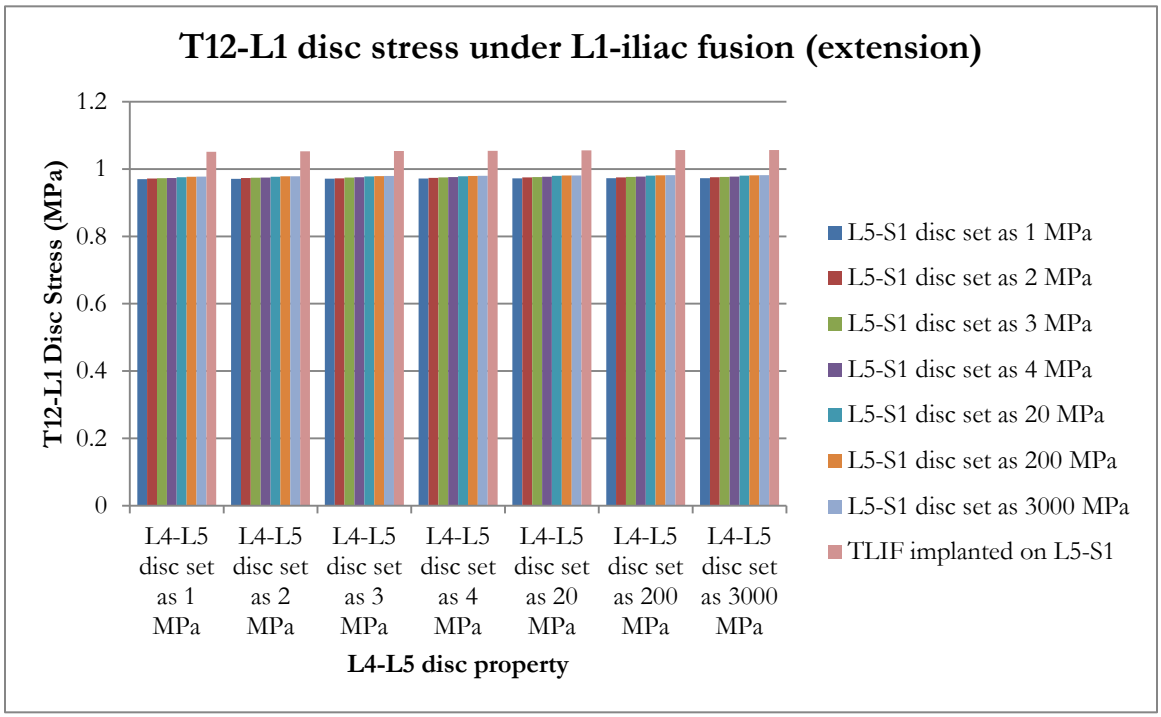

Figure 4.4. T12-L1 disc stress with L1-iliac fusion during extension motion

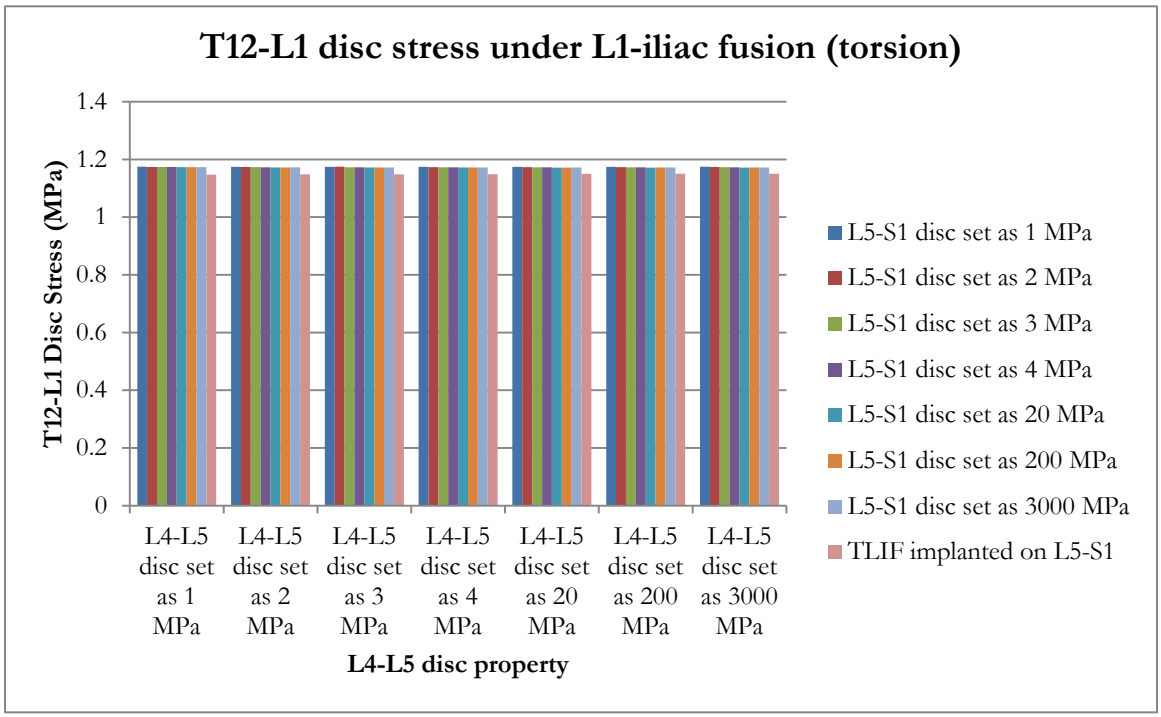

Figure 4.5. T12-L1 disc stress with L1-iliac fusion during torsion motion

The T12-L1 disc stresses under two other fusion models (L2-iliac and T10-iliac) are presented in Figures 4.6-4.11 As before, we find that the T12-L1 disc stresses are insensitive to mechanical properties on bottom two disc levels. These results further prove that any changes in the stresses induced on the T12-L1 disc are directly related to the spinal rigidity provided by rod-screw constructs. As mentioned previously, the results from the models using healthy disc parameters are selected to do the comparison.

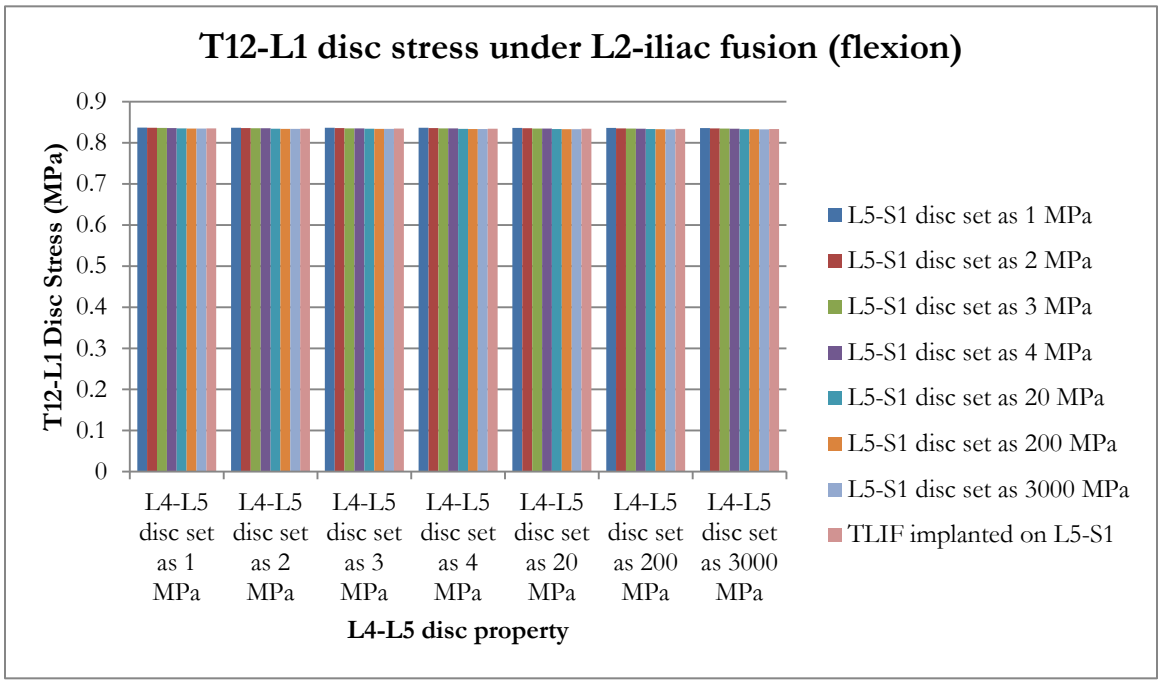

Figure 4.6. T12-L1 disc stress with L2-iliac fusion during flexion motion

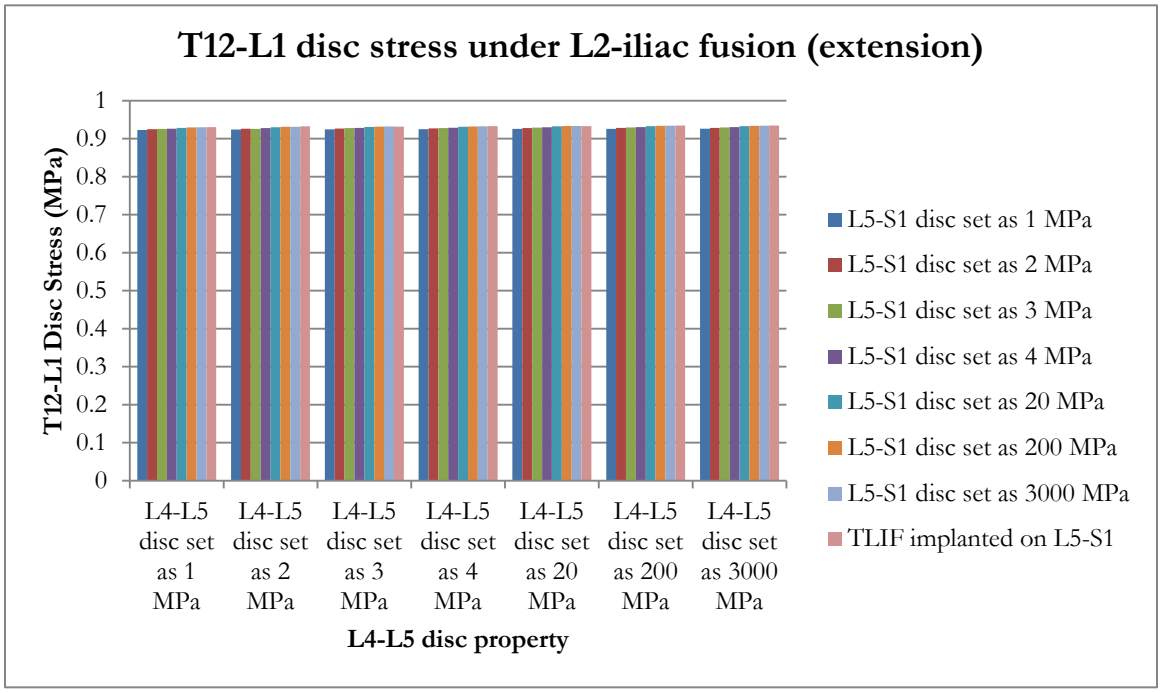

Figure 4.7. T12-L1 disc stress with L2-iliac fusion during extension motion

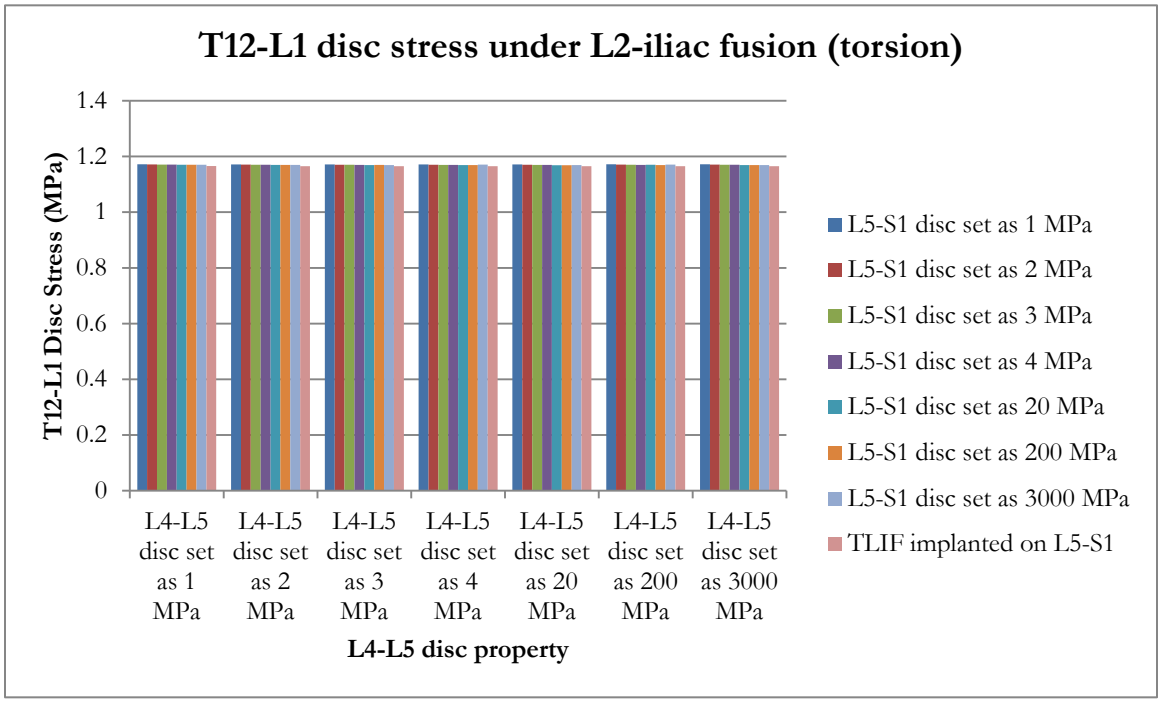

Figure 4.8. T12-L1 disc stress with L2-iliac fusion during torsion motion

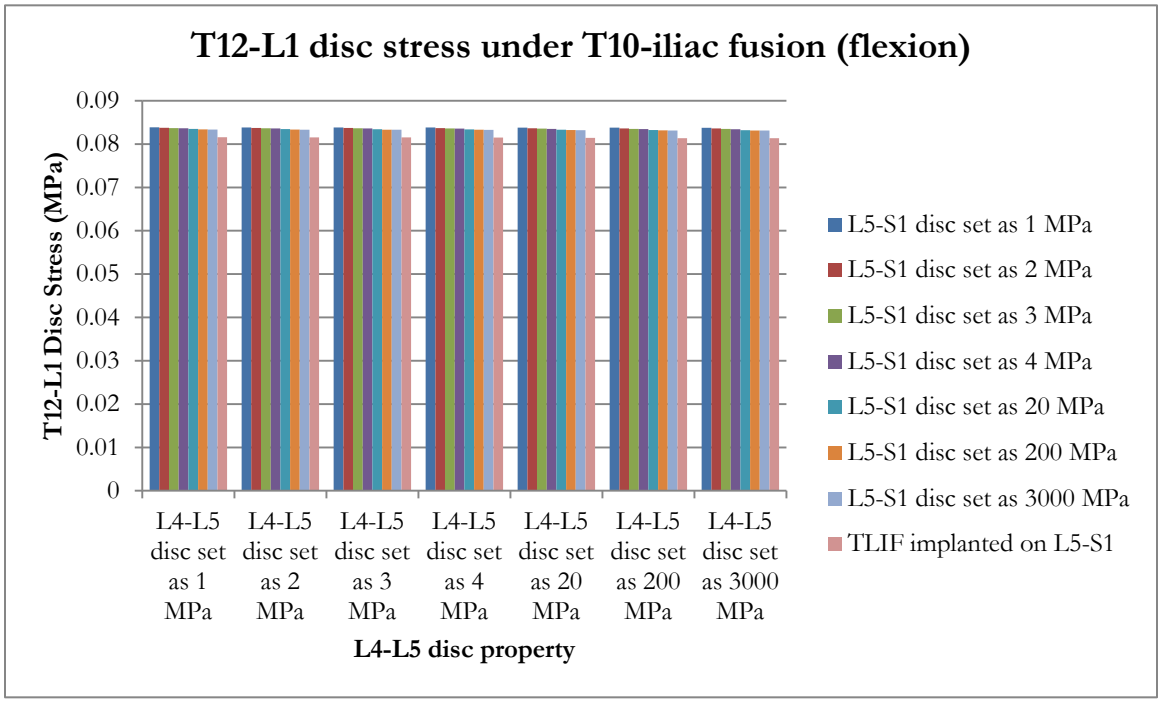

Figure 4.9. T12-L1 disc stress with T10-iliac fusion during flexion motion

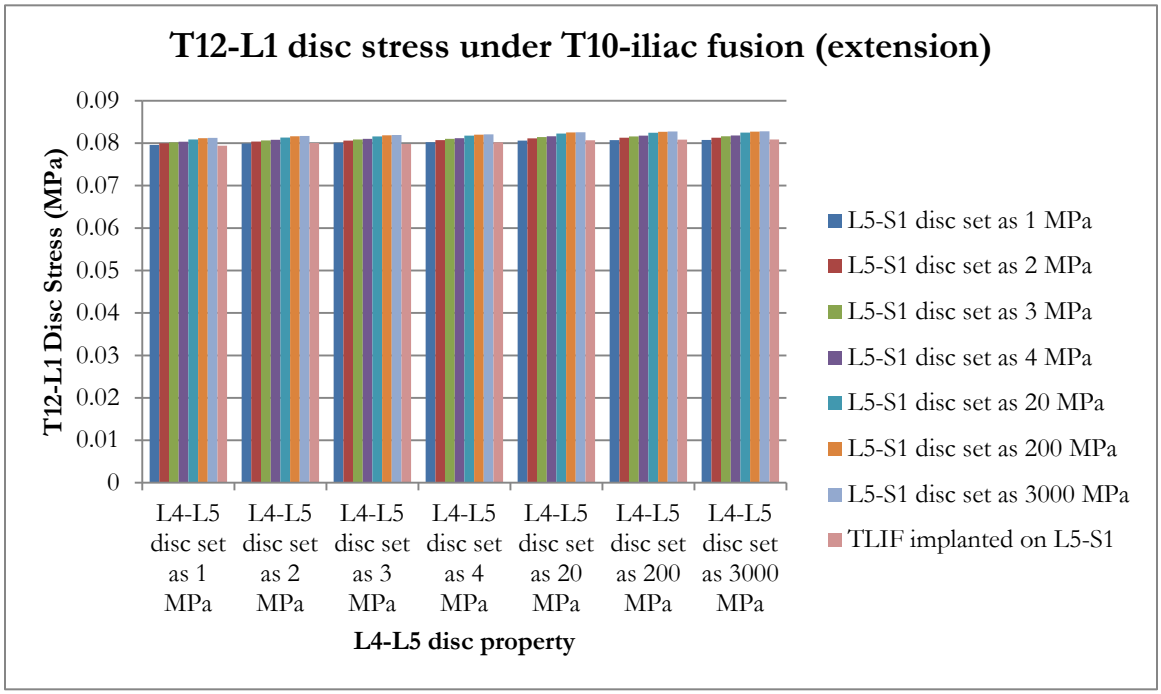

Figure 4.10. T12-L1 disc stress with T10-iliac fusion during extension motion

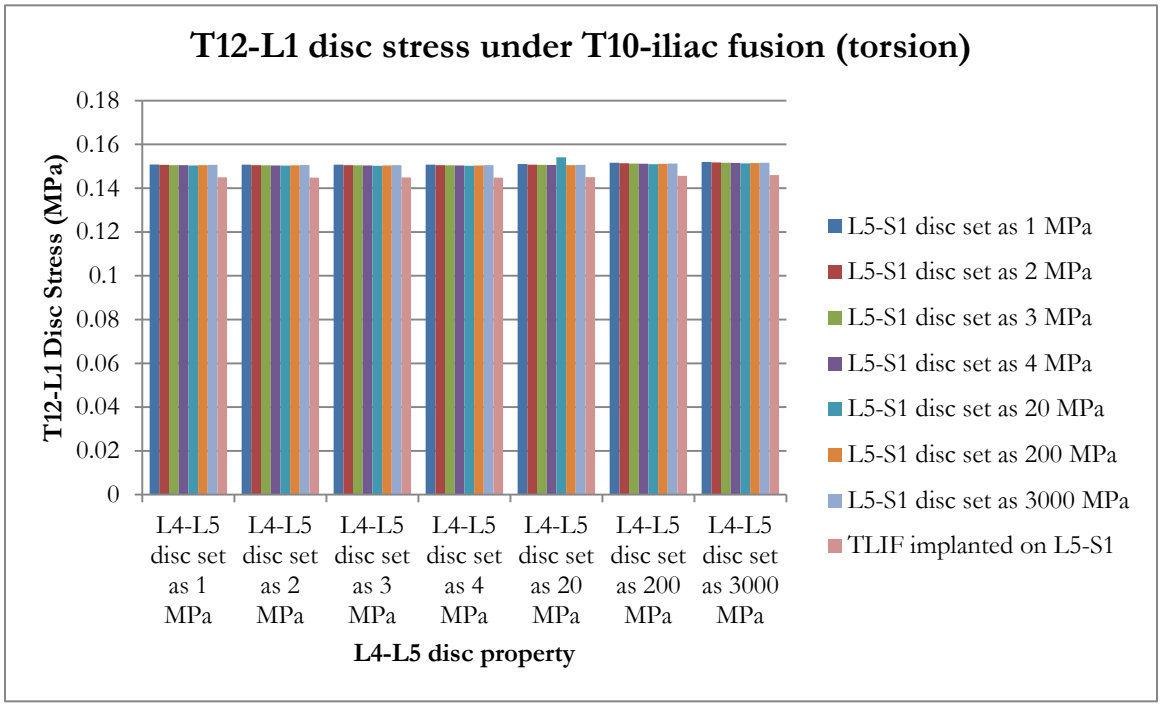

Figure 4.11. T12-L1 disc stress with T10-iliac fusion during torsion motion

Similar results for the T10-T11 and T11-T12 discs are found as well. This again suggests that changes in adjacent disc stresses are mostly related to the rod-screw fusion levels. Since no significant difference in stress is observed as the disc stiffness parameters are varied, the results from the models using healthy disc parameters are selected when examining the effect of the different levels of fusion surgery on the T10-T11 and T11-T12 disc stresses. The comparison is presented in Figure 4.12 and Figure 4.13. Surprisingly, no significant difference is noticed between the L1-iliac fusion and L2-iliac fusion among all three discs under all motions. Also, the values are quite close to the nonfused control model. The largest percentage differences compared with the control model are 18.8% and 13.0% (Figure 4.13) for the L1-iliac and L2-iliac fusion respectively, which are less than anticipated. Under the same loadings, the spinal range of motion is decreased by increased stiffness due to fusion compared to the control model. However, the stress level doesn't increase significantly due to the higher spinal rigidity. The T12-L1 disc under the T10-iliac fusion is 90.1% reduced from the control model. Since T12-L1 is in the range of rod-screw fusion levels, the rod and screws bear much of the load, which leads to the reduced stresses in the T12-L1 disc under all the loadings.

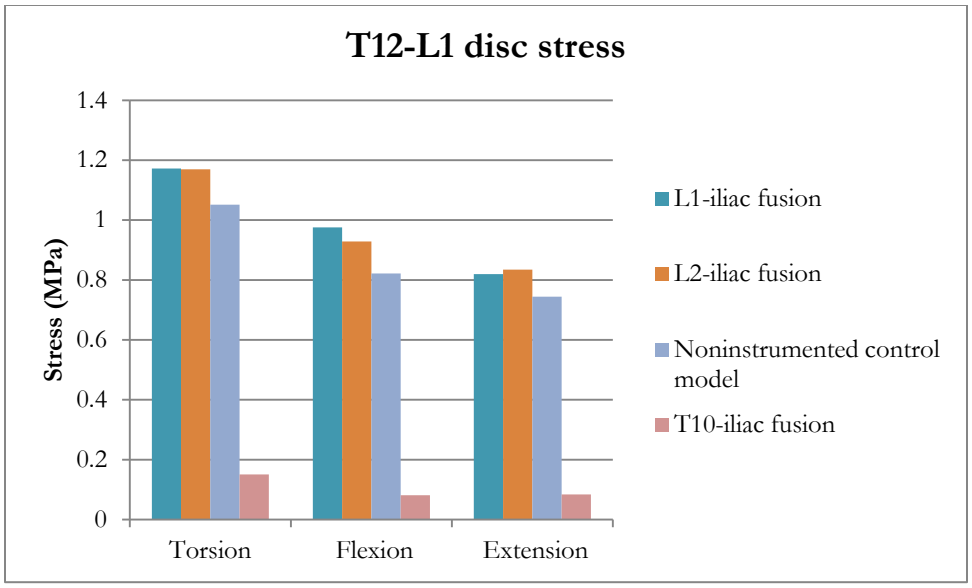

Figure 4.12. T12-L1 disc stress comparison among all fusion models during flexion, extension, and torsion motions

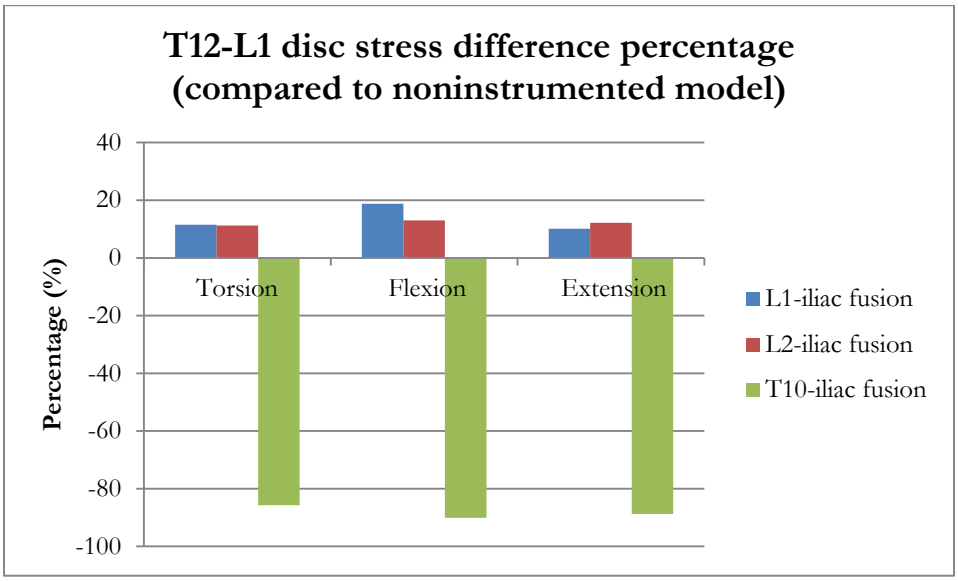

Figure 4.13. T12-L1 disc stress difference percentage between fusion models and noninstrumented model during flexion, extension, and torsion motions

The T11-T12 and T10-T11 disc stresses are presented in Figure 4.14 and 4.16. Similarly, there is no significant difference between the disc stresses induced in the L1-iliac and L2-iliac fusion models. On the T11-T12 disc, the largest percentage differences compared to noninstrumented control model are 24.5% and 26.0% for the L1-iliac and L2-iliac fusion respectively (Figure 4.15). While for the T10-T11 disc, the largest percentage differences compared with control model are 31.2% and 27.5% for the L1-iliac and L2-iliac fusion respectively (Figure 4.17). The results show that the stress increase on adjacent discs due to fusion surgery is less than anticipated, suggesting that factors other than stress increase may be the cause of adjacent disc failure after fusion surgery.

The T10-iliac fusion significantly reduced the T12-L1 disc stress compared with the control model. A T10-iliac fusion provides increased stability by connecting the lumbar spine with the thoracic region, which is the least mobile of all the spinal regions. From T10 up to T1, the thoracic vertebrae attach to the rib cage, which gives the thoracic spine strong rigidity. Note that the T10-iliac fusion may dramatically restrict spinal mobility.

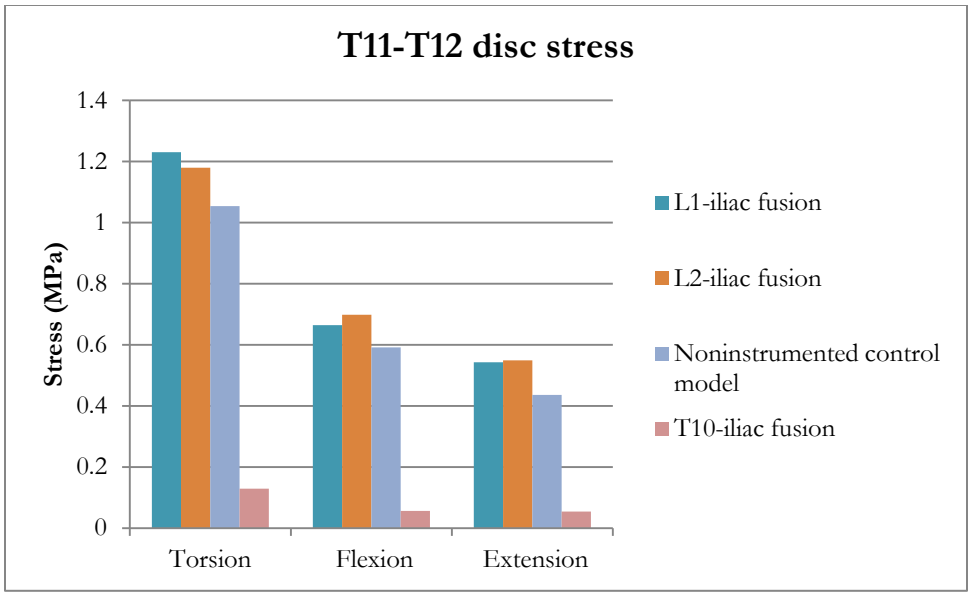

Figure 4.14. T11-T12 disc stress comparison among all fusion models during flexion, extension, and torsion motions

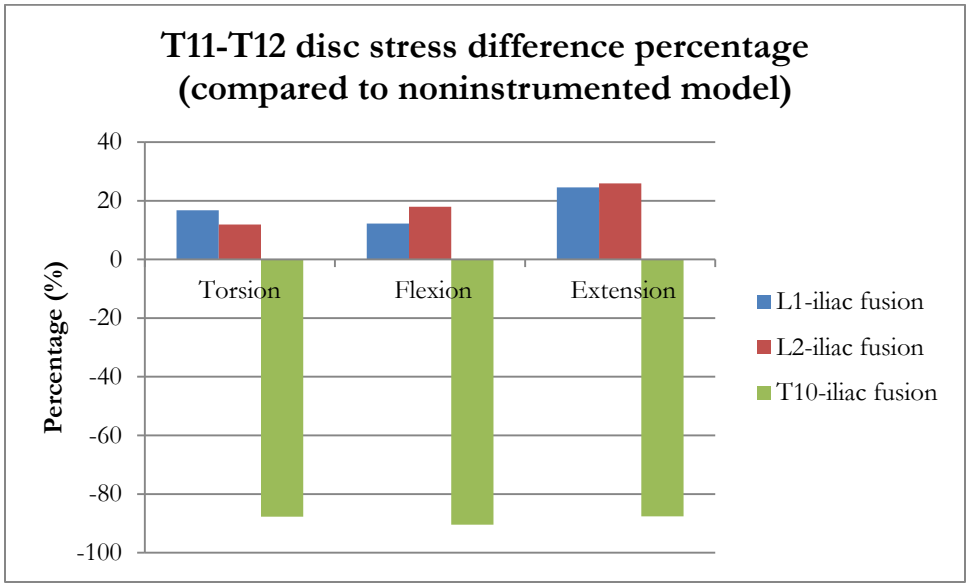

Figure 4.15. T11-T12 disc stress difference percentage between fusion models and noninstrumented model during flexion, extension, and torsion motions

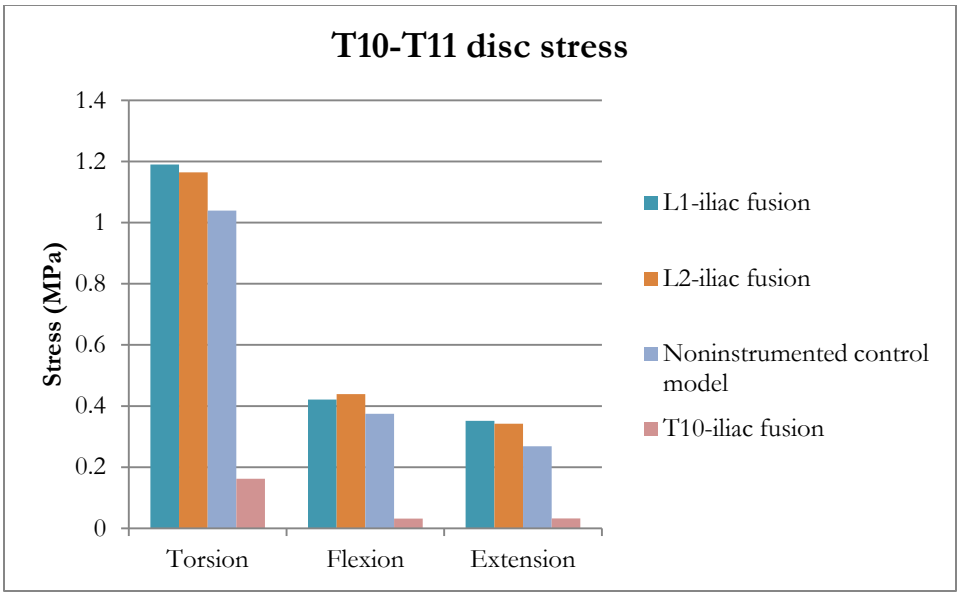

Figure 4.16. T10-T11 disc stress comparison among all fusion models during flexion, extension, and torsion motions

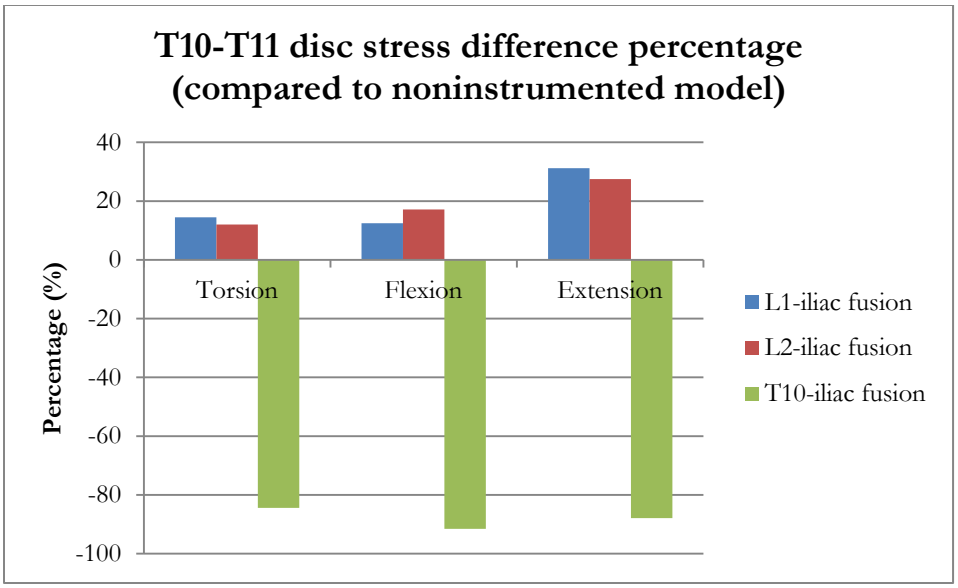

Figure 4.17. T10-T11 disc stress difference percentage between fusion models and noninstrumented model during flexion, extension, and torsion motions

4.4 Conclusion

In this chapter, four configurations of models are created to investigate how the fusion level affects on adjacent disc stress. The results show less than expected increases in adjacent disc stresses after fusion when compared with a noninstrumented control model under the same loadings. Therefore, factors other than stress increase may be the cause of adjacent disc failure after fusion surgery, such as genetic spinal diseases, infections, and damage to adjacent discs during fusion surgery.

Chapter 5

Conclusions

This dissertation presents a validated, computationally efficient finite element model of the human spine which includes the entire thoracic and lumbar portions of the spine. The model was then used to conduct parametric studies to determine the stresses induced in the spine and in spinal fusion instrumentation during flexion, torsion and extension, as the intervertebral disc stiffness values were varied to simulate different types of disc degeneration. Currently used fusion instrumentation, and novel spinal instrumentation, were both studied using the model. The stresses induced in discs adjacent to the fused portion of the spine were also studied. The main contributions of this research are summarized below:

- The finite element model of the spine presented in this dissertation encompasses the entire thoracic and lumbar portions of the human spine.

- The finite element model of the spine presented in this dissertation is computationally efficient, enabling analyses to be run very quickly, hence enabling extensive parametric analyses to be performed.

- The studies presented in this dissertation examine the effect of different types of disc degeneration on the stresses induced in the rods used in fusion surgeries.

- Parametric studies have been presented regarding the effect of different types of interbody spacers on the stresses induced in the rods used in fusion surgeries. The results indicate that for some degenerative disc conditions, the use of interbody spacers can significantly reduce the stresses induced in the rods, while for the other cases, the use of interbody spacers has little effect on the stresses induced in the rods.

- Parametric studies have been presented regarding the effect of posterior connectors on the stresses induced in the rods used in fusion surgeries. The results show that adding a truss-type structure to the fusion hardware can help to considerably reduce the stresses induced in the fusion rods, particularly under torsional loading. Under specific circumstances, DLink connectors are shown to further reduce the rod stress.

- Parametric studies have been presented regarding the effect of different types of interbody spacers on the stresses induced in adjacent discs after lumbar fusion surgery. Surprisingly, the results show that the stress increase on adjacent discs due to fusion surgery is less than anticipated, suggesting that factors other than an increase in stress may be the cause of adjacent disc failure after fusion surgery.

References

[1] Deen HG , Birch BD , Wharen RE , et al. Lateral mass screw-rod fi xation of the cervical spine: a prospective clinical series with 1-year follow-up . Spine J 2003 ; 3 : 489 – 95 .

[2] Fischgrund JS, Mackay M et al (1997). 1997 Volvo Award winner in clinical studies. Degenerative lumbar spondylolisthesis with spinal stenosis: a prospective, randomized study comparing decompressive laminectomy and arthrodesis with and without spinal instrumentation. Spine 22:2807–2812

[3] Sweet FA, Lenke LG, Bridwell KH, et al. Maintaining lumbar lordosis with anterior single solid-rod instrumentation in thoracolumbar and lumbar adolescent idiopathic scoliosis. Spine 1999;24:1655–62.

[4] Newton PO, Parent S, Marks M, et al. Prospective evaluation of 50 consecutive scoliosis patients surgically treated with thoracoscopic anterior instrumentation. Spine 2005;30(suppl 17):100–9.

[5] Bono CM, Lee CK (2004). Critical analysis of trends in fusion for degenerative disc disease over the past 20 years: influence of technique on fusion rate and clinical outcome. Spine 29:455–463

[6] Harms J, Jeszenszky D. The unilateral transforaminal approach for posterior lumbar interbody fusion. Orthop Traumatol, vol. 6, pp. 88–99, 1998.

[7] Chad D. Cole, Todd D. McCall et al., "Comparison of low back fusion techniques: transforaminal lumbar interbody fusion (TLIF) or posterior lumbar interbody fusion (PLIF) approaches," Curr Rev Musculoskelet Med, vol. 2, pp. 118-126, 2009.

[8] McCullen GM, Yuan HA. Artificial disc: current developments in artificial disc replacement. Curr Opin Orthop 2003;14:138–43.

[9] Baker JK, Reardon PR, Reardon MJ, Heggeness MH. Vascular injury in anterior lumbar surgery. Spine 1993;18:2227–30.

[10] Rajaraman V, Vingan R, Roth P, Heary RF, Conklin L, Jacobs GB. Visceral and vascular complications resulting from anterior lumbar interbody fusion. J Neurosurg 1999;91:60–4.

[11] Erasmo L. Artificial disc replacement using posterior approach. Patent US, editor; 2007.

[12] Iris Busscher, Joris J. W. Ploegmakers et al (2010). Comparative Anatomical Dimensions of the Complete Human and Porcine Spine. Eur Spine J 19: 1104-1114

[13] Naresh Kumar, Sandeep Kukreti et al (2000). Anatomy of Deer Spine and Its Comparison to the Human Spine. The Anatomical Record 260: 189-203

[14] Sun-Ren Sheng, Xiang-Yang Wang et al (2010). Anatomy of Large Animal Spines and Its Comparison to the Human Spine: a Systematic Review. Eur Spine J 19: 46-56

[15] Guan Y, Yoganandan N et al (2006). Validation of a clinical finite element model of the human lumbosacral spine. Med Biol Eng Comput 44:633–641

[16] Chen CS, Cheng CK et al (2001). Stress analysis of the disc adjacent to interbody fusion in lumbar spine. Med Eng Phys 23:483–491

[17] Goel VK, Kim YE et al (1988). An analytical investigation of the mechanics of spinal instrumentation. Spine 13:1003–1011

[18] Shirazi-Adl SA, Shrivastava SC et al (1984). Stress analysis of thelumbar disc-body

unit in compression. A three-imensional nonlinear finite element study. Spine 9:120–134

[19] Yamamoto I, Panjabi MM. Three-dimensional movements of the whole lumbar spine and lumbosacral joint. Spine, vol. 14, pp. 1256-1260, 1989.

[20] Peng XQ, Guo ZY, Moran B. An anisotropic hyperelastic constitutive model with fiber-matrix shear interaction for the human annulus fibrosus. J Appl Mech, vol. 73(5), pp. 815–824, 2006.

[21] Antonius Rohlmann, Nagananda K. Burra, Thomas Zander, Georg Bergmann. Comparison of the effects of bilateral posterior dynamic and rigid fixation devices on the loads in the lumbar spine: a finite element analysis. European Spine Journal, Vol. 16(8), pp. 1223-1231, 2007.

[22] Eberlein R, Holzapfel GA, Schulze-Bauer CAJ. An anisotropic model for annulus tissue and enhanced finite element analysis of intact lumbar disc bodies. Comp Meth Biomech Biomed Eng, vol. 4, pp. 209–229, 2000.

[23] Ching-Sung Kuo, Hsuan-Teh Hu et al.. Biomechanical analysis of the lumber spine on facet joint force and intradiscal pressure-a finite element study. BMC Musculoskeletal Disorders, vol.11, 2010.

[24] Eberlein R, Holzapfel GA, Schulze-Bauer CAJ (2000). An anisotropic model for annulus tissue and enhanced finite element analysis of intact lumbar disc bodies. Comp Meth Biomech Biomed Eng 4:209-229

[25] Pintar FA, Yoganandan N et al (1992). Biomechanical properties of human lumbar spine ligaments. J Biomech 25:1351–1356

[26] Wu HC, Yao RF (1976). Mechanical behavior of the human annulus fibrosus. J Biomech 9:1–7

[27] Kim Y (2007). Finite element analysis of anterior lumbar interbody fusion: threaded cylindrical cage and pedicle screw fixation. Spine 32:2558–2568

[28] Spilker R. Mechanical behavior of a simple model of an intervertebral disk under compressive loading. J Biomech 1980;13:895–901.

[29] Steven M. Kurtz, John N. Devine (2007). PEEK Biomaterials in Trauma, Orthopedic, and Spinal Implants. Biomaterials 28:4845-4869

[30] Dick JC, Zdeblick TA, Bartel BD, et al. Mechanical evaluation of cross-link designs in rigid pedicle screw systems. Spine 1997;22:370–5.

[31] Wood KB, Wentorf FA, Ogilvie JW, et al. Torsional rigidity of scoliosis constructs. Spine 2000;25:1893–8.

[32] Kim YJ, Bridwell KH, Lenke LG, et al. Pseudarthrosis in primary fusions for adult idiopathic scoliosis: incidence, risk factors, and outcome analysis. Spine 2005;30:468–74.

[33] Richards BR, Emara KM. Delayed infections after posterior TSRH spinal instrumentation for idiopathic scoliosis: revisited. Spine 2001;26: 1990–6.

[34] Esses SI. Mechanical stability of thoracolumbar pedicle screw fixation: the effects of crosslinks. Spine 1997;22:1573.

[35] Lynn G, Mukherjee DP, Kruse RN, et al. Mechanical stability of thoracolumbar pedicle screw fixation. The effect of crosslinks. Spine 1997;22:1568– 72, discussion 73.

[36] Brodke DS, Bachus KN, Mohr RA, et al. Segmental pedicle screw fixation or cross-links in multilevel lumbar constructs. a biomechanical analysis. Spine J 2001;1:373–9.

[37] Lim TH, Kim JG, Fujiwara A, et al. Biomechanical evaluation of diagonal fixation in pedicle screw instrumentation. Spine 2001;26:2498–503.

[38] Valdevit A, Kambic HE, McLain RF. Torsional stability of cross-link configurations:a biomechanical analysis. Spine J 2005;5:441–5.

[39] Lim TH, Eck JC, An HS. Biomechanics of transfixation in pedicle screw instrumentation. Spine 1996;21:2224–9.

[40] An HS, Lim TH, You JW, et al. Biomechanical evaluation of anterior thoracolumbar spinal instrumentation. Spine 1995;20:1979–83.

[41] Duffield RC, Carson WL, Chen LY, et al. Longitudinal element size effect on load sharing, internal loads, and fatigue life of trilevel spinal implant construct. Spine 1993;18:1695–703.

[42] Goel VK, Nye TA, Clark CR, et al. A technique to evaluate an internal spinal device by use of the Selspot system: An application to Luque closed loop. Spine 1987;12:150–9.

[43] Lim TH, An HS, ed. Principles and Techniques of Spine Surgery. Baltimore: Williams & Wilkins, 1998:63–89.

[44] Lim TH, Goel VK. Load sharing characteristics in the stabilized lumbar motion segment: A finite element study. J Musculoskeletal Res 1998;2:55–64.

[45] McLain R, Kambic H, Valdevit A. Torsional stability of various cross-link configurations. Hawaii: International Society for the Studies of Lumbar Spine, 1999:214B.

[46] McNamara MJ, Dawson JM, Meyer L, et al. Evaluation of cross-linking members in a porcine laminectomy model. NASS 1992:107.

[47] Panjabi MM. Biomechanical evaluation of spinal fixation devices: I. A conceptual framework. Spine 1988;13:1129–34.

[48] Texada RP, Mukherjee DP, Mayeux RH, et al. Thoracolumbar fracture fixation: A novel arrangement of crosslinks. Anaheim, CA: Orthopaedic Research Society, 1999:992.

[49] Dick JC, Jones MP, Zdeblick TA, et al. A biomechanical comparison evaluating the use of intermediate screws and crosslinkage in lumbar pedicle fixation. NASS 1993:142.

[50] Lim TH, An HS, Hong JH, et al. Biomechanical evaluation of anterior and posterior fixations in an unstable calf spine model. Spine 1997;22:261–6.

[51] Lim TH, Eck JC, An HS, et al. Biomechanics of transfixation in pedicle screw instrumentation. Spine 1996;21:2224–9

[52] Kamra Majid, Manasa Gudipally, Mir Hussain, et al. The biomechanical effect of transverse connectors use in a pre- and postlaminectomy model of the posterior cervical spine. Spine 2011; 36: 1694-1701

[53] Tae-Hong Lim, Jesse G. Kim, Atsushi Fujiwara, et al. Biomechanical evaluation of diagonal fixation in pedicle screw instrumentation. Spine 2001; 26: 2498-2503

[54] Lee CK (1988). Accelerated degeneration of the segment adjacent to a lumbar fusion. Spine 13:375–377

[55] Park P, Garton HJ et al (2004). Adjacent segment disease after lumbar or lumbosacral fusion: review of the literature. Spine 29:1938–1944

[56] Shono Y, Kaneda K et al (1998). Stability of posterior spinal instrumentation and its effects on adjacent motion segments in the lumbosacral spine. Spine 23:1550–1558

[57] Rahm MD, Hall BB (1996) Adjacent-segment degeneration after lumbar fusion with instrumentation: a retrospective study. J Spinal Disord 9:392–400

[58] Kim YE, Goel VK, Weinstein JN, Lim TH. Effect of disc degeneration at one level on the adjacent level in axial mode. Spine 1991;16:331–5.

[59] Lee CK. Accelerated degeneration of the segment adjacent to a lumbar fusion. Spine 1988;13:375–7.

[60] Louw JA, Dommissee GF, Roos MF. Spinal stenosis following anterior spinal fusion. Spine 1988;13:952–3.

[61] Schlegel JD, Smith JA, Schleusener RL. Lumbar motion segment pathology adjacent to thoracolumbar, lumbar, and lumbosacral fusions. Spine 1996;21:970–81.

[62] Takahashi K, Kitahara H, Yamagata M, Murakami M, Takata K, Miyamoto K, Mimura M, Takahashi Y, Moriya H. Long-term results of anterior interbody fusion for treatment of degenerative spondylolisthesis. Spine 1990;15:1211–5.

[63] Lehmann TR, Tozz JE, Weinstein JN, Reinarz SJ, El-Khoury G. Long term follow up of lower lumbar fusion patient. Spine 1987;12:97–103.

[64] Lee CK, Langrana NA. Lumbosacral spinal fusion. A biomechanical study. Spine 1984;9:574–81.

[65] Frymoyer JW, Hanley E, Howe J, Kuhlmann D, Matteri R. Disc excision and spine fusion in the management of lumbar disc disease. Spine 1978;3:1–6.

[66] Inoue S, Watanabe T, Goto S, Takahashi K, Takata K, Sho E. Degenerative spondylolisthesis, pathophysiology and results of anterior interbody fusion. Clin Orthop 1988;227:90–8.

[67] Bastian L, Lange U, Knop C, Tusch G, BlauthM. Evaluation ofthemobility of adjacent segments after posterior thoracolumbar fixation: a biomechanical study. Eur Spine J 2001;10:295–300.

[68] Kumar MN, Jacquot F, Hall H. Long-term follow-up of functional outcomes and radiographic changes at adjacent levels following lumbar spine fusion for degenerative disc disease. Eur Spine J 2001;10:309–13.

[69] Bono CM, Lee CK. Critical analysis of trends in fusion for degenerative disc disease over thepast 20 years—influence oftechnique onfusionrate andclinical outcome. Spine 2004;29:455–63.

[70] Hilibrand, A.S., Carlson, G.D., Palumbo, M.A., Jones, P.K., Bohlman, H.H., 1999. Radiculopathy and myelopathy at segments adjacent to the site of a previous anterior cervical arthrodesis. J. Bone Joint Surg. Am. 81, 519–528.

[71] Goffin, J., Geusens, E., Vantomme, N., Quintens, E., Waerzeggers, Y., Depreitere, B., Van Calenbergh, F., Van Loon, J., 2004. Long-term follow-up after interbody fusion of the cervical spine. J. Spinal Disord. Tech. 17, 79–85.

[72] Gore DR, Sepic SB. Anterior cervical fusion for degenerated or protruded discs. A review of one hundred forty-six patients. Spine (Phila Pa 1976) 1984;9:667–71.

[73] Eck, J.C., Humphreys, S.C., Lim, T.H., Jeong, S.T., Kim, J.G., Hodges, S.D., An, H.S., 2002. Biomechanical study on the effect of cervical spine fusion on adjacent-level intradiscal pressure and segmental motion. Spine 27, 2431–2434.

APPENDIX

Appendix A

Fusion Rods Material Substitution - Titanium

A.0.1 Parametric study of stresses induced in the spine and in associated spinal fusion hardware, as intervertebral disc conditions are varied parametrically with respect to stiffness with titanium rods instead of cobalt chrome

In the study, based on the basic methods of chapter 2 of this dissertation, cobalt rods are replaced by titanium material to see whether it can reduce the rod stress. A 3D spine model from T1 to the pelvis is created in this work to study the spinal degeneration process as intervertebral disc conditions are varied parametrically with respect to stiffness. The rod-screw construct fusion in this model starts from T2 all the way down to iliac wing. As discussed earlier, a model with ALIF implanted in both L4-L5 and L5-S1 levels is presented in Figure 2.12. A variety of spinal fusion instrumentation constructs are studied. ALIF is placed at the center between vertebrae, and TLIF is located as anteriorly as possible.

As in Chapter 2, in this study, finite element analysis is used to show the potential to provide surgeons with guidance as to when to implant one or two interbody devices to reduce the risk of rod breakage.

All nodes on the bottom of the pelvis are fixed in all directions. The annulus fibrosus in the intervertebral discs is modeled as linear elastic material in this work. Interbody devices (TLIF and ALIF) are made out of poly ether ether ketone (PEEK) [29]. The rod is made out of titanium. The other material properties are the same as the ones used in L1-S1 validation model. All material information of this T1-Pelvis model is listed in Table A.1.

Table A.1. Material and mechanical properties in T1-Pelvis model

Component	Element type	Young's Modulus (MPa)	Cross-section (mm^2)	Poisson's ratio
Cortical bone	Shell	12000	-	0.3
Trabecular bone	Solid	100	-	0.2
Annulus fibrosus	Solid	Parametric Study	-	0.3
Posterior elements	Solid	3500	-	0.25
Ligaments	Spring			
Anterior longitudinal		7.8(<12%) 20(>12%)	63.7	-
Posterior longitudinal		10(<11%) 20(>11%)	20.0	-
Intertransverse		10(<18%) 58.7(>18%)	1.8	-
Interspinous		10(<14%) 11.6(>14%)	40.0	-
Ligamentum flavum		15(<6.2%) 19.5(>6.2%)	40.0	-
Capsular		7.5(<25%) 32.9(>25%)	30.0	-
Supraspinous		8(<20%) 15(>20%)	30.0	-
Sacrum	Solid	12000	-	0.3
Fusion rods (Titanium)	Solid	116000	-	0.32
Fusion screws (Titanium)	Solid	116000	-	0.32
Interbody device (PEEK)	Solid	3800	-	0.3

After consulting with surgeons, based on surgical practice, a TLIF cannot be implanted on the spinal level below ALIF if there is already one ALIF implanted. Therefore, totally 8 models are

modeled to include all the possible interbody device combinations (Table 2.4).

A 40 N concentrate force is applied at the center of the spine model to simulate the extension/flexion motions. A 10 Nm moment is imposed on the spine to create the torsion motion.

Figure A.1-A.3 show the maximum rod stress on models with no spacers implanted and with spacers implanted in the L4-L5 spacer model models during extension, flexion and torsion motions, as the L4-L5 and L5-A1 disc stiffness parameters are varied parametrically from 1 MPa to 3000 MPa; these values are chosen to reflect the range of stiffness values which have been observed in the human spine during cadaver studies, with the normal stiffness value of the human spine being 4 MPa [23]. For this study all of the discs above L4-L5 are assumed to be healthy, i.e. their disc stiffness values are set to 4 MPa. As the results show, during extension and flexion motions, larger maximum rod stresses occur when the disc properties are set as degeneratively soft (Young's modulus of 1 MPa). As mentioned above, in accordance with the biomechanics literature, a healthy disc is modeled as having a Young's modulus of 4 MPa [23]. Once disc properties are stiffer than 4 MPa, the maximum rod stress decreases and becomes lower than the stresses that occur when the discs are healthy; this is most likely due to the fact that more rigid discs take up more of the load than do healthier, softer discs. Disc properties can become stiffer during a process called self-fusion, in which the discs become more rigid; this of course reduces flexibility in the spine, but does have the positive effect of the maximum rod stress which occurs in the rods used in spinal fusion surgery. Of course, during the months after the implantation of spinal fusion rods, the discs which are now immobilized tend to self-fuse and become rigid, leading to less stress on the rods, but the initial disc stiffness is very important in that it affects the stresses induced in the rods in the months occurring immediately after surgery. Based on the results, we see that replacing a degeneratively soft L4-L5 disc with an interbody device can significantly reduce the maximum rod stress. However, if the discs are already stiffer prior to surgery due to a degenerative process, the implantation of an interbody device may not be necessary.

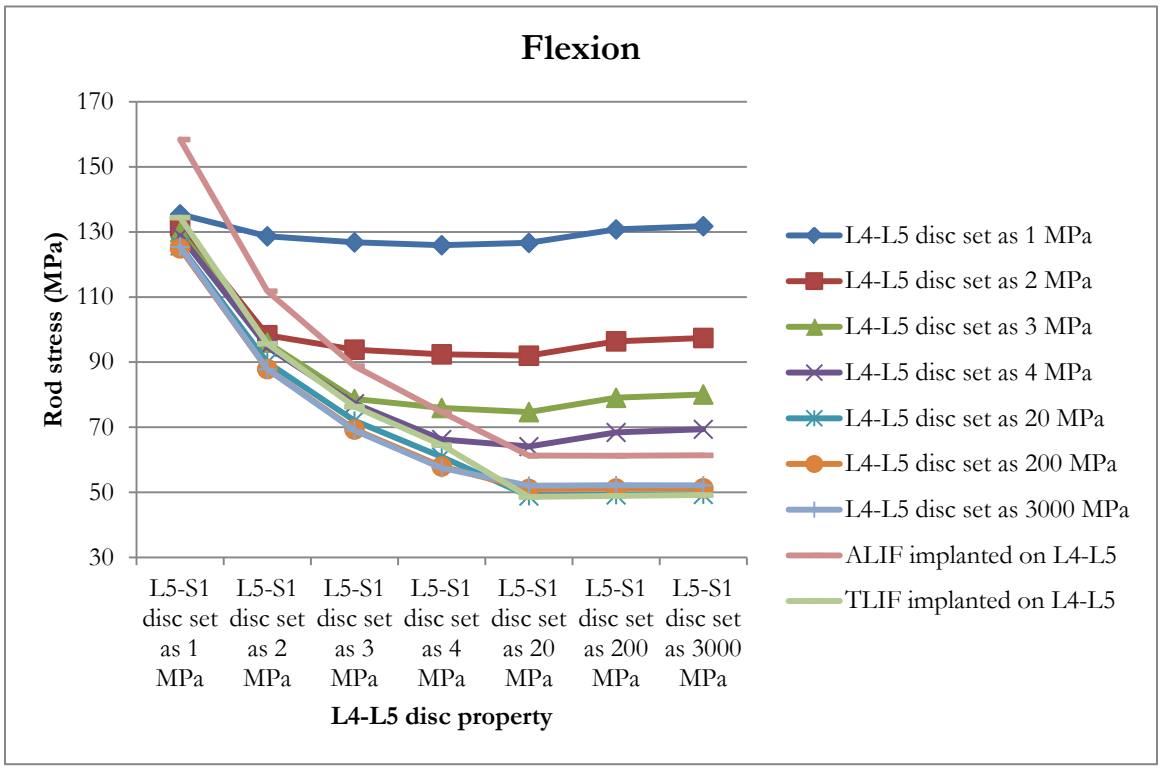

Figure A.1. Maximum rod stress (MPa) on non-spacer model and L4-L5 spacer models during disc degeneration in flexion motion

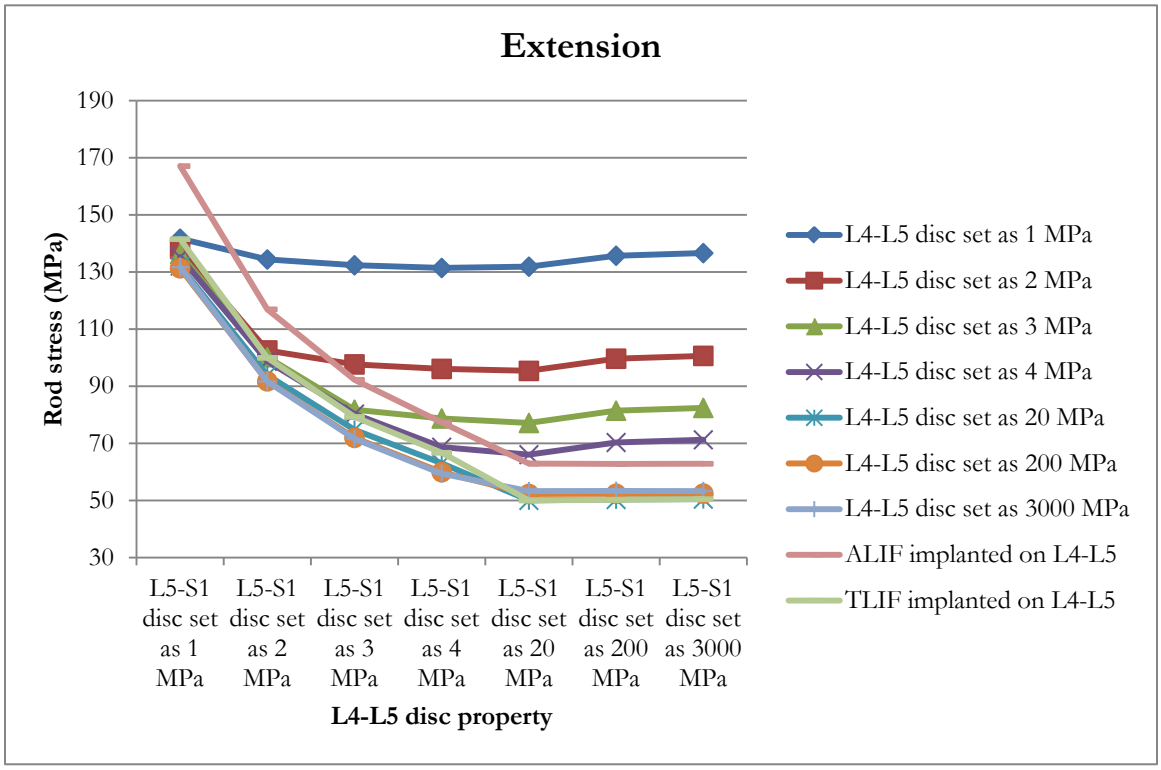

Figure A.2. Maximum rod stress (MPa) on non-spacer model and L4-L5 spacer models during disc degeneration in extension motion

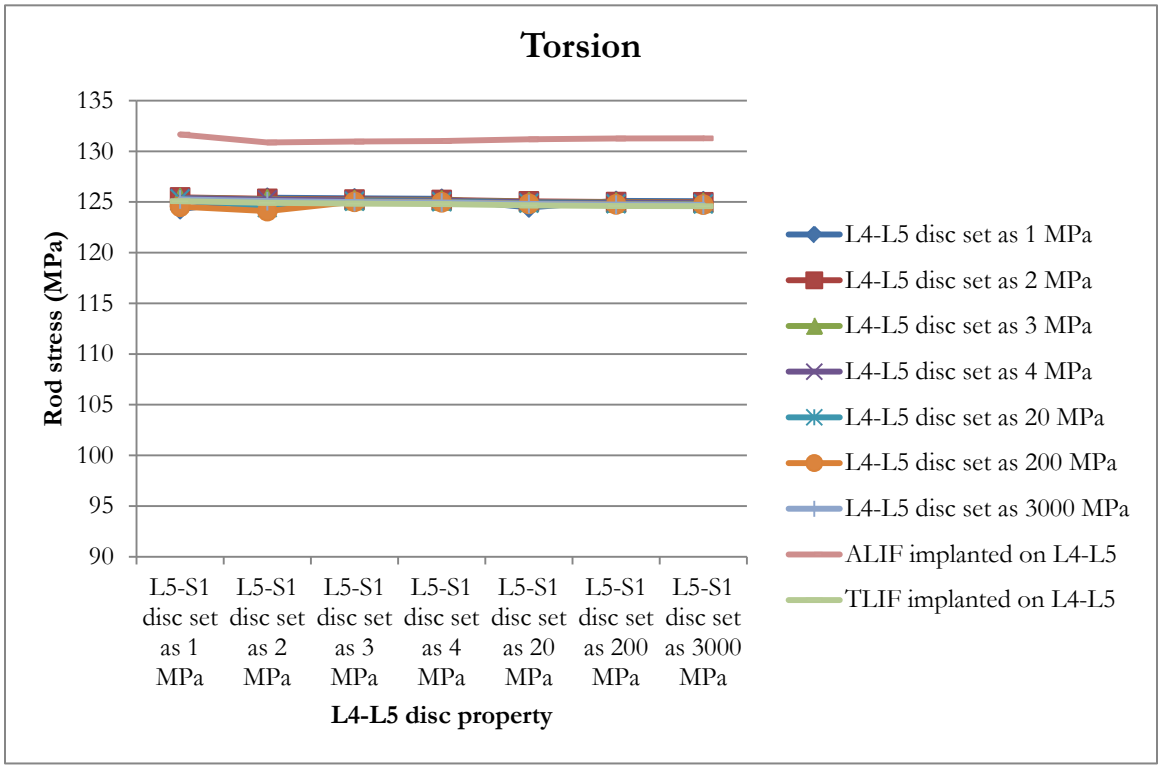

Figure A.3. Maximum rod stress (MPa) on non-spacer model and L4-L5 spacer models during disc degeneration in torsion motion

Figure A.1-A.3 also illustrate if both L4-L5 and L5-S1 discs are degeneratively soft (i.e. with a Young's modulus of 1 MPa), just replacing L4-L5 disc with an interbody device doesn't reduce the maximum rod stress during extension and flexion motions. In fact, in some cases adding an interbody device induces an even larger maximum rod stress. For example, in the model with an ALIF implanted on L4-L5 (yellow dot curve), when L5-S1 is degeneratively soft we have that in extension the maximum rod stress is 17.9% higher than the model where both discs are degeneratively soft. A similar situation also occurs during flexion motion.

Figure A.4-A.6 depict the maximum rod stress on models with an ALIF implanted at the L4-L5 level, and the L5-S1 stiffness varied parametrically (including a case where an ALIF is also implanted at L5-S1, as discussed below), during extension, flexion, and torsion. The motivation for this study is to investigate when a second interbody device should be implanted to reduce the risk of rod breakage. As discussed previously, if the L5-S1 disc is degeneratively soft, an interbody device implanted on L4-L5 doesn't reduce the maximum rod stress. In surgical practice, a second interbody device is often implanted to further provide the spine with more rigidity. In this case, an ALIF is already placed between L4 and L5. According to surgical protocols, a TLIF normally wouldn't be implanted between spinal levels below ALIF implant. Therefore, one model with an additional ALIF implanted at the L5-S1level is created.

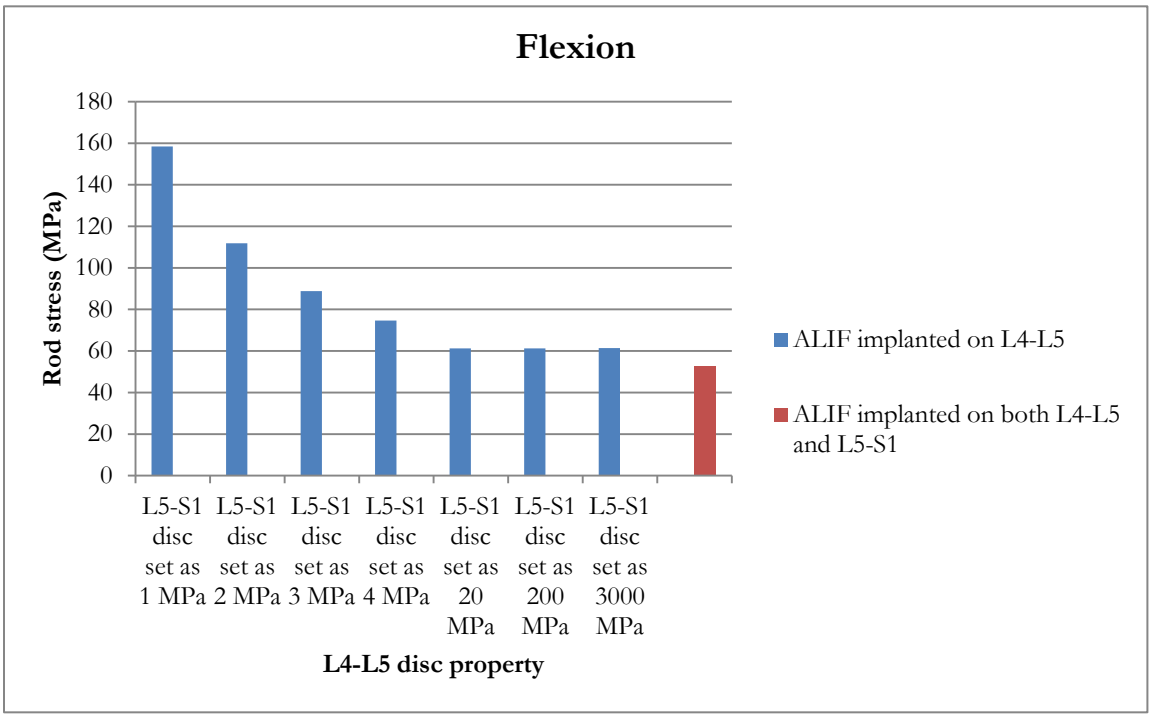

Figure A.4. Maximum rod stress (MPa) on models with ALIF implanted on the L4-L5 level during disc degeneration in flexion motion

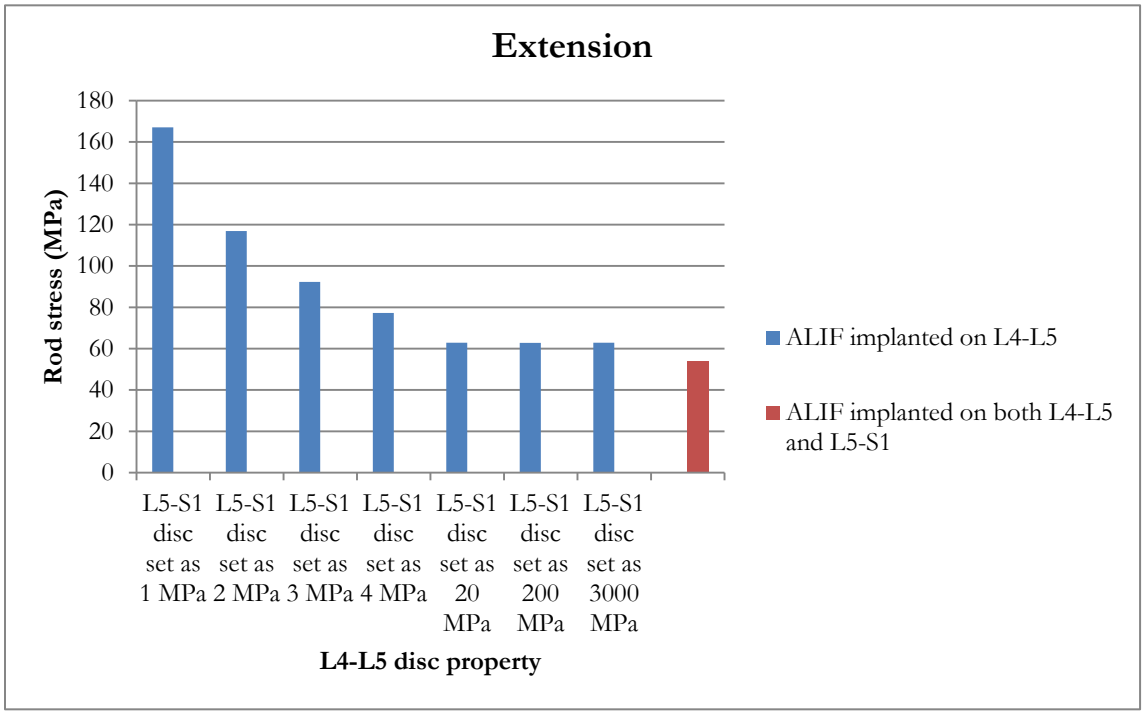

Figure A.5. Maximum rod stress (MPa) on models with ALIF implanted on the L4-L5 level during disc degeneration in extension motion

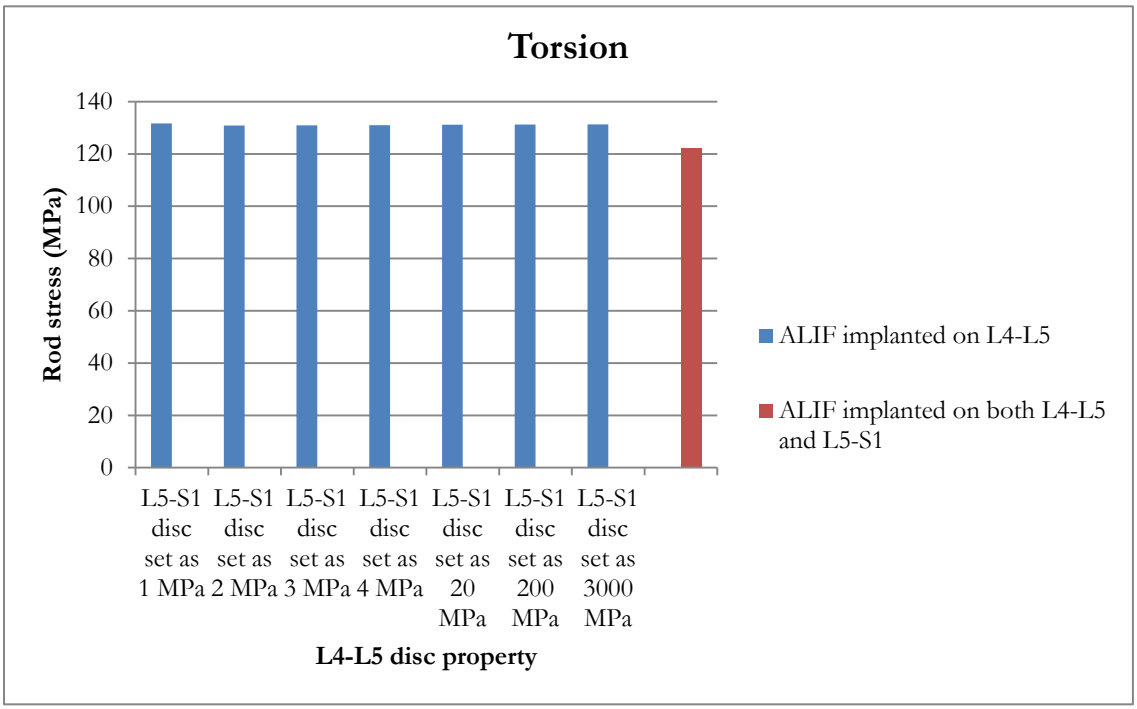

Figure A.6. Maximum rod stress (MPa) on models with ALIF implanted on the L4-L5 level during disc degeneration in torsion motion

Von Mises stress of each model is tabulated to compare the maximum rod stress. For the model with an ALIF implanted on L4-L5 (blue bars), we see that the highest maximum rod stress occurs when the L5-S1 disc's Young's modulus is set as 1 MPa. For both extension and flexion motions, the maximum rod stress decreases when the L5-S1 disc becomes stiffer, as expected. The maximum rod stress decreases 62.4% as the L5-S1 disc property is varied from 1 MPa to 3000 MPa under extension. The percentage difference is 61.2% under flexion.

During extension and flexion motions, a second ALIF spacer (red bars) can significantly reduce the maximum rod stress if the L5-S1 disc is degeneratively soft. If the L5-S1 disc is stiffer than normal (i.e. its Young's modulus is higher than 4 MPa), the second ALIF on L5-S1 has no significant impact on reducing the maximum rod stress. Similarily, there is no significant difference between the two models under torsional loading for all of the parameter values investigated.

Figure A.7-A.9 demonstrate the maximum rod stress on models with a TLIF implanted on L4-L5 during disc degeneration in extension, flexion and torsion motions. The study assumes the surgical scenario of a patient who has a TLIF implanted between L4 and L5 disc already. In surgical practice, either an ALIF or a TLIF can be implanted at the L5-S1 disc level if necessary. To match standard surgical protocols, two models with either an ALIF or TLIF implanted at the L5-S1 level are modeled.

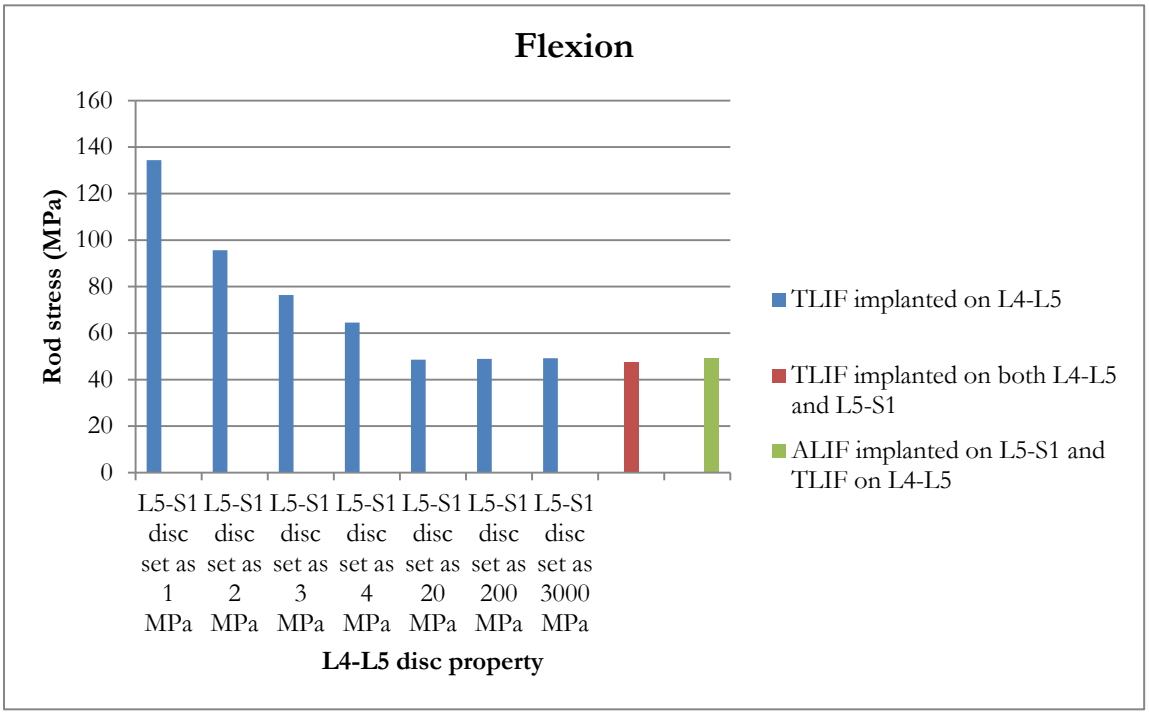

Figure A.7. Maximum rod stress (MPa) on models with TLIF implanted on the L4-L5 level during disc degeneration in flexion motion

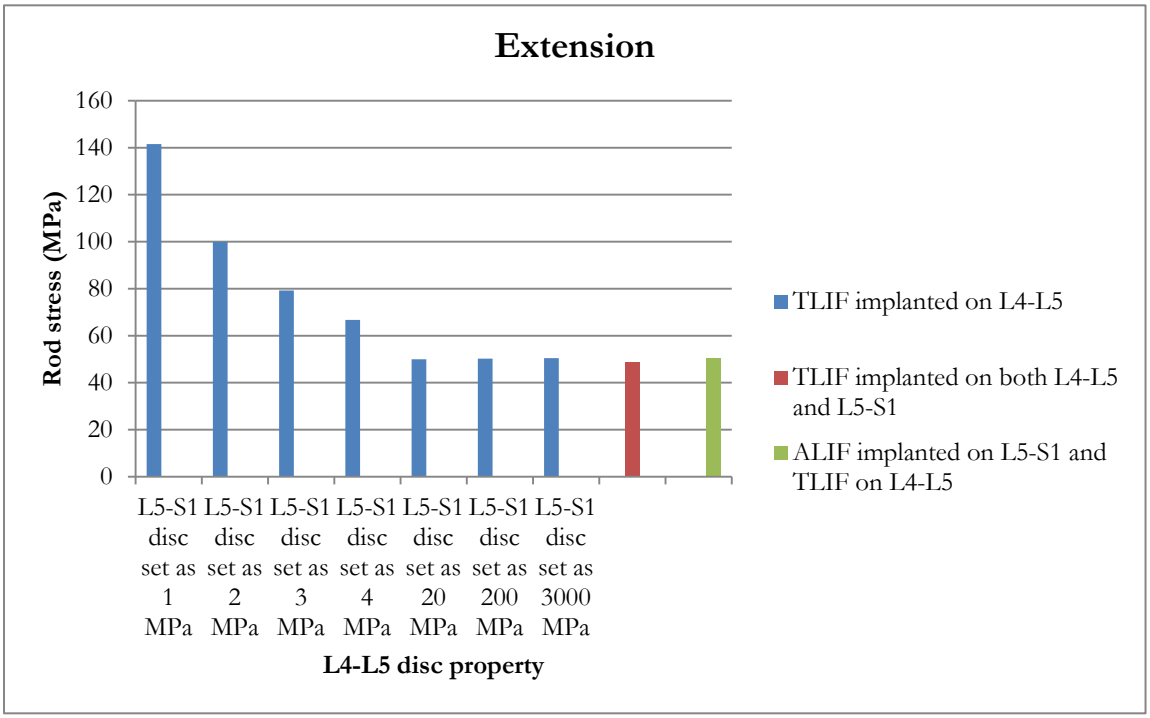

Figure A.8. Maximum rod stress (MPa) on models with TLIF implanted on the L4-L5 level during disc degeneration in extension motion

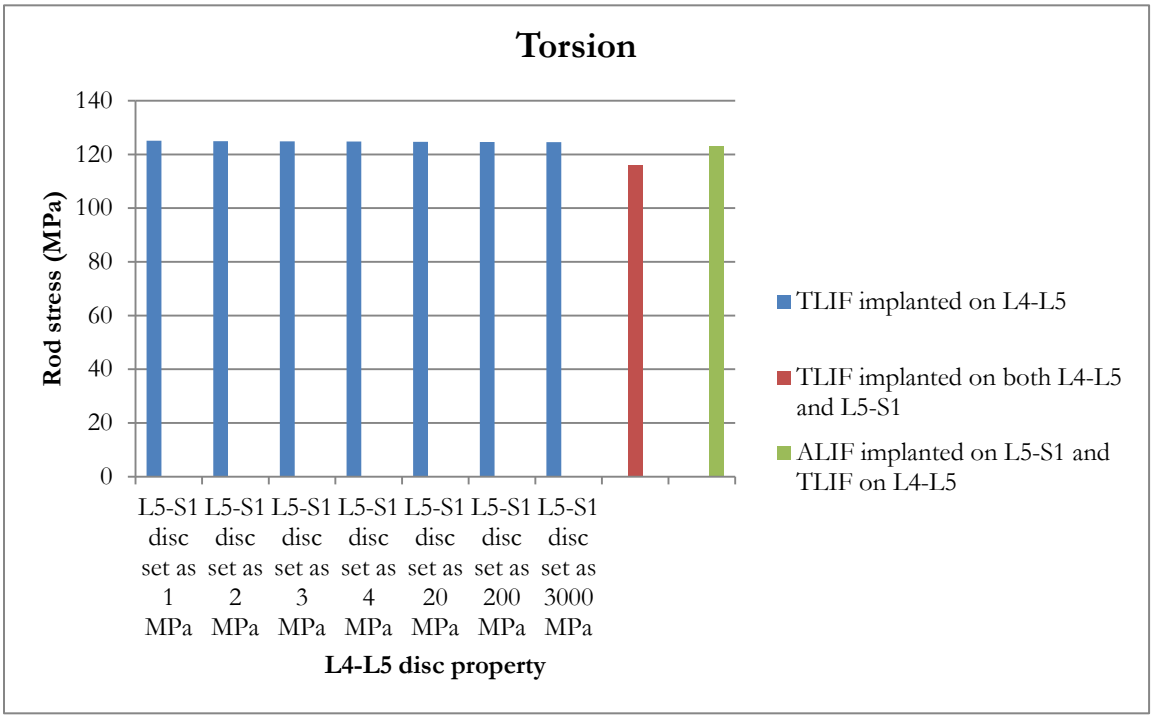

Figure A.9. Maximum rod stress (MPa) on models with TLIF implanted on the L4-L5 level during disc degeneration in torsion motion

For the model with a TLIF implanted on L4-L5 (blue bars), the maximum rod stress decreases when the L5-S1 disc gets stiffer under extension and flexion motions. 63.4% and 63.5% percentage differences are noticed, respectively, for extension and flexion when the L5-S1 disc stiffness property is changed from 1 MPa to 3000 MPa.

As Figure A.7-A.9 depict, either ALIF (green bars) or TLIF (red bars) can significantly reduce the maximum rod stress if L5-S1 disc is degeneratively soft. In this case, a second spacer can be critical to prevent the risk of rod breakage. Similarly as discussed earlier, no spacer would be necessary if the disc is already degeneratively stiff prior to surgery. During torsion motion, we see that all the models generate similar maximum rod stresses.

Note that there is no significant difference between an ALIF and TLIF at reducing the maximum rod stress. As the name implies, ALIF requires surgeons to operate from the anterior side of the patient. Currently, most of the spinal fusion is implanted on the posterior side, such as rod-screw constructs, so implanting an ALIF increases both the surgical difficulty and time, which are directly related to the surgical cost and also increase the possibility of post-surgical complications. Also, in some cases, vascular injuries have been seen to occur with the anterior surgical approach. A TLIF, however, can be implanted from the posterior side, where the rod-screws construct is located; since a TLIF serves a similar function in reducing the risk of rod breakage, a TLIF may be a better option than an ALIF for some cases in which the spacer is being implanted to replace a degeneratively soft disc for the purpose of reducing the stresses induced in the fusion rods.

Figure A.10-A.12 present the maximum rod stresess for the non-spacer model and the L5-S1 spacer models during extension, flexion, and torsion motions. As discussed earlier, the interbody devices implanted on L4-L5 are already studied. In Figure A.4, the simulation focuses on how the interbody devices influence on spinal performance when they are implanted on L5-S1.

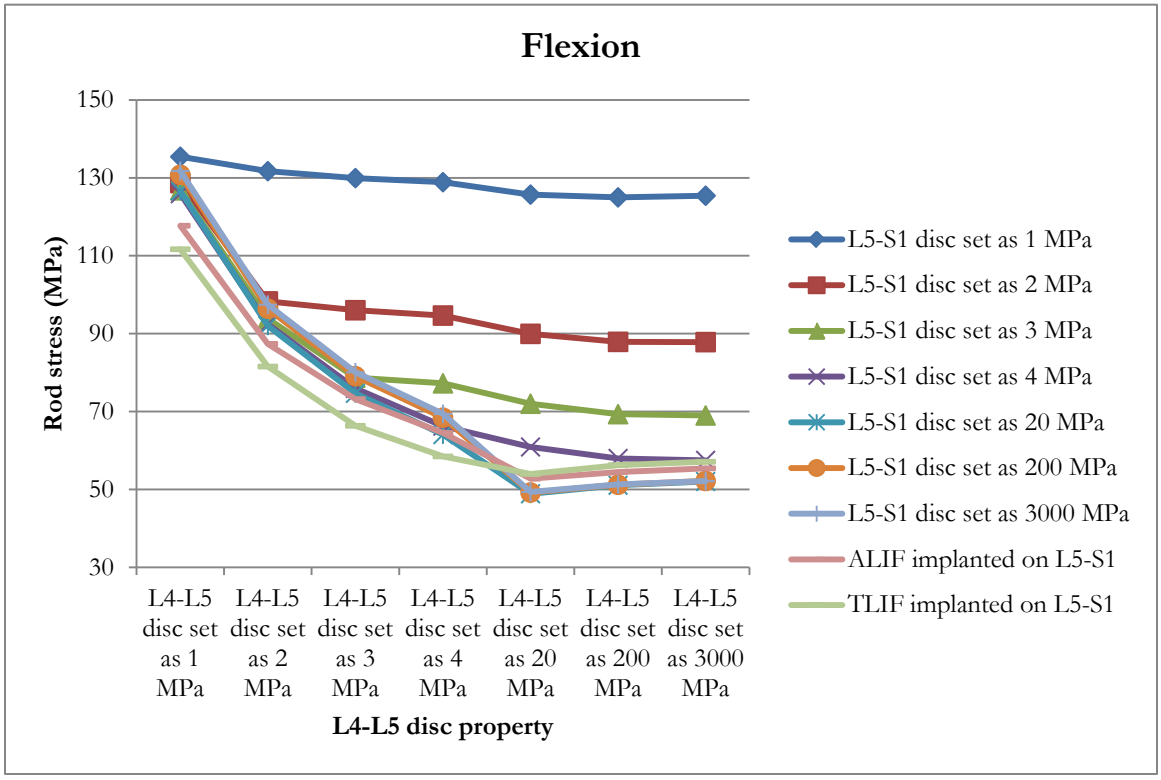

Figure A.10. Maximum rod stress (MPa) on non-spacer model and L5-S1 spacer models during disc degeneration in flexion motion

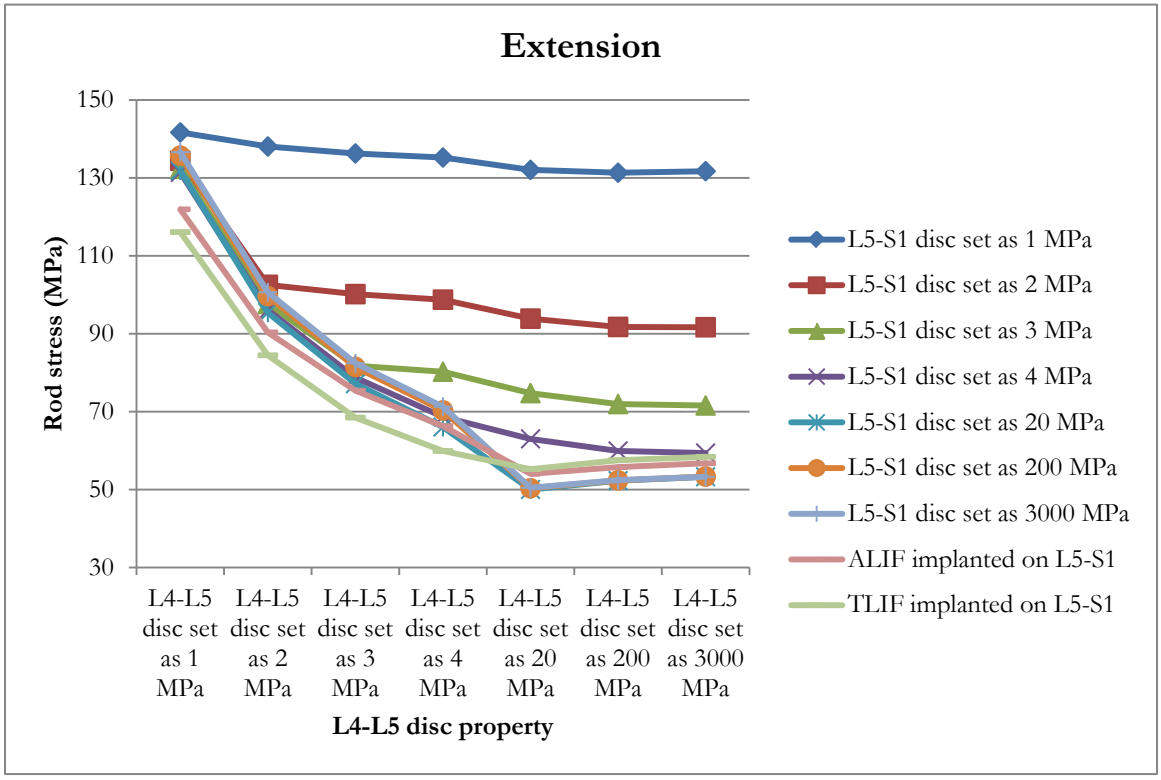

Figure A.11. Maximum rod stress (MPa) on non-spacer model and L5-S1 spacer models during disc degeneration in extension motion

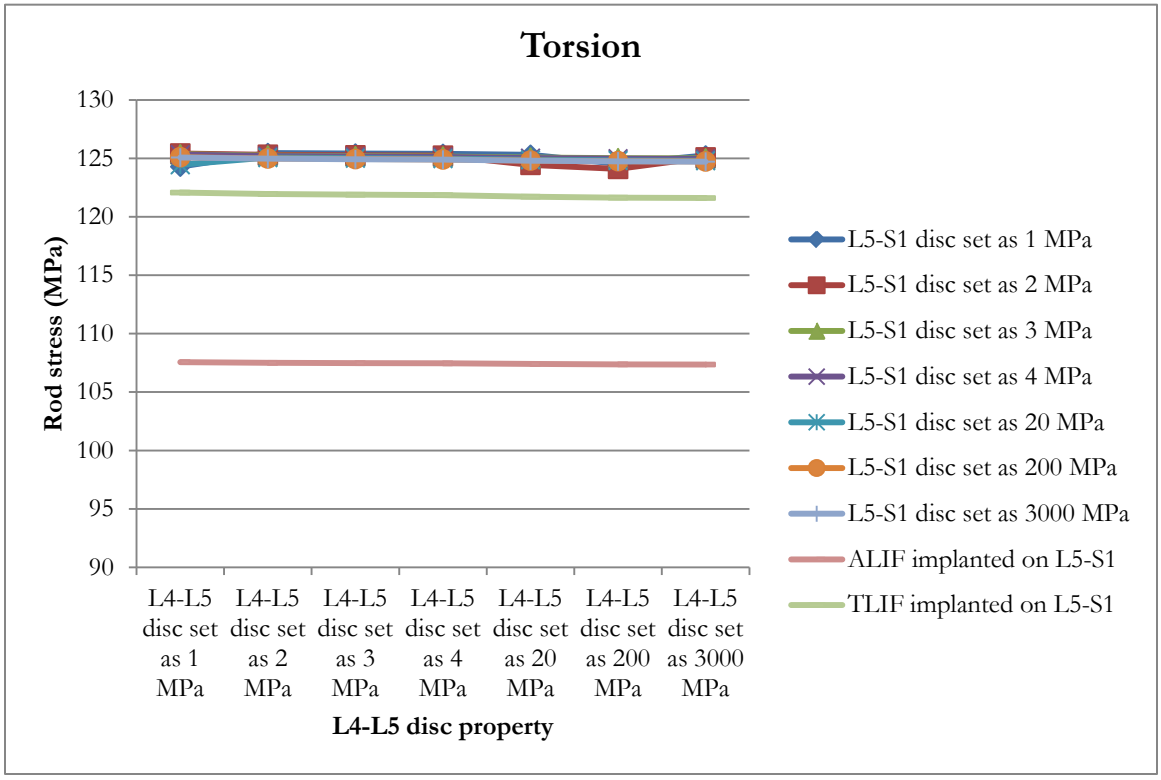

Figure A.12. Maximum rod stress (MPa) on non-spacer model and L5-S1 spacer models during disc degeneration in torsion motion

During extension and flexion motions, the results show that an interbody device can significantly reduce the maximum rod stress if the L5-S1 disc is degeneratively soft. When the L5-S1 disc gets stiffer (i.e. its Young's modulus is higher than 4 MPa), neither an ALIF nor a TLIF affects a significant reduction of the maximum rod stress. However, it is also noticed that the maximum rod stress is still considerably high even with interbody device implanted when L4-L5 disc is degeneratively soft, which necessitates the requirement of a second interbody device. Under torsional loading, all the models generate similar maximum rod stress. Figure A.13-A.15 show the maximum rod stress on models with an ALIF implanted on the L5-S1 level in extension, flexion, and torsion motions. In this simulation, an ALIF is already implanted to replace the L5-S1 disc. L4-L5 disc conditions are varied parametrically with respect to disc stiffness to study its influence on rod stresses. Since an ALIF is first placed at the bottom lumbar disc level (L5-S1), either ALIF or TLIF can be placed at L4-L5 based on surgical protocol. Therefore, two additional models are created.

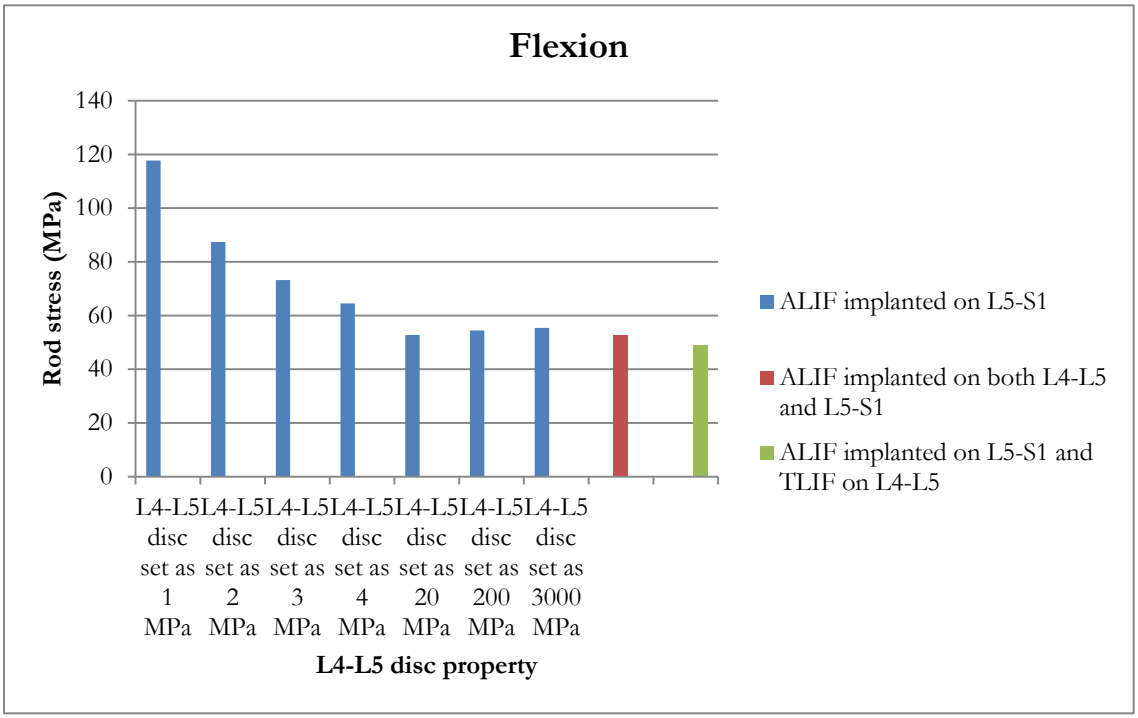

Figure A.13. Maximum rod stress (MPa) on models with ALIF implanted on the L5-S1 level during disc degeneration in flexion motion

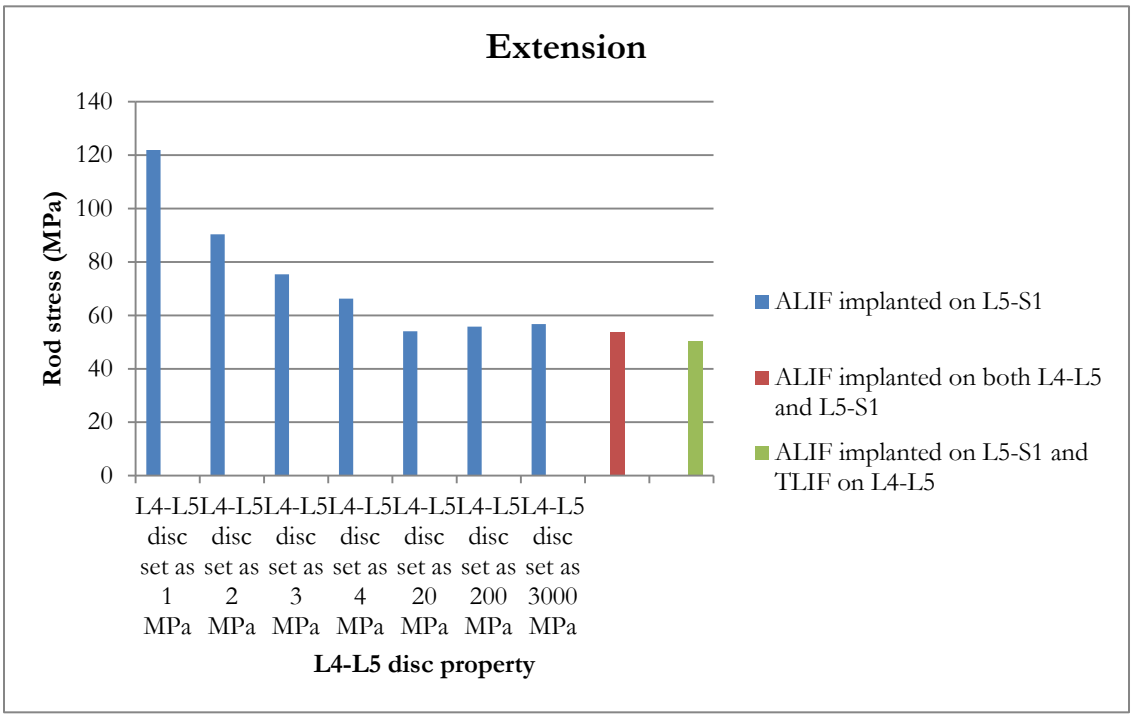

Figure A.14. Maximum rod stress (MPa) on models with ALIF implanted on the L5-S1 level during disc degeneration in extension motion

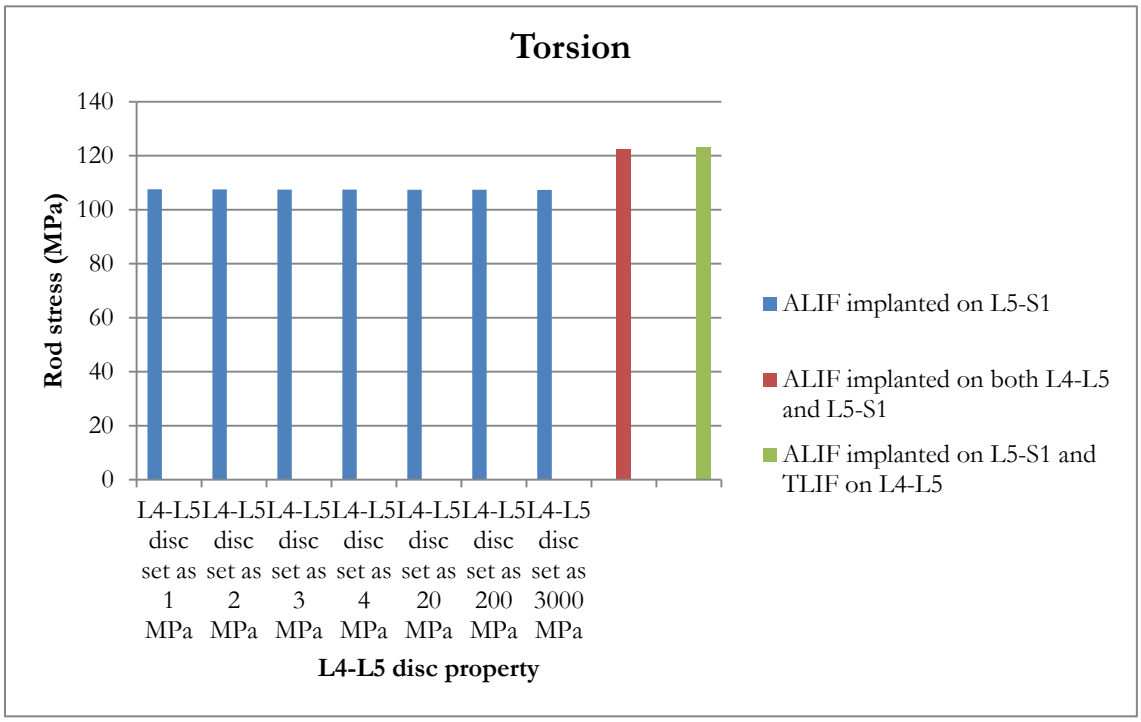

Figure A.15. Maximum rod stress (MPa) on models with ALIF implanted on the L5-S1 level during disc degeneration in torsion motion

For the model with an ALIF implanted on L5-S1 (blue bars), the maximum rod stresses are reduced by 53.5% and 52.9% under extension and flexion respectively when the L4-L5 disc property varies from 1 MPa to 3000 MPa. As discussed earlier, the maximum rod stress is still quite high when the L4-L5 disc is degeneratively soft. A second interbody device replacement on the L4-L5 level (red and green bars) can significantly reduce the maximum rod stress when L4-L5 disc is degeneratively soft. If the L4-L5 disc becomes stiffer (Young's modulus is higher 4 MPa), a second interbody device implant is not necessary. The maximum rod stress decreased automatically due to the higher spinal rigidity provided by stiffer discs. No significant difference is noticed between an ALIF and TLIF at reducing the maximum rod stress as they are used as the second interbody device.

Finally, in the last simulation, a TLIF is first placed at L5-S1 level. Similarly, two additional models with either ALIF or TLIF implanted on L5-S1 are modeled to investigate the necessity of a second interbody device. The maximum rod stress on models with a TLIF implanted on the L5-S1 level during disc degeneration in extension, flexion and torsion motions is presented in Figure A.16-A.18.

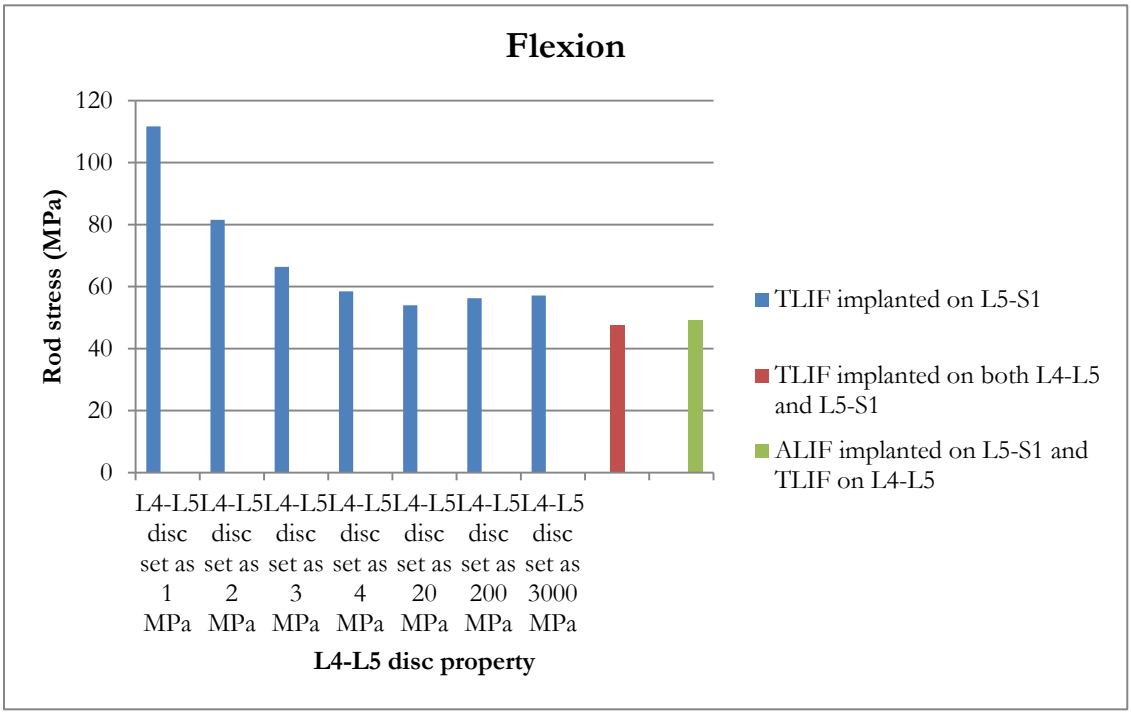

Figure A.16. Maximum rod stress (MPa) on models with TLIF implanted on the L5-S1 level during disc degeneration in flexion motion

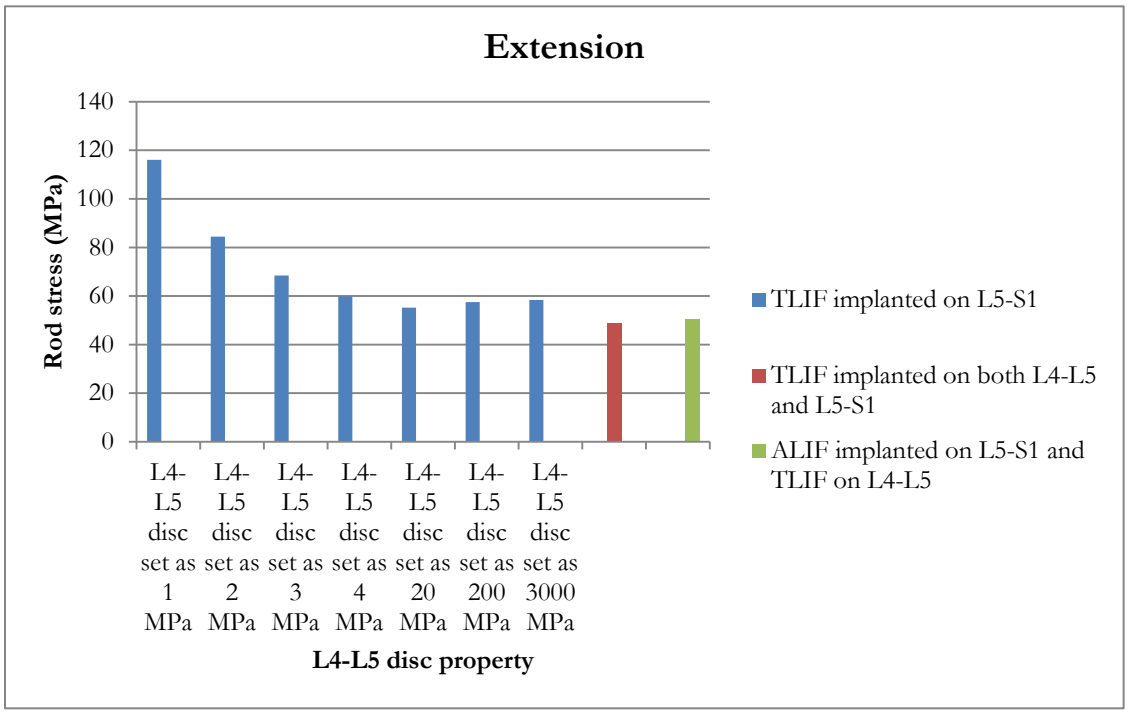

Figure A.17. Maximum rod stress (MPa) on models with TLIF implanted on the L5-S1 level during disc degeneration in extension motion

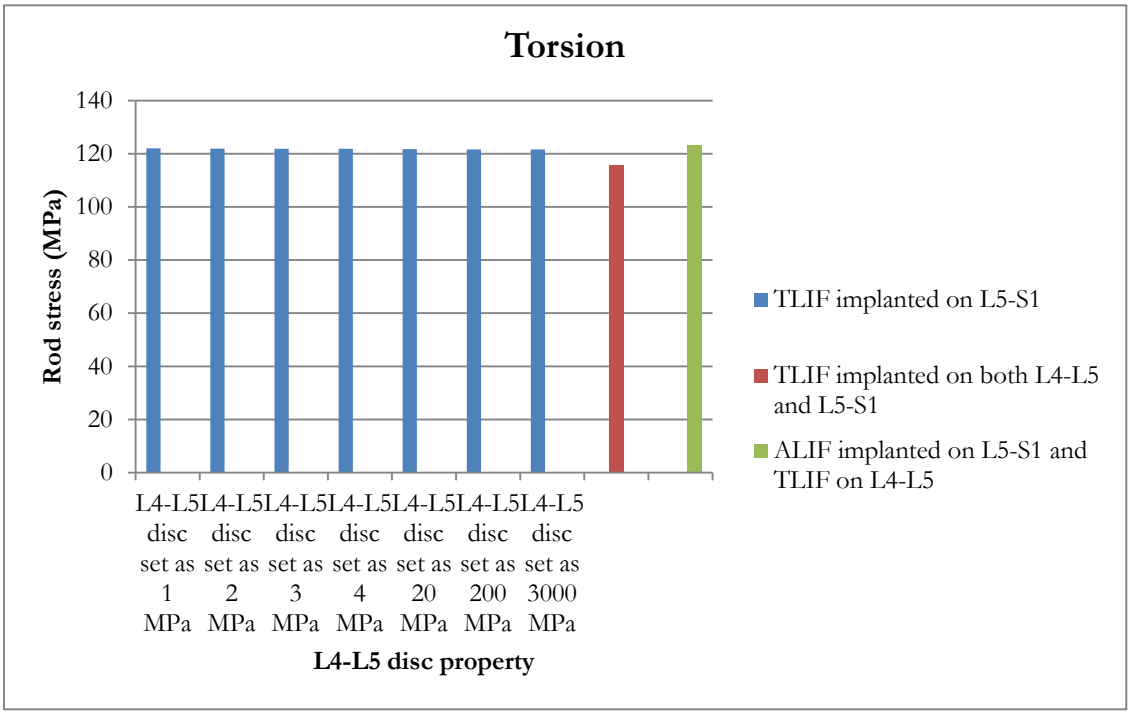

Figure A.18. Maximum rod stress (MPa) on models with TLIF implanted on the L5-S1 level during disc degeneration in torsion motion

During extension and flexion motions, 49.7% and 48.9% percentage decreases are noticed in the maximum rod stresses respectively when the L4-L5 disc property is varied from 1 MPa to 3000 MPa. It is critical to use a second interbody device at the L4-L5 level if the disc is diagnosed as degeneratively soft, in terms of reducing the maximum rod stress.

Currently, surgeons implant either an ALIF or a TLIF as the second interbody device on the L4-L5 level in this situation. However, our results indicate the a TLIF can yield similar results to an ALIF, as far as reducing the maximum rod stress is concerned, when it is placed as anteriorly as possible between in vertebrae. As we mentioned before, considering the surgical difficulty and associated cost of implanting an ALIF, a TLIF should be considered as a simpler alternative to an ALIF when replacing a degeneratively soft disc, if the primary reason for implanting a spacer is to reduce rod stress.

A.0.2 Titanium rods vs. cobalt chrome

The maximum rod stresses studied in Chapter 2 were made of cobalt chrome. As seen in this appendix, similar trends are seen in the stresses induced when the analysis is repeated for titanium rods. As with the cobalt chrome rods, an interbody spacer can significantly reduce the rod stress when it replaces a degeneratively soft disc, and if the second disc is also degeneratively soft, a second spacer is required to replace it, since the rod stress remains considerably high unless the second spacer is inserted. However, while the titanium rods exhibit similar trends as the cobalt chrome rods, titanium rods also experiences significantly less stress compared to cobalt chrome. In extension, the rod stress reduction achieved by replacing cobalt chrome with titanium can be as great as 26.7%. In flexion motion, rod stress reduction achieved by replacing cobalt chrome with titanium can be as great as 27.0%. In torsion motion, the effect is less dramatic, as the rod stress reduction achieved by replacing cobalt chrome with titanium is around 10%. Since both materials have similar yield strength (yield strength of cobalt chrome is 960 MPa and yield strength of titanium is 940 MPa), this study suggest that using titanium as the rod material has the potential to significantly reduce the risk of rod breakage, due to the fact that the stresses in the rods will be lower when compared with the same loads applied to cobalt

chrome rods.